

Contrastive Network Representation Learning

Zihan Dong¹, Xin Zhou², Ryumei Nakada¹, Lexin Li², and Linjun Zhang¹

¹Rutgers University ²University of California at Berkeley

September 16, 2025

Abstract

Network representation learning seeks to embed networks into a low-dimensional space while preserving the structural and semantic properties, thereby facilitating downstream tasks such as classification, trait prediction, edge identification, and community detection. Motivated by challenges in brain connectivity data analysis that is characterized by subject-specific, high-dimensional, and sparse networks that lack node or edge covariates, we propose a novel contrastive learning-based statistical approach for network edge embedding, which we name as Adaptive Contrastive Edge Representation Learning (ACERL). It builds on two key components: contrastive learning of augmented network pairs, and a data-driven adaptive random masking mechanism. We establish the non-asymptotic error bounds, and show that our method achieves the minimax optimal convergence rate for edge representation learning. We further demonstrate the applicability of the learned representation in multiple downstream tasks, including network classification, important edge detection, and community detection, and establish the corresponding theoretical guarantees. We validate our method through both synthetic data and real brain connectivities studies, and show its competitive performance compared to the baseline method of sparse principal components analysis.

1 Introduction

Representation learning has emerged as a central problem in statistics and machine learning, aiming to discover meaningful low-dimensional latent features or embeddings that capture the underlying structure of observed data (Xu and Qu, 2025). Within this paradigm, network representation learning seeks to embed network data into a low-dimensional space while preserving its essential key topological and semantic properties. Such learned representations often enable more effective graph-based data analysis, supporting downstream tasks including graph classification, trait prediction, edge selection, and community detection. See Cai et al. (2018); Zhang et al. (2020) for systematic reviews on network representation learning.

Our motivation stems from brain connectivity analysis, a vital field in neuroscience that studies how different brain regions interact and communicate with each other. It provides crucial insights into brain function and structure, as well as the mechanisms underlying numerous neurological and psychiatric disorders. It relies on neuroimaging modalities, such as functional magnetic resonance imaging (fMRI) and diffusion magnetic resonance imaging (dMRI). There has been a rapid advancement in brain connectivity analysis through the use of graph theory tools (Wang et al., 2021). Central to this development is the notion that brain connectivity can be represented as a graph, where nodes correspond to brain regions,

and edges capture functional, structural, or directional interactions between regions. It also exhibits some unique features. Each individual subject has a connectivity network derived from a neuroimaging modality, and the subject-to-subject variation is typically large. The underlying network is often sparse, containing only a small subset of nonzero edges, yet high-dimensional, with hundreds of nodes and tens of thousands of edges. Moreover, unlike gene network or social network, brain connectivity network usually contains little node or edge attribute information (Fornito et al., 2013).

Numerous approaches have been developed for network representation learning. Depending on the target of the embedding, these methods can be broadly categorized into node embedding, which learns a vector representation for each node in the network; edge embedding, which captures relationships between pairs of nodes; and whole-graph or subgraph embedding, which generates representations for an entire graph or its subsets. The last category of methods, e.g., graph2vec (Narayanan et al., 2017), often build upon the first category, by employing node embedding as the first step. For node embedding, there have been many proposals. Notable examples include deepwalk (Perozzi et al., 2014), node2vec (Grover and Leskovec, 2016), high-order proximity preserved embedding (Ou et al., 2016), graph convolutional networks (Kipf and Welling, 2016), and graphSAGE (Hamilton et al., 2017), among many others. In contrast, for edge embedding, there have been much fewer solutions. Notable examples include edge2vec (Wang et al., 2020), dual hypergraph transformation (Jo et al., 2021a), attrE2vec (Bielak et al., 2022), and edge-wise bipartite graph representation learning (Wang et al., 2024).

There is a line of network representation solutions that employ contrastive learning techniques (You et al., 2020; Zhu et al., 2020, 2021; Xia et al., 2022). Contrastive learning is a self-supervised approach that learns meaningful representations by teaching models to distinguish between similar (positive) and dissimilar (negative) pairs of data (Chen et al., 2020). The core idea is to bring representations of similar inputs closer in the embedding space, while pushing apart dissimilar ones, implicitly regularizing the learned representations (Ji et al., 2023). This technique is particularly useful for network representation learning, as it does not require labeled data, and it encourages robust representations that generalize well on downstream tasks. There has also been some recent work studying statistical properties of contrastive learning (Gui et al., 2023, 2025; Wang, 2023, 2025; Lin and Mei, 2025)

Despite their success, however, several challenges remain in applying current node or edge embedding methods to brain connectivity analysis. In particular, most existing solutions require node attributes, and are not effective in handling heterogeneous and sparse networks. Moreover, there is very limited literature providing theoretical guarantees when networks are heterogeneous and sparse.

In this article, we propose a new contrastive learning-based statistical model and accompanying methodology, which we name as Adaptive Contrastive Edge Representation Learning (ACERL), for network edge embedding. Our proposal offers several advantages and novel contributions. First, ACERL constructs network embedding by contrasting positive and negative pairs, and unlike most existing embedding solutions, does *not* require additional node or edge attribute information. It can effectively capture meaningful structural information, and is naturally suited to handle data heterogeneity by learning representation through data-driven augmentation. It further incorporates iterative truncation to induce sparsity in the learned network representation. Second, we introduce an adaptive random masking mechanism, which dynamically adjusts the augmentation process based on the signal-to-noise ratio to enhance feature extraction. This mechanism improves robustness in the presence of heterogeneous noise, and enables effective handling of

sparsity by iteratively refining informative features. We note that the principles of this technique extend beyond heterogeneous networks, offering a novel and principled approach to feature extraction from heterogeneous data in general. Third, we establish sharp performance guarantees, and show that ACERL achieves the minimax optimal rate of convergence, which is significantly faster than most existing contrastive learning methods in the literature. To the best of our knowledge, this is the first minimax optimality result for contrastive network embedding in sparse and heterogeneous settings. Finally, we demonstrate the applicability of the learned representation in multiple downstream tasks, including network classification, important edge detection, and community detection, and derive the corresponding theoretical guarantees. We validate ACERL through both synthetic data and real brain connectivity studies, and show its competitive performance compared to the baseline solution.

We adopt the following notation throughout this article. For a set \mathcal{I} , let $|\mathcal{I}|$ denote its size, and \mathcal{I}^c its complement. Let $a \vee b = \max\{a, b\}$, and $a \wedge b = \min\{a, b\}$. We use c and C to denote absolute positive constants that may vary from place to place. For two positive sequences $\{a_n\}, \{b_n\}$, write $a_n \lesssim b_n$ if $a_n \leq Cb_n$ for all n , $a_n \gtrsim b_n$ if $b_n \lesssim a_n$, and $a_n \asymp b_n$ if $a_n \lesssim b_n$ and $b_n \lesssim a_n$. Write $a_n = o(b_n)$ if $\lim_n a_n/b_n = 0$, $a_n = O(b_n)$ if $a_n \leq Cb_n$, and $a_n = \Omega(b_n)$ if $a_n \geq Cb_n$ for all n and some positive C . For a matrix A , let $\|A\|_{\text{sp}}$ and $\|A\|_F$ be its spectral norm and Frobenius norm. Let $\|A\|_{2,0}$ be the $(2, 0)$ -matrix-norm defined as the number of non-zero rows of A , and $\|A\|_{2,\infty}$ the $(2, \infty)$ -matrix-norm defined as the maximum ℓ_2 norm among all rows of A . Let $A_{\mathcal{I}\mathcal{J}}$ be its $|\mathcal{I}| \times |\mathcal{J}|$ submatrix formed by a_{ij} with $(i, j) \in \mathcal{I} \times \mathcal{J}$ for two sets \mathcal{I}, \mathcal{J} . For two matrices A, B of the same dimension, let $\langle A, B \rangle = \text{tr}(A^\top B)$ denote the trace inner product, and $\text{dist}(A, B) = \min_O \|AO - B\|_F$, where O is an orthogonal rotation matrix.

The rest of the article is organized as follows. Section 2 introduces the model and the estimation procedure. Section 3 presents the theoretical analysis, and Section 4 studies several downstream tasks. Section 5 compares to a key alternative method, sparse principal components analysis (sPCA). Section 6 presents the simulations, and Section 7 illustrates with two real-world brain connectivity studies. The Supplementary Appendix collects all proofs and additional results.

2 Model and Estimation

2.1 Model Set-up

Consider a graph $\mathcal{G} = \mathcal{V} \times \mathcal{E}$ with the node set \mathcal{V} and the edge set \mathcal{E} . Let $v = |\mathcal{V}|$ denote the total number of nodes, and $d = |\mathcal{E}|$ the total number of edges. For an undirected acyclic graph, $d = v(v - 1)/2$, and for a directed acyclic graph, $d = v^2$. To simplify the presentation, we focus on the undirected graph in this article, whereas all results can be naturally extended to the directed graph.

For an individual subject $i \in [n]$, let $x_i = (x_{i1}, \dots, x_{id})^\top \in \mathbb{R}^d$ denote the vectorized connectivity strength of all edges. Suppose each edge $e \in \mathcal{E}$ has a corresponding latent edge embedding representation $q_e \in \mathbb{R}^r$, and each subject i has a low-dimensional latent subject embedding representation $z_i \in \mathbb{R}^r$, where r is the dimension of the latent feature space. We consider the following generative model,

$$x_i = Q^* z_i + \xi_i, \quad (2.1)$$

where $\xi_i \in \mathbb{R}^d$ is an independent zero mean sub-Gaussian noise. Here we model the connectivity strength, represented by the e th entry $x_{i,e}$ of vector x_i , through the inner

product $\langle q_e, z_i \rangle$, which, intuitively, measures the alignment between the latent edge embedding q_e and the subject embedding z_i . For identifiability, we assume $\text{Cov}(z_i) = I_r$. We also assume $\text{Cov}(\xi_i) = \Sigma^* = \text{diag}(\sigma_1^*, \dots, \sigma_d^*)$, and throughout this article, we focus on the *heteroscedastic* case, where $\sigma_1^*, \dots, \sigma_d^*$ can be different. Let $Q^* = (q_1, \dots, q_d) \in \mathbb{R}^{d \times r}$ denote the *edge embedding matrix* that collects all latent edge representation q_e 's, and $Z = (z_1, \dots, z_n) \in \mathbb{R}^{r \times n}$ denote the *subject embedding matrix* that collects all latent subject representation z_i 's. Due to rotational invariance, Q^* and Z are only identifiable up to an orthogonal transformation. Moreover, in numerous applications, the graph is inherently sparse. Correspondingly, we introduce a sparsity constraint on Q^* , such that $\|Q^*\|_{2,0} \leq s^*$, where s^* denotes the true sparsity level.

Following model (2.1), we define $q_{Q^*}(x) = Q^{*\top} x : \mathbb{R}^d \rightarrow \mathbb{R}^r$, which is a linear representation function that maps the network data x_i to its latent representation. Following this formulation, learning the edge embedding matrix Q^* is the same as learning the linear representation q_{Q^*} that is parameterized by Q^* . Toward that end, we employ contrastive learning, leveraging its capabilities of learning latent representation without label information and handling heterogeneous noise.

Before turning to estimation, we make a few remarks about our model (2.1). First, the edge embedding q_e is crucial for downstream tasks such as edge detection and community detection, whereas the subject embedding z_i is crucial for downstream tasks such as patient classification. For an edge e , the connectivity strength $x_{i,e} = \langle q_e, z_i \rangle$ becomes stronger if the subject embedding z_i aligns with the edge embedding q_e . Second, in this model, we essentially vectorize all the edges. We note that this is a common practice in edge embedding (Wang et al., 2024; Jo et al., 2021b; Goyal et al., 2018). More importantly, there are typically no inherent structural constraints on the adjacency matrices for most networks. As such, representing edges in a vectorized form is mathematically equivalent to using their adjacency matrices. Such formulation is not only simple, but also provides a flexible framework that can be naturally extended to incorporate additional structural constraints if there are any. For instance, for the downstream task of community detection that we study in Section 4.3, the corresponding adjacency matrix satisfies a block-wise structure up to a permutation. In such a case, we extend our model to explicitly reflect the underlying community structure among the nodes, allowing for a more structured and refined analysis. Finally, we remark that, in this article, we primarily focus on linear latent representation learning. Despite its simplicity, it is widely adopted in the literature of both network embedding (Roweis and Saul, 2000; Cui et al., 2018) and principal components-based analysis (Cai et al., 2013; Gao and Ma, 2023), thanks to its interpretability and computational efficiency. We believe it serves as a solid starting point, whereas its theoretical properties already require careful characterization.

2.2 Construction of augmented views with adaptive masking

Contrastive learning begins with applying a data augmentation technique, for instance, masking, to generate two correlated views, $h_1(x_i)$ and $h_2(x_i)$, of a given data instance x_i , then constructing positive pairs from these views and negative pairs from unrelated instances. However, current contrastive learning methods use a fixed masking strategy, which struggles in the presence of heteroscedastic noise, and can actually introduce significant bias into the learned representations. To overcome this hurdle, we propose an *adaptive* random masking mechanism to construct augmented views of the raw data. Specifically, we utilize two augmentation functions,

$$h_1(x_i) = Ax_i, \quad h_2(x_i) = (I - A)x_i,$$

where $A = \text{diag}(a_1, \dots, a_d) \in \mathbb{R}^{d \times d}$ is the diagonal masking matrix, and the diagonal elements $\{a_e\}_{e=1}^d$ are independent random variables sampled from the following distribution with the masking parameter $p = (p_1, \dots, p_d)^\top \in [0, 1]^d$,

$$a_e = \begin{cases} 0 & \text{with probability } \frac{1-p_e}{2} \\ \frac{1}{2} & \text{with probability } p_e \\ 1 & \text{with probability } \frac{1-p_e}{2} \end{cases}. \quad (2.2)$$

Again, the key here is an adaptive adjustment of the masking probability p_e . All existing contrastive learning methods set a *fixed* masking probability of $p_e = 0$ for all edges $e \in \mathcal{E}$. In contrast, we propose to adjust p_e *adaptively* based on the signal-to-noise ratio, which may vary significantly in the heterogeneous noise setting. We describe the detailed adaptive adjustment procedure in Section 2.4, and provide its rigorous theoretical guarantee in Section 3. At the high level, the masking probability p_e directly controls the degree of information shared between the two views. That is, when $a_e = 0$ or $a_e = 1$, the corresponding feature is completely masked in one of the views, and when $a_e = 1/2$, the feature information is shared between the two views. As such, when the estimated signal-to-noise ratio is large, we increase p_e , making a_e more likely equal 1/2, which in turn helps retain more shared information. Conversely, when the estimated signal-to-noise ratio is low, we decrease p_e , making a_e more likely equal to 0 or 1, which decreases information sharing between the views. This way, we are able to control the trade-off between complete masking for denoising in highly noisy edges and the preservation of shared feature information across views in less noisy edges. Such an adaptive strategy thus allows our method to effectively handle heterogeneous noise across the network. To the best of our knowledge, our proposal is among the first contrastive learning approach with adaptive masking.

2.3 Contrastive loss function

After obtaining the augmented views, we construct the positive pair and the negative pairs for $h_j(x_i)$, $i \in [n], j \in [2]$, as,

$$\mathcal{B}_{h_j(x_i)}^{\text{pos}} = \{h_w(x_i) : w \in [2] \setminus \{j\}\}, \quad \mathcal{B}_{h_j(x_i)}^{\text{neg}} = \{h_w(x_{i'}) : w \in [2] \setminus \{j\}, i' \in [n] \setminus \{i\}\}.$$

That is, we form the positive pair by taking the other view of the same sample x_i , because intuitively two augmented views of the same sample contain more similar information. Meanwhile, we form the negative pair by taking the counterpart view of other samples $x_{i'} \in [n] \setminus \{i\}$, because the training samples are usually independent from each other and thus contain different information.

We then estimate the edge embedding matrix Q^* by minimizing the distance between the positive pairs while maximizing the distance between the negative pairs. That is, we minimize the following loss function with respect to $Q \in \mathbb{R}^{d \times r}$,

$$\mathcal{L}(Q) = \frac{1}{n} \sum_{i=1}^n \sum_{j=1}^2 \ell\left(h_j(x_i), \mathcal{B}_{h_j(x_i)}^{\text{pos}}, \mathcal{B}_{h_j(x_i)}^{\text{neg}}; q_Q\right) + R(Q), \quad (2.3)$$

where ℓ is a contrastive loss function, and $R(Q)$ is a regularization term. For ℓ , we employ the triplet contrastive loss, which is widely used in contrastive learning (see, e.g., Hadsell et al., 2006; He et al., 2018), and is defined as,

$$\ell(h_j(x_i), \mathcal{B}_{h_j(x_i)}^{pos}, \mathcal{B}_{h_j(x_i)}^{neg}, q_Q) = - \sum_{x \in \mathcal{B}_{h_j(x_i)}^{pos}} \frac{\langle q_Q(h_j(x_i)), q_Q(x) \rangle}{|\mathcal{B}_{h_j(x_i)}^{pos}|} + \sum_{x \in \mathcal{B}_{h_j(x_i)}^{neg}} \frac{\langle q_Q(h_j(x_i)), q_Q(x) \rangle}{|\mathcal{B}_{h_j(x_i)}^{neg}|}. \quad (2.4)$$

2.4 Two-level iterative estimation

Next, we develop an estimation procedure to iteratively minimize the contrastive loss while updating the masking parameter, aiming to preserve essential structural information while at the same time to mitigate noise. Our algorithm consists of two levels of iterations: during the *inner* iteration, we estimate the embedding matrix Q^* based on the current masking parameter p_e , and during the *outer* iteration, we update p_e based on the current estimate of Q^* .

More specifically, during the inner iteration, given the input network data $\mathcal{D} = \{x_i\}_{i=1}^n \subset \mathbb{R}^d$ and the current masking parameter p , we employ the contrastive loss function (2.3) to estimate Q^* . We set the regularization term $R(Q) = \|QQ^\top\|_F^2/8$ to prevent Q from growing arbitrarily large and to ensure numerical stability. We set the regularization parameter to 1/8 to simplify the method and theory development, while we allow a more flexible choice of this parameter. We provide more discussion in Appendix B.1. The loss function in (2.3) then becomes,

$$\begin{aligned} \mathcal{L}(Q; \mathcal{D}, A) = & -\frac{1}{n} \sum_i \langle Q^\top Ax_i, Q^\top(I - A)x_i \rangle + \\ & \frac{1}{n^2} \sum_{i,j} \langle Q^\top Ax_i, Q^\top(I - A)x_j \rangle + \frac{1}{8} \|QQ^\top\|_F^2. \end{aligned} \quad (2.5)$$

To minimize (2.5), we employ gradient decent. To further enforce sparsity, we apply the hard thresholding function $HT(Q, s)$ with the working sparsity level $s \in \mathbb{N}$, by keeping the s rows of Q with the largest ℓ_2 norms and setting all other rows to zeros. We run the inner iterations for T times.

During the outer iteration, we update the masking parameter $p = (p_1, \dots, p_d)^\top$ based on the current estimate of Q^* , by setting

$$p_e^{(k)} = \frac{\|\widehat{q}_e^{(k-1)}\|_2}{\sqrt{\widehat{\text{Var}}(x_e)}} \wedge 1, \quad (2.6)$$

where $\widehat{q}_e^{(k-1)}$ is the estimate of q_e at the $(k-1)$ th iteration, and the sample variance $\widehat{\text{Var}}(x_e) = \sum_i^n x_{i,e}^2/n - (\sum_i^n x_{i,e}/n)^2$. Since $x_{ie} = q_e^\top z_i + \xi_{ie}$, we note that $\|\widehat{q}_e^{(k-1)}\|_2$ can be interpreted as the estimated signal strength of edge e at the k th iteration. When the estimated signal is strong, we increase p_e to retain more shared information between the augmented views. When the estimated signal is weak, we decrease p_e to encourage stronger masking augmentation, which in effect facilitates denoising. We run the outer iterations for K times.

We also briefly discuss the initial value and tuning parameters. For the initial edge embedding estimator $\widehat{Q}^{(0)}$, let $M = n^{-1}XX^\top - n^{-2}X1_n1_n^\top X^\top \in \mathbb{R}^{d \times d}$, $X = (x_1, \dots, x_n) \in \mathbb{R}^{d \times n}$, $1_n = (1, \dots, 1)^\top \in \mathbb{R}^n$, $D(M)$ be the diagonal matrix with the same diagonal elements of M , and $\Delta(M) = M - D(M)$. We then apply the Fantope projection method (Vu et al., 2013) to $\Delta(M)$ and apply PCA to obtain an initial estimator for $\widehat{Q}^{(0)}$. For the latent dimension r and the sparsity level s , we recommend some graph-based empirical

Algorithm 1 ACERL .

- 1: **Input:** Network edge data $\mathcal{D} = \{x_i\}_{i=1}^n \subset \mathbb{R}^d$, initial edge embedding matrix $\widehat{Q}^{(0)}$; initial masking parameter p , dimension of the representation space r , working sparsity level s , step size $\eta > 0$, number of inner iterations T , number of outer iterations K .
- 2: **for** $k \in [K]$ **do**
- 3: Set $\widehat{Q}_{(0)}^{(k)} = \widehat{Q}^{(k-1)}$.
- 4: **for** $t \in [T]$ **do**
- 5: Generate $A_{(t)}^{(k)} = \text{diag} \left(a_{(t),1}^{(k)}, \dots, a_{(t),d}^{(k)} \right)$ following (2.2).
- 6: Update the edge embedding matrix estimate as
$$\begin{aligned}\widehat{Q}_{(t)}^{(k)} &\leftarrow \widetilde{Q}_{(t-1)}^{(k)} - \eta \partial_Q \mathcal{L} \left(\widetilde{Q}_{(t-1)}^{(k)}; \mathcal{D}, A_{(t)}^{(k)} \right), \\ \widetilde{Q}_{(t)}^{(k)} &\leftarrow HT \left(\widehat{Q}_{(t)}^{(k)}, s \right).\end{aligned}$$
- 7: **end for**
- 8: Set $\widehat{Q}^{(k)} = \widetilde{Q}_{(T)}^{(k)}$.
- 9: Update the masking parameter $p_e^{(k+1)} = \frac{\|\widehat{q}_e^{(k)}\|_2}{\sqrt{\text{Var}(x_e)}} \wedge 1$ following (2.6).
- 10: **end for**
- 11: **Output:** Edge embedding matrix estimator $\widehat{Q} = \widehat{Q}^{(K)}$.

approach, and give more details in Section 6. For the number of inner and outer iterations T and K , we suggest setting them to be of the order of $\log n$. We set the step size η between 0.1 and 1, and our numerical experiments show that the results are not overly sensitive within this range.

We summarize the above estimation procedure in Algorithm 1.

3 Theoretical Guarantees

We establish the theoretical guarantee for our proposed method, in particular, the minimax optimal convergence rate of the estimator from Algorithm 1. We first obtain the upper bound for the estimator at the k th outer iteration, then the upper bound of the estimated edge embedding matrix Q^* .

We note that, since our goal is to learn Q^* up to an orthogonal transformation, we present our results in the form of $Q^*Q^{*\top}$. Consider the spectral decomposition

$$Q^*Q^{*\top} = U^* \Lambda^* U^{*\top}, \quad \text{where } \Lambda^* = \text{diag}(\lambda_1^{*2}, \dots, \lambda_r^{*2}) \in \mathbb{R}^{r \times r},$$

with the diagonal elements in a descending order, and $U^* \in \mathbb{R}^{d \times r}$ is orthonormal. Moreover, since the random masking is generated at each iteration of the gradient descent, generating multiple masking matrices A 's can be viewed as averaging over different samples. Consequently, the gradient updates can be interpreted as stochastic gradient descent on the following expected loss (3.1) over the randomness of A .

$$\mathcal{L}(Q) = \mathbb{E}_A[\mathcal{L}(Q; \mathcal{D}, A)]. \quad (3.1)$$

We begin with a set of regularity conditions.

Assumption 3.1. Suppose $\sigma_{(1)}^{*2} \asymp 1$, where $\sigma_{(j)}^{*2}$ denotes the j th largest of $\sigma_1^{*2}, \dots, \sigma_d^{*2}$.

Assumption 3.2. Suppose $\lambda_1^{2*} \asymp 1$, and $\kappa_{\Lambda^*} = \lambda_1^{*2}/\lambda_r^{*2} < c_1$ for some constant c_1 .

Assumption 3.3. Suppose the incoherent constant of U^* , i.e., $I(U^*) = \|U^*\|_{2,\infty}^2$, satisfies that $I(U^*) \leq c_2/r$ for some sufficiently small constant $c_2 > 0$.

Assumption 3.4. Suppose the initial edge embedding matrix estimator $\widehat{Q}^{(0)}$ satisfies that $\|\widehat{Q}^{(0)}\widehat{Q}^{(0)\top} - Q^*Q^{*\top}\|_F \leq \lambda_r^{*3}/(20\lambda_1^*)$.

We make some remarks on these conditions. Assumption 3.1 allows heterogeneous noise levels. Assumption 3.2 ensures that the signal strengths across coordinates are of the same order. Additionally, they assume that the signals and noise variances are of a constant order. These conditions are commonly imposed in the literature (see, e.g., Zhang et al., 2022; Gao and Ma, 2023; Johnstone and Lu, 2009; Vu and Lei, 2013). Assumption 3.3 intuitively quantifies the extent to which the signals are evenly distributed across coordinates. It implies that the signal coordinates are correlated, and they can be distinguished from random noise. Similar conditions have also been considered in the literature of low-rank matrix analysis (see, e.g., Candès and Recht, 2009; Zhang et al., 2022). Assumption 3.4 is about the initial estimator $\widehat{Q}^{(0)}$, which is obtained by applying the Fantope projection method in our case. By Vu et al. (2013, Theorem 3.3) and Assumption 3.3, we have that $\|\widehat{Q}^{(0)}\widehat{Q}^{(0)\top} - Q^*Q^{*\top}\|_F \lesssim s^*/\sqrt{r}$. Consequently, our initial estimator $\widehat{Q}^{(0)}$ satisfies Assumption 3.4.

We now present our main theoretical results in two parts, first for the estimator at a fixed k th outer iteration, then for the estimator when k increases to K .

Theorem 3.1. For a given $k = 1, \dots, K$, define the masking-adjusted covariance matrix estimation error as,

$$W^{(k-1)} = \sup_{\mathcal{I} \subset [d] \text{ with } |\mathcal{I}|=2s+s^*} \left\| \left(\Delta(M) + P^{(k)2} D(M) - Q^*Q^{*\top} \right)_{\mathcal{I}\mathcal{I}} \right\|_{sp} \quad (3.2)$$

where $P^{(k)} = \text{diag}(p_1^{(k)}, \dots, p_d^{(k)})$, and $M, \Delta(M)$ and $D(M)$ are as defined in Section 2.4. Suppose $W^{(k-1)} \leq c_3\lambda_r^{*3}/(\lambda_1^*\sqrt{r})$ for some sufficiently small positive constant c_3 , and $\|\widetilde{Q}_{(0)}^{(k)}\widetilde{Q}_{(0)}^{(k)\top} - Q^*Q^{*\top}\|_F \leq \lambda_r^{*3}/(20\lambda_1^*)$. Set the step size $\eta \leq 6/(43\lambda_1^{*2})$, and the sparsity level $s \geq 36s^*/(\lambda_r^{*4}\eta^2)$. Then, for all $t \geq 1$, we have

$$\text{dist}(\widetilde{Q}_{(t+1)}^{(k)}, Q^*) \leq \xi^t \text{dist}(\widetilde{Q}_{(0)}^{(k)}, Q^*) + \frac{3}{\lambda_r^*} \sqrt{\frac{sr}{s^*}} W^{(k-1)}. \quad (3.3)$$

where $\xi = 1 - \lambda_r^{*2}\eta/2$.

We first briefly remark that, as $\text{dist}(\widetilde{Q}_{(t+1)}^{(k)}, Q^*)$ gradually decays, the conditions for $W^{(k-1)}$ and $\widetilde{Q}_{(0)}^{(k)}$ in this theorem hold for all k once they hold for $k = 0$. Further details can be found in the proof. Theorem 3.1 provides an upper bound of the distance between Q^* and $\widetilde{Q}_t^{(k)}$ for a fixed outer iteration k while the number of inner iterations t increases. This bound consists of two terms, the first is an optimization error term that decays geometrically as t increases, and the second is a statistical error term that accounts for the irreducible error due to finite samples and does not diminish as t increases. As such, when t increases, the first term is to be dominated by the second term, which relies on $W^{(k-1)}$. Note that $W^{(k-1)}$ depends only on the masking parameter p , which varies with the outer iterations, but not the inner iterations. In the next theorem, we establish the estimation error of our edge embedding estimator by characterizing the evolution of $W^{(k-1)}$ when the outer iteration k increases to K .

Theorem 3.2. Suppose Assumptions 3.1 to 3.4 hold, and $s^* \log d \ll n$. Set the step size $\eta \leq 6/(43\lambda_1^{*2})$, and the sparsity level $s \geq 36s^*/(\lambda_r^{*4}\eta^2)$. For inner iterations, we run $T^{(k)} = \Omega(\log n \wedge \log(2^k r))$ times, and for outer iterations, we run $K = \Omega(\log n)$ times. Then, with probability at least $1 - ce^{-cs \log d}$, we have

$$\left\| \widehat{Q}^{(K)} \widehat{Q}^{(K)\top} - Q^* Q^{*\top} \right\|_F \lesssim \frac{s}{s^*} \sqrt{\frac{s^* r \log d}{n}}. \quad (3.4)$$

Theorem 3.2 shows a controlled deviation of our final estimated edge embedding matrix $\tilde{Q}^{(K)}$ after K outer iterations from the ground truth Q^* . In particular, the factor s/s^* accounts for the selection of the sparsity level, and since s can be chosen as the same order of s^* , the error remains $\sqrt{s^* r \log d/n}$ up to a constant.

We also remark that Theorem 3.2 essentially shows ACERL achieves the minimax optimal rate of convergence. This is because, when the noise is homogeneous, i.e., when $\sigma_1^* = \dots = \sigma_d^*$ in model (2.1), our problem reduces to sPCA. Since the homogeneous noise setting is a special case of the heterogeneous one, the results established for sPCA under the homogeneous setting (Cai et al., 2013; Vu and Lei, 2013) provide a direct minimax lower bound for ACERL, which is $\sqrt{s^*(r + \log d)/n}$. This implies that, when r is finite, ACERL achieves the minimax optimal rate. We further study and compare with sPCA under the heterogeneous setting in Section 5.

Finally, we remark on the advantage of adaptive masking. As shown in Theorem 3.2, ACERL removes the bias term, an issue that is often further amplified in a sparse setting. Ji et al. (2023) studied standard contrastive learning in the classical non-sparse setting with fixed masking, and established the estimation error rate of $\sqrt{rd/n} + (r^{3/2} \log d)/d$. We can easily modify our proposed method to incorporate the non-sparse setting. That is, we still consider model (2.1), but impose no sparsity constraint. Accordingly, for estimation, we modify Algorithm 1 slightly by dropping the hard thresholding step, $\tilde{Q}_{(t)}^{(k)} \leftarrow HT(\widehat{Q}_{(t)}^{(k)}, s)$. Then, we can establish the corresponding estimation error rate of the non-sparse estimator.

Assumption 3.5. Suppose the incoherent constant of U^* satisfies that $I(U^*) \leq c_4$ for some sufficiently small constant $c_4 > 0$.

Corollary 3.1. Suppose Assumptions 3.1, 3.2 and 3.5 hold, and that $r < d \ll n$. We run the outer iterations $K = \Omega(\log n)$ times. Then, with probability at least $1 - ce^{-c\sqrt{n/d} \wedge d}$, we have

$$\left\| \widehat{Q}^{(K)} \widehat{Q}^{(K)\top} - Q^* Q^{*\top} \right\|_{sp} \lesssim \sqrt{\frac{d}{n}}. \quad (3.5)$$

Compared to Ji et al. (2023), our method offers two main advantages. First, our condition is milder. That is, our Assumption 3.5, which is the counterpart of Assumption 3.3 in the non-sparse setting, is weaker than the condition in Ji et al. (2023), which required the incoherence constant to satisfy $I(U^*) = O((r \log d)/d)$. Second, our algorithm achieves a sharper error rate. That is, Corollary 3.1 establishes a Frobenius norm error of $\sqrt{rd/n}$, which improves upon the rate $\sqrt{rd/n} + (r^{3/2} \log d)/d$ obtained in Ji et al. (2023). The improvement comes from masking, where fixed masking introduces a bias term, and our adaptive masking successfully removes it.

4 Downstream Tasks

We next investigate how network edge embedding can facilitate downstream tasks, in particular, subject classification, edge selection, and node community detection. For each

task, we discuss the underlying model, our solution based on edge embedding, the evaluation criterion, and the theoretical quantification of task performance.

4.1 Subject classification task

For the task of subject classification, we consider a binary classification model setting, where for the subject $i \in [n]$,

$$y_i \mid z_i \sim \text{Bernoulli}(F(\langle z_i, w^* \rangle)), \quad (4.1)$$

in which y_i is the binary label, z_i is the latent subject embedding that connects with the observed feature vector x_i through model (2.1), $w^* \in \mathbb{R}^r$ is a unit-norm coefficient vector, and $F : \mathbb{R} \rightarrow [0, 1]$ is a monotonically increasing function satisfying $1 - F(u) = F(-u)$ for all $u \in \mathbb{R}$. This formulation covers many standard classification models, including the logistic model and the probit model. Our goal is to classify a new subject, based on the feature information x_0 , into one of the two classes.

Given the training data $\{x_i, y_i\}_{i=1}^n$, we first obtain the estimated edge embedding matrix \hat{Q} following Algorithm 1. Note that this estimation step only uses $\{x_i\}_{i=1}^n$, and thus is unsupervised. We then estimate the corresponding patient embedding as,

$$\hat{z}_i = (\hat{Q}^\top \hat{Q})^{-1} \hat{Q}^\top x_i, \quad i \in [n].$$

Given $\{\hat{z}_i, y_i\}_{i=1}^n$, we fit a classification model and obtain the estimated coefficient \hat{w} . Finally, for a new testing data point x_0 , we obtain the classifier,

$$\delta_{\hat{Q}, \hat{w}}(x_0) = \mathbb{1} \left\{ F \left(\hat{w}^\top \hat{z}_0 \right) \geq \frac{1}{2} \right\} = \mathbb{1} \left\{ F \left(\hat{w}^\top (\hat{Q}^\top \hat{Q})^{-1} \hat{Q}^\top x_0 \right) \geq \frac{1}{2} \right\},$$

where $\mathbb{1}(\cdot)$ is the indicator function.

We evaluate the classifier using the usual 0-1 loss, $\mathcal{L}_c(\delta) = \mathbb{1} \{y_0 \neq \delta(x_0)\}$, for a classifier δ . We then establish the theoretical bound for the excess risk of classification,

$$\inf_{w \in \mathbb{R}^r} \mathbb{E}_0 \left[\mathcal{L}_c \left(\delta_{\hat{Q}, w} \right) \right],$$

where $\mathbb{E}_0[\cdot]$ is the expectation with respect to (y_0, x_0, z_0) . Since our goal is to evaluate the performance of classification task based on the learned edge embedding \hat{Q} , rather than the specific procedure to train the classifier, we take the infimum over $w \in \mathbb{R}^r$ to select the best classifier within the family $\{\delta_{\hat{Q}, w} \mid w \in \mathbb{R}^r\}$ in our evaluation.

Theorem 4.1. *Suppose the eigenvalues of the noise covariance matrix Σ^* are all of a constant order. Suppose z_0 and ξ_0 are Gaussian random variables. In addition, for the edge embedding estimation error, $E(\hat{Q}) = \|\hat{Q}\hat{Q}^\top - Q^*Q^{*\top}\|_F$, suppose*

$$E(\hat{Q}) \leq \sigma_{(d)}^2 \wedge \frac{1}{2}, \quad (4.2)$$

where $\sigma_{(d)}$ is the smallest eigenvalue of Σ . Then, the excess risk for classification is bounded as:

$$\inf_{w \in \mathbb{R}^r} \mathbb{E}_0 \left[\mathcal{L}_c \left(\delta_{\hat{Q}, w} \right) \right] - \inf_{w \in \mathbb{R}^r} \mathbb{E}_0 [\mathcal{L}_c(\delta_{Q^*, w})] \lesssim E(\hat{Q}).$$

We first note that the condition on $E(\hat{Q})$ in (4.2) is satisfied by Theorem 3.2. Meanwhile, the Gaussian variable assumption is made for simplicity and is commonly used when evaluating the excess risk (Ji et al., 2023; Xu and Hsu, 2019). Besides, this assumption

can be relaxed. Then Theorem 4.1 shows that the excess classification error is controlled by the estimation error of the learned edge embedding. For the downstream subject classification task, the classification error when using our edge embedding estimator would not be worse than the oracle case when using the true edge embedding by more than $(s/s^*)\sqrt{(s^*r \log d)/n}$.

4.2 Edge selection task

For the task of edge selection, we adopt a simple yet effective strategy; i.e., we deem the edges with larger ℓ_2 -norms of their embeddings more important. Correspondingly, after we obtain the estimated edge embedding matrix \hat{Q} following Algorithm 1, we compute the norm $\|\hat{q}_e\|_2$ for each edge e , and select the top s edges with the largest norm values.

We evaluate the selection performance based on the estimated support, $\hat{\mathcal{C}} = \{e : \|\hat{q}_e\|_2 \text{ ranks among the } s^* \text{ largest values in } \{\|\hat{q}_j\|_2\}_{j=1}^d\}$, and compare it to the true support, $\mathcal{C} = \{e : \|q_e\|_2 \text{ ranks among the } s^* \text{ largest values in } \{\|q_j\|_2\}_{j=1}^d\}$. We next establish the theoretical guarantee of the support recovery.

Theorem 4.2. *Suppose the assumptions of Theorem 3.2 hold. Suppose*

$$\|q_e\|_2 \gtrsim \frac{s}{s^*} \sqrt{\frac{s^*r \log d}{n}}, \quad \text{if } \|q_e\|_2 \neq 0.$$

Then, with probability at least $1 - ce^{-cs \log d}$, we have $\hat{\mathcal{C}} = \mathcal{C}$.

We first note that the signal gap condition is quite weak. When the first r eigenvalues of Λ^* are at a constant level, we have $\|q_e\| \approx r/d$, which is much larger than $(s/s^*)\sqrt{(s^*r \log d)/n}$. Then Theorem 4.2 shows that, by leveraging the estimation error bound in Theorem 3.2, all important edges can be reliably identified by ranking the norms of the estimated edge embeddings.

4.3 Node community detection task

For the task of community detection, we consider a stochastic block model setting (Holland et al., 1983; Lei and Rinaldo, 2015). Recall that, under our model (2.1), the norm of the edge embedding represents the connectivity strength between two nodes. For community detection, we introduce an additional structure to (2.1), by assuming that, if two edges that connect the node pairs from the same pair of communities, then the norms of their embeddings would be the same. This in turn induces a stochastic block model in the embedding space, and enables community detection based on the edge embedding matrix \hat{Q} . More specifically, suppose the node set \mathcal{V} with $v = |\mathcal{V}|$ nodes is partitioned into G disjoint communities $\mathcal{C}_1, \dots, \mathcal{C}_G$, where each node belongs to exactly one community. We consider the following model,

$$x_i = Q^* z_i + \xi_i, \quad \|q_e\|^2 = S_{u_e u'_e}, \quad S = \Theta B \Theta^\top \in \mathbb{R}^{v \times v}, \quad (4.3)$$

where e denotes an edge connecting the nodes u_e and u'_e , $\Theta \in \mathbb{R}^{v \times G}$ is the membership matrix that encodes the community to which the each node belongs, with each row containing exactly one element of one and all remaining elements zero, $B \in \mathbb{R}^{G \times G}$ is the inter-community connection strength matrix, with its (g, g') th entry $b_{gg'}$ representing the connection strength between community \mathcal{C}_g and $\mathcal{C}_{g'}$, and $\text{rank}(B) = G$, and $S = \Theta B \Theta^\top \in \mathbb{R}^{v \times v}$ is the corresponding similarity matrix, which captures the overall connection strengths between all pairs of nodes. Our goal is to recover the community membership matrix Θ .

Given the observed network data $\{x_i\}_{i=1}^n$, we first obtain the estimated edge embedding matrix \widehat{Q} following Algorithm 1. We then estimate the similarity matrix \widehat{S} , by setting $\widehat{S}_{u_e u'_e} = \widehat{S}_{u'_e u_e} = \|\widehat{q}_e\|_2$, and setting the diagonal entries to zero. We then conduct spectral clustering for community detection, by applying the $(1 + \epsilon)$ -approximate k -means clustering (Kumar et al., 2004; Lei and Rinaldo, 2015) to the normalized and Laplacian transformed similarity matrix \widehat{S} . We denote the final estimated community membership matrix as $\widehat{\Theta}$. We give more details of this community detection procedure based on edge embedding in Appendix C.3.

We evaluate the community detection accuracy using two criteria. The first is the overall relative error that measures the overall percentage of mis-clustered nodes,

$$\mathcal{L}(\widehat{\Theta}, \Theta) = v^{-1} \min_J \|\widehat{\Theta}J - \Theta\|_0,$$

over all $G \times G$ permutation matrices J . The second is the worst-case community-wise misclassification error,

$$\widetilde{\mathcal{L}}(\widehat{\Theta}, \Theta) = \min_J \max_g v_g^{-1} \|(\widehat{\Theta}J)_{G_g} - \Theta_{G_g}\|_0,$$

over all $G \times G$ permutation matrices J and over $g \in [G]$, $G_g = G_g(\Theta) = \{1 \leq i \leq v : \Theta_{ig} = 1\}$, $v_g = |G_g| = \sum_{i=1}^v \Theta_{ig}$ is the size of community g , $g \in [G]$. Note that $0 \leq \mathcal{L}(\widehat{\Theta}, \Theta) \leq \widetilde{\mathcal{L}}(\widehat{\Theta}, \Theta) \leq 2$. As such, $\widetilde{\mathcal{L}}$ is a stronger criterion than \mathcal{L} , in the sense that $\widetilde{\mathcal{L}}$ requires the estimator to perform well among all communities, while \mathcal{L} allows some small communities to have large relative errors. We next establish the theoretical bound for these two criteria.

Theorem 4.3. *Let $\rho_G = \max_{g \in [G]} B_{gg}$, $\tau_v = \min_{j \in [v]} D_{jj}/v$, where D is the diagonal degree matrix with $D_{vv} = \sum_{v'} S_{v,v'}$, and λ_G be the smallest absolute nonzero eigenvalue of the normalized Laplacian matrix $L = D^{-\frac{1}{2}}SD^{-\frac{1}{2}}$. Suppose $128(2 + \epsilon)\rho_G^2 G^2 / (\tau_v^2 v^2 \lambda_G^2) \leq 1$. In addition, for the edge embedding estimation error, suppose*

$$E(\widehat{Q}) = o(\tau_v \sqrt{v} \wedge \rho_G), \quad (4.4)$$

Then, the community detection errors are bounded as:

$$\widetilde{\mathcal{L}}(\widehat{\Theta}, \Theta) \leq 128(2 + \epsilon) \frac{\rho_G^2 G^2}{\tau_v^2 v^2 \lambda_G^2}, \quad \mathcal{L}(\widehat{\Theta}, \Theta) \leq 128(2 + \epsilon) \frac{\rho_G^2 G^2 v'_{\max}}{\tau_v^2 v^3 \lambda_G^2},$$

where v'_{\max} is the second largest community size.

We first note that the condition on $E(\widehat{Q})$ in (4.4) is satisfied by Theorem 3.2. Moreover, when the community sizes are balanced, i.e., $v_{\max}/v_{\min} = O(1)$, where $v_{\min} = \min_{1 \leq g \leq G} v_g$ and $v_{\max} = \max_{1 \leq g \leq G} v_g$, and $\tau_v = \Omega(\log v/v)$, we have that $128(2 + \epsilon)\rho_G^2 G^2 / (\tau_v^2 v^2 \lambda_G^2) \leq O(G^2 / \log^2 v)$. Consequently, when the number of communities satisfies that $G = o(\log v)$, we have that the condition $128(2 + \epsilon)\rho_G^2 G^2 / (\tau_v^2 v^2 \lambda_G^2) \leq 1$ holds. Then Theorem 4.3 shows the community detection error remains small, as long as the edge embedding error is small.

5 Comparison with Sparse PCA

Our proposed method is closely related to another popular unsupervised dimension reduction method, i.e., sparse principal components analysis. There have been several methods studying the theoretical properties of sPCA in detail (Cai et al., 2013; Vu and Lei, 2013;

Vu et al., 2013; Gao and Ma, 2023). However, they all focus on the homogeneous noise setting. In contrast, ACERL considers the heterogeneous noise setting. In this section, we study sPCA under heterogeneous noise, by establishing the lower bound for its embedding estimation as well as downstream classification, and comparing with ACERL. To the best of our knowledge, this is the first work to theoretically study sparse PCA under heterogeneous noise.

We begin with a brief review of sPCA, which seeks the latent embedding through the top r eigenvectors $U_x \in \mathbb{R}^{d \times r}$ of the covariance matrix $\Sigma_x = \mathbb{E}[XX^\top] \in \mathbb{R}^{d \times d}$, where $X = (x_1, \dots, x_n) \in \mathbb{R}^{d \times n}$, while imposing additional sparsity that $\|U_x\|_{2,0} \leq s^*$. Actually, sPCA is closely related to our latent model (2.1), under which $\Sigma_x = Q^*Q^{*\top} + \Sigma^* = U^*\Lambda^*U^{*\top} + \Sigma^*$, $U^* \in \mathbb{R}^{d \times r}$, $\Lambda^* \in \mathbb{R}^{r \times r}$. When the noise is homogeneous, i.e., $\sigma_1^* = \dots = \sigma_d^* = \sigma^*$, $\Sigma_x = U^*(\Lambda^* + \sigma^*I_d)U^{*\top}$. Therefore, sPCA recover the target U^* through the top eigenvectors \widehat{U}_x of the sample covariance matrix $\widehat{\Sigma}_x$.

Next, we study the estimation performance of sPCA under the heterogeneous noise setting. We establish the lower bound for the sPCA estimator, and demonstrate that heteroskedastic noise leads to a fundamental deterioration in its statistical performance. We first note that the existing sPCA methods (Cai et al., 2013; Vu and Lei, 2013; Vu et al., 2013; Gao and Ma, 2023) all satisfy the following assumption.

Assumption 5.1. Suppose $\|\widehat{U}_x\widehat{U}_x^\top - U_xU_x^\top\|_F \leq c_5$, with probability at least $1 - ce^{-cs \log d}$, for some constants $c_5 > 0$.

Theorem 5.1. Suppose Assumptions 3.3 and 5.1 hold. Then,

$$\sup_{(Q^*, \Sigma^*) \in \mathcal{M}_s} \mathbb{P}\left(\|\widehat{U}_x\widehat{U}_x^\top - U^*U^{*\top}\|_F \gtrsim \sqrt{r}\right) \geq 1 - ce^{-cs \log d},$$

over the parameter space \mathcal{M}_s of (Q^*, Σ^*) , such that $\|Q^*\|_{2,0} \leq s^*$ and Q^* satisfies Assumptions 3.2, 3.3, and Σ^* satisfies Assumption 3.1.

Theorem 5.1 shows that, under heterogeneous noise, the worst-case scenario of sPCA incurs an estimation error of at least $O(\sqrt{r})$. In contrast, as shown in Theorem 3.2, our estimator achieves an error rate of $(s/s^*)\sqrt{(s^*r \log d)/n}$ that is much smaller. Moreover, under heterogeneous noise, the top r eigenvalues of the sample covariance matrix are distorted due to the heterogeneous structure of the noise. As a result, sPCA is likely to fail in recovering the true signal subspace.

Next, we investigate the impact of sPCA on the downstream task of subject classification. Given the sPCA estimator \widehat{U}_x and a new data x_0 , its low-dimensional embedding is computed as $\widehat{z}_0 = \widehat{\Lambda}_r^{-\frac{1}{2}}\widehat{U}_x^\top x_0$, where $\widehat{\Lambda}_r = \text{diag}(\widehat{\sigma}_1, \dots, \widehat{\sigma}_r)$. Following Section 4.1, the corresponding classifier is $\delta'_{\widehat{U}_x, \widehat{w}}(x_0) = \mathbb{1}\left\{F(\widehat{w}^\top \widehat{\Lambda}_r^{-\frac{1}{2}}\widehat{U}_x^\top x_0) \geq 1/2\right\}$. Similar to Theorem 4.1, we take the infimum over $w \in \mathbb{R}^r$ to select the best classifier within the family $\{\delta_{\widehat{Q}, w} \mid w \in \mathbb{R}^r\}$ in our evaluation.

Theorem 5.2. Suppose $\sigma_{(1)}^{*2} \asymp 1$ and $\kappa_\Sigma = \sigma_{(1)}^{*2}/\sigma_{(d)}^{*2} \asymp 1$. Suppose z_0 and ξ_0 are Gaussian random variables. In addition, suppose

$$E_{U^*}^2(\widehat{U}_x) \geq r - \frac{\sigma_{(1)}^2}{\kappa_\Sigma(1 + \sigma_{(1)}^2)} + \frac{c_6}{\kappa_\Sigma}, \quad (5.1)$$

for some constant $c_6 > 0$, where $E_{U^*}^2(\widehat{U}_x) = \|\widehat{U}_x \widehat{U}_x^\top - U^* U^{*\top}\|_F$. Then, the excess risk for classification is bounded as

$$\inf_{w \in \mathbb{R}^r} \mathbb{E}_0 \left[\mathcal{L}_c \left(\delta'_{\widehat{U}_x, w} \right) \right] - \inf_{w \in \mathbb{R}^r} \mathbb{E}_0 [\mathcal{L}_c(\delta_{Q^*, w})] \geq c_P,$$

where c_P is a positive constant that depends only on c_6 , $\sigma_{(1)}^{*2}$, and κ_Σ .

We first note that the condition in on $E_{U^*}^2(\widehat{U}_x)$ in (5.1) is satisfied by applying Theorem 5.1. Then this theorem shows that the classification based on sPCA suffers a poor performance due to heterogeneous errors. In contrast, as shown in Theorem 4.1, our method leads to a much better classification performance, demonstrating its advantage in the presence of heterogeneous errors.

6 Simulation Studies

We conduct intensive simulations to investigate the empirical performance of our ACERL method through the three downstream tasks. We also compare ACERL with sPCA, following the implementation of Seghouane et al. (2019). We exclude graph neural networks (GNNs) from comparison, as our preliminary study indicates that GNNs perform poorly when node feature information is unavailable.

We simulate the model following (2.1),

$$x_{i,e} = 1.25 c_e q_e^\top z_i + \sigma_\xi \xi_{i,e},$$

where for every $i \in [n]$ and $e \in [d]$, we draw the entry of z_i and q_e independently from a standard normal distribution, and the noise $\xi_{i,e}$ independently from a normal distribution with mean zero and standard deviation e/d . We set the number of nodes $v = \{45, 55, 64\}$, such that the number of edges $d = \{990, 1485, 2016\}$ and the number of edges are close to $\{1000, 1500, 2000\}$, respectively. We set the dimension of the latent space $r = \{10, 20\}$. We use the binary vector $c = (c_1, \dots, c_d)$ to represent important edges, set the true sparsity level $s^* = 50$, and randomly set s^* entries of c as 1 and the rest as 0. We use the constant σ_ξ to control the magnitude of the noise level, and set $\sigma_\xi = \{0, 2, 4, 6\}$ to represent no, small, medium and large noise, respectively. In addition, for the subject classification task, we assign each subject is to a binary class based on whether the first entry or the second entry in the subject embedding is larger. We set the sample size $n = \{250, 500, 750\}$, and use the first 60% data for training and the remaining 40% for testing. We train ACERL or sPCA based on the training data, and report the performance of each task based on the testing data. We replicate all experiments 50 times. For the subject classification task, we employ a support vector machine classifier. For the edge detection task, we choose a working sparsity level $s = 150$. For the community detection task, we consider a smaller non-sparse network, by setting the number of nodes $v = \{15, 18, 21\}$, such that the number of edges $d = \{105, 153, 210\}$, and setting all edges important. We generate $x_{i,e} = 5\sqrt{c_{u_e} c_{u'_e}} f(u_e, u'_e) q_e^\top z_i + \sigma_\xi \xi_{i,e}$, where $c_{u_e}, c_{u'_e}$ are uniformly independently drawn from $\text{Uniform}(0.1, 1.1)$, and $f(c_{u_e}, c_{u'_e}) = 10^{-|c_{u_e} - c_{u'_e}|}$.

Table 1 reports the classification accuracy for the subjection classification task. Table 2 reports the selection accuracy for the edge selection task, and Table 3 reports the rand index of node clustering for the community detection task. In all these tables, we see that the performance improves with a larger sample size, a smaller number of edges, or a smaller noise level, which agrees with our theory. Furthermore, ACERL achieves a better performance than sPCA across all tasks and settings.

Table 1: Subject classification task: average classification accuracy (in percentage) and standard error (in parenthesis), across different noise levels.

n	v	d	σ_ξ	$r = 10$				$r = 20$			
				0	2	4	6	0	2	4	6
250	45	990	ACERL	100.0(0.0)	100.0(0.0)	98.8(1.4)	78.1(5.6)	100.0(0.0)	100.0(0.0)	100.0(0.3)	90.9(3.6)
			sPCA	94.8(2.5)	92.2(3.5)	82.2(5.1)	72.0(5.5)	93.7(3.0)	87.2(3.9)	78.4(5.8)	68.5(6.6)
	45	1485	ACERL	100.0(0.0)	100.0(0.0)	97.9(2.0)	72.8(6.7)	100.0(0.0)	100.0(0.0)	99.9(0.4)	90.2(3.0)
			sPCA	96.0(2.2)	91.3(3.2)	78.7(5.7)	67.9(5.4)	92.8(2.8)	87.2(3.6)	74.8(5.8)	67.7(5.2)
	45	2016	ACERL	100.0(0.0)	100.0(0.0)	98.1(1.4)	67.4(7.3)	100.0(0.0)	100.0(0.0)	99.8(0.6)	87.9(4.1)
			sPCA	96.1(1.8)	90.5(3.1)	77.3(5.5)	66.1(7.0)	92.5(2.9)	87.0(4.5)	73.7(5.3)	66.1(5.8)
500	45	990	ACERL	100.0(0.0)	100.0(0.0)	100.0(0.0)	93.6(3.0)	100.0(0.0)	100.0(0.0)	100.0(0.0)	96.9(2.2)
			sPCA	97.3(1.4)	93.6(1.9)	86.2(3.4)	75.0(4.8)	96.3(1.5)	91.2(2.4)	81.1(3.7)	72.1(4.6)
	45	1485	ACERL	100.0(0.0)	100.0(0.0)	99.9(0.4)	90.9(3.6)	100.0(0.0)	100.0(0.0)	100.0(0.0)	97.8(1.5)
			sPCA	97.3(1.2)	93.5(1.8)	84.0(4.0)	71.3(5.2)	96.4(1.8)	90.6(3.1)	79.1(4.1)	70.9(5.1)
	45	2016	ACERL	100.0(0.0)	100.0(0.0)	99.8(0.8)	89.6(3.9)	100.0(0.0)	100.0(0.0)	100.0(0.0)	97.4(2.1)
			sPCA	97.2(1.4)	93.3(2.3)	83.2(3.7)	70.4(5.4)	96.1(1.5)	90.1(2.4)	80.0(4.6)	70.6(4.8)
750	45	990	ACERL	100.0(0.0)	100.0(0.0)	100.0(0.0)	96.6(2.1)	100.0(0.0)	100.0(0.0)	100.0(0.0)	99.3(0.9)
			sPCA	97.8(1.0)	94.7(1.5)	86.5(3.4)	77.3(4.8)	97.2(1.0)	92.4(2.1)	83.0(4.2)	73.7(3.8)
	45	1485	ACERL	100.0(0.0)	100.0(0.0)	100.0(0.0)	96.5(2.0)	100.0(0.0)	100.0(0.0)	100.0(0.0)	99.5(1.0)
			sPCA	98.0(0.9)	93.8(1.7)	85.2(3.9)	75.4(4.8)	96.8(1.2)	91.8(1.9)	81.6(4.9)	72.8(4.5)
	45	2016	ACERL	100.0(0.0)	100.0(0.0)	100.0(0.0)	94.9(2.7)	100.0(0.0)	100.0(0.0)	100.0(0.0)	99.2(1.3)
			sPCA	97.6(0.9)	93.8(1.5)	84.5(3.8)	72.1(5.3)	96.9(0.9)	91.4(1.9)	80.5(4.1)	73.0(5.0)

Table 2: Edge selection task: the average selection accuracy (in percentage) and the standard error (in parenthesis) of important edges under the working sparsity level $s = 150$ when the true sparsity level $s^* = 50$.

n	v	d	σ_ξ	$r = 10$				$r = 20$			
				0	2	4	6	0	2	4	6
250	45	990	ACERL	100.0(0.0)	100.0(0.0)	98.8(1.4)	78.1(5.6)	100.0(0.0)	100.0(0.0)	100.0(0.3)	90.9(3.6)
			sPCA	100.0(0.0)	100.0(0.0)	98.0(2.0)	69.2(6.5)	100.0(0.0)	100.0(0.0)	99.8(0.6)	85.4(4.8)
	45	1485	ACERL	100.0(0.0)	100.0(0.0)	97.9(2.0)	72.8(6.7)	100.0(0.0)	100.0(0.0)	99.9(0.4)	90.2(3.0)
			sPCA	100.0(0.0)	100.0(0.0)	96.8(2.8)	64.6(6.3)	100.0(0.0)	100.0(0.0)	99.8(0.6)	84.6(4.3)
	45	2016	ACERL	100.0(0.0)	100.0(0.0)	98.1(1.4)	67.4(7.3)	100.0(0.0)	100.0(0.0)	99.8(0.6)	87.9(4.1)
			sPCA	100.0(0.0)	100.0(0.0)	96.5(2.2)	59.0(7.3)	100.0(0.0)	100.0(0.0)	99.5(0.9)	81.8(4.5)
500	45	990	ACERL	100.0(0.0)	100.0(0.0)	100.0(0.0)	93.6(3.0)	100.0(0.0)	100.0(0.0)	100.0(0.0)	96.9(2.2)
			sPCA	100.0(0.0)	100.0(0.0)	99.7(0.7)	87.1(5.2)	100.0(0.0)	100.0(0.0)	100.0(0.0)	94.4(2.9)
	45	1485	ACERL	100.0(0.0)	100.0(0.0)	99.9(0.4)	90.9(3.6)	100.0(0.0)	100.0(0.0)	100.0(0.0)	97.8(1.5)
			sPCA	100.0(0.0)	100.0(0.0)	99.7(0.7)	83.5(4.9)	100.0(0.0)	100.0(0.0)	100.0(0.0)	94.6(2.3)
	45	2016	ACERL	100.0(0.0)	100.0(0.0)	99.8(0.8)	89.6(3.9)	100.0(0.0)	100.0(0.0)	100.0(0.0)	97.4(2.1)
			sPCA	100.0(0.0)	100.0(0.0)	99.5(1.0)	81.0(5.9)	100.0(0.0)	100.0(0.0)	100.0(0.0)	94.0(2.9)
750	45	990	ACERL	100.0(0.0)	100.0(0.0)	100.0(0.0)	96.6(2.1)	100.0(0.0)	100.0(0.0)	100.0(0.0)	99.3(0.9)
			sPCA	100.0(0.0)	100.0(0.0)	100.0(0.3)	92.4(3.7)	100.0(0.0)	100.0(0.0)	100.0(0.0)	97.3(1.8)
	45	1485	ACERL	100.0(0.0)	100.0(0.0)	100.0(0.0)	96.5(2.0)	100.0(0.0)	100.0(0.0)	100.0(0.0)	99.5(1.0)
			sPCA	100.0(0.0)	100.0(0.0)	100.0(0.3)	91.6(3.2)	100.0(0.0)	100.0(0.0)	100.0(0.0)	97.5(2.4)
	45	2016	ACERL	100.0(0.0)	100.0(0.0)	100.0(0.0)	94.9(2.7)	100.0(0.0)	100.0(0.0)	100.0(0.0)	99.2(1.3)
			sPCA	100.0(0.0)	100.0(0.0)	99.9(0.4)	89.4(4.2)	100.0(0.0)	100.0(0.0)	100.0(0.0)	97.4(1.8)

In the simulations so far, we fix the latent space dimension r at the true values, and fix the sparsity level s at a predefined value. Next, we discuss how to choose r and s given the data. For r , we recommend to adopt a similar approach as PCA and use the explained variance percentage. Figure 1 shows the percentage of explained variance when $n = 250$, $d = 990$, and $r = 10$ under different noise levels, with the red line corresponding to the component at the true value of $r = 10$. We observe a relatively clear gap around the true value of r . For s , we recommend to examine the empirical distribution of $\|\hat{Q}_e\|$ to help determine the threshold value. Figure 2 shows the violin plot when $n = 500$, $d = 990$, and $r = 10$ under different noise levels, with the horizontal line corresponding to the true

Table 3: Community detection task: the average rand index of node clustering (in percentage) and the standard error (in parenthesis).

n	v	d	σ_ξ	$r = 10$				$r = 20$			
				0	2	4	6	0	2	4	6
250	15	105	ACERL	82.7(14)	82.3(14)	64.2(22)	57.1(8.5)	82.3(14)	76.0(14)	45.7(8.1)	52.0(10)
			sPCA	55.4(11)	46.1(9.0)	40.4(10)	41.9(5.1)	44.8(4.7)	42.1(9.7)	40.4(6.3)	41.3(8.6)
	18	153	ACERL	88.4(14)	82.6(14)	83.1(14)	91.4(14)	82.4(14)	85.0(19)	73.5(16)	51.4(11)
			sPCA	50.1(7.4)	45.8(9.6)	39.9(7.8)	44.2(12)	42.4(6.7)	34.0(0.0)	46.0(10)	40.0(9.5)
	21	210	ACERL	88.4(9.8)	96.9(6.3)	93.0(11)	88.8(14)	88.7(23)	91.1(18)	71.7(20)	52.4(12)
			sPCA	45.0(6.7)	42.1(10)	44.6(12)	42.3(8.8)	51.4(6.8)	39.2(6.8)	37.4(7.5)	38.4(7.2)
500	15	105	ACERL	82.3(14)	88.2(14)	63.6(8.4)	64.0(13)	82.3(14)	77.1(12)	62.5(18)	60.6(8.4)
			sPCA	54.3(8.1)	47.0(5.5)	44.6(10)	46.5(7.3)	49.0(4.4)	48.2(7.4)	51.2(1.1)	56.0(3.5)
	18	153	ACERL	94.6(11)	94.2(12)	88.9(14)	92.5(15)	90.6(12)	88.4(14)	70.2(18)	63.5(21)
			sPCA	46.9(11)	53.6(1.4)	44.2(8.4)	49.5(7.9)	46.8(8.3)	43.9(8.1)	52.3(9.7)	50.2(4.0)
	21	210	ACERL	89.5(13)	100(0.0)	76.7(22)	81.8(15)	100(0.0)	96.9(6.3)	88.6(14)	71.3(20)
			sPCA	45.1(6.6)	47.4(9.8)	48.2(8.2)	46.5(12)	54.3(1.7)	56.2(3.7)	47.1(9.4)	43.1(8.3)
750	15	105	ACERL	82.7(14)	78.5(19)	62.9(20)	63.4(13)	83.0(14)	70.9(0.8)	79.8(17)	66.1(16)
			sPCA	51.0(1.7)	51.2(1.3)	45.9(11)	46.9(12)	49.0(4.4)	55.4(2.6)	53.3(3.5)	55.0(14)
	18	153	ACERL	88.8(14)	82.7(14)	82.9(14)	87.3(13)	89.5(13)	88.8(14)	68.4(15)	79.7(19)
			sPCA	51.8(7.2)	47.6(6.8)	56.2(4.0)	52.5(2.3)	51.5(3.0)	56.7(6.6)	42.6(8.7)	51.6(2.9)
	21	210	ACERL	84.1(13)	100(0.0)	90.7(11)	89.5(13)	94.4(11)	95.3(9.3)	89.1(13)	73.7(14)
			sPCA	48.4(7.5)	51.5(4.3)	50.7(6.5)	46.0(10)	54.3(1.7)	48.5(6.6)	43.3(10)	42.5(9.0)

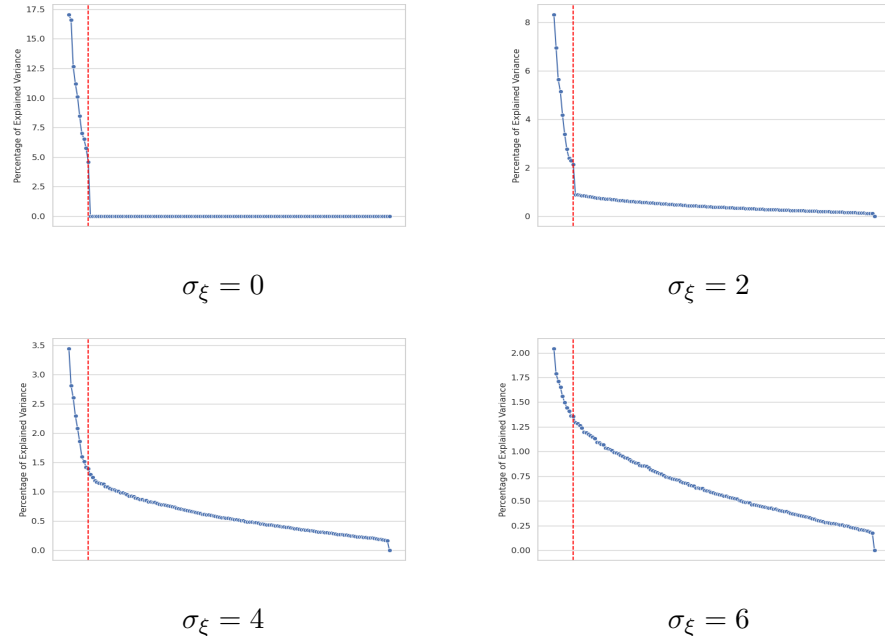


Figure 1: Percentage of explained variance for each component or $n = 250$, $d = 990$, and $r = 10$ under different noise levels. The red line corresponds to the component at the true value of $r = 10$.

sparsity level.

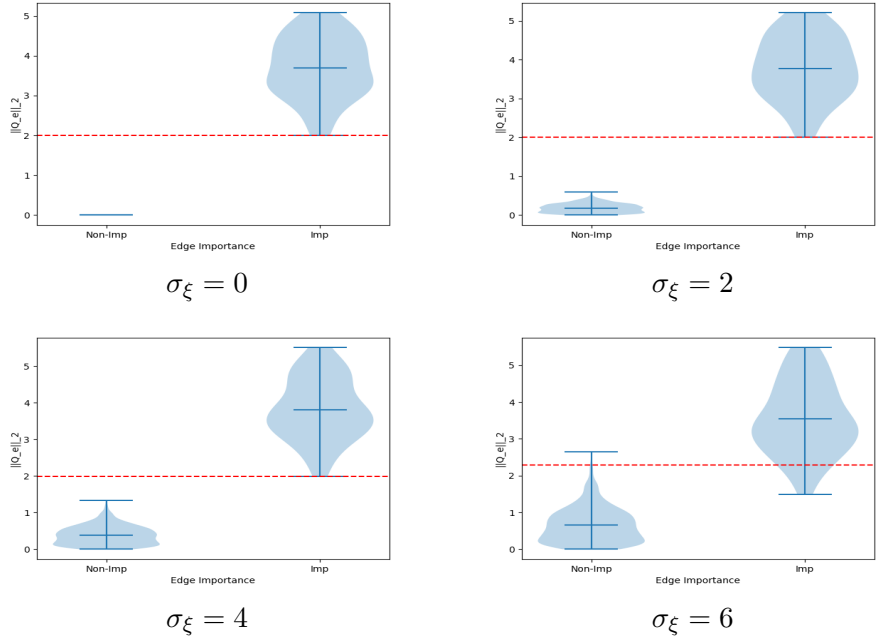


Figure 2: Violin plot for the ℓ_2 norms of the edge embeddings for ACERL . The red line corresponds to the true sparsity level.

7 Brain Connectivity Analysis

Brain connectivity analysis examines the structural and functional relationships between different regions of the brain, providing insight into how neural circuits are organized and interact. It plays a crucial role in neuroscience by helping researchers understand the mechanisms underlying normal brain development, cognitive functions, and aging. Moreover, alterations in connectivity patterns are often associated with neurological and psychiatric disorders such as Alzheimer’s disease, autism, and schizophrenia. Connectivity analysis models the brain as a network, where regions are represented as nodes and their interactions as edges, and network representation learning helps to uncover hidden brain patterns, identify potential biomarkers, and predict disease states (Fornito et al., 2013). Next, we illustrate our ACERL method with two brain connectivity analysis examples.

7.1 Autism Brain Imaging Data Exchange

The first example is the Autism Brain Imaging Data Exchange (ABIDE), which studies autism spectrum disorder, a prevalent neurodevelopmental disorder with symptoms including social difficulties, communication deficits, stereotyped behaviors and cognitive delays (Di Martino et al., 2014). The dataset, after preprocessing, consists of 786 subjects, among whom 430 are diagnosed with autism, and 356 are healthy controls. Each subject received a resting-state functional magnetic resonance imaging (fMRI) scan, which is summarized as a 116×116 functional connectivity network, with nodes corresponding to 116 brain regions-of-interest (ROIs) based on the standard Automated Anatomical Labelling brain atlas, and edges measuring the mutual information of the fMRI signals between all pairs of ROIs.

We applied ACERL and sPCA to this data, and carried out two downstream tasks: classifying the subjects into the two classes, and identifying potentially important brain

Table 4: Trait classification accuracy (misclassification error rate) for the ABIDE study, and trait prediction accuracy (mean squared error) for the HCP study.

	(a) ABIDE	(b) HCP			
		Trait (i)	Trait (ii)	Trait (iii)	Trait (iv)
ACERL	39.9 (0.9)	0.0201(0.0009)	0.0207(0.0009)	0.1149(0.0133)	0.2102(0.0065)
sPCA	41.5 (1.8)	0.0211(0.0015)	0.0223(0.0011)	0.1211(0.0092)	0.2187(0.0039)

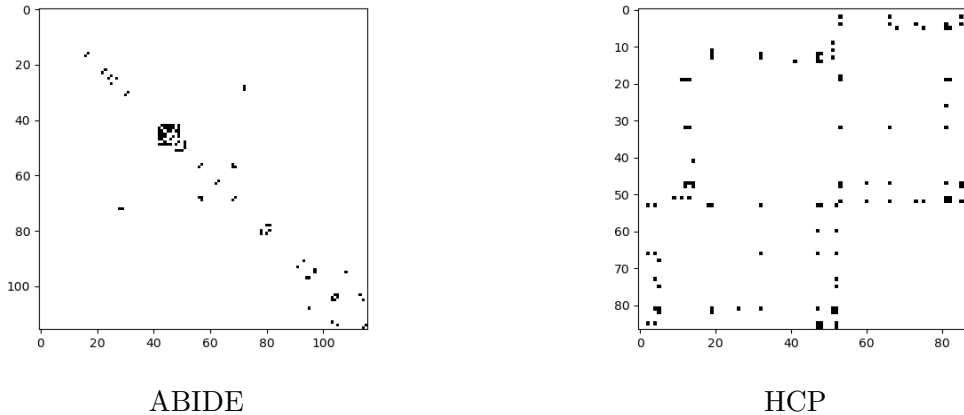


Figure 3: Sparse graph for ABIDE and HCP data at the sparsity level $s = 100$.

regions. We transformed the mutual information measure by its square. We randomly split the data, using 60% for training and the remaining 40% for testing. We repeated the split 50 times, and report the results based on 50 replications. We employed a support vector machine classifier. We chose $r = 10$ as the dimension of the latent space, by the percentage of explained variance.

Table 4(a) reports the misclassification error rate on the testing data, where we see that ACERL outperforms sPCA. Figure 3(a) reports the sparse edge adjacency matrix when setting the sparsity level at $s = 100$. There are four nodes with noticeably larger degrees, corresponding to four brain regions: right superior occipital gyrus, left calcarine sulcus, right calcarine sulcus, and left cuneus. These regions align well with the ASD literature. Notably, they are all part of the occipital lobe, which is primarily responsible for interpreting and processing visual information. Visual perception difference is a well-documented feature of ASD, often reflected in how individuals perceive faces, objects, and motion. The calcarine sulcus and cuneus play key roles in these visual functions and are closely linked to the altered visual processing commonly observed in ASD, such as heightened sensitivity to visual details alongside difficulties with integrating global visual information (Edgar et al., 2015; Eilam-Stock et al., 2016; Zoltowski et al., 2021).

7.2 Human Connectome Project

The second example is the Human Connectome Project (HCP), which aims to map the structural and functional connectivity networks of human brain and to understand their associations with behavioral traits (Essen et al., 2013). The dataset we analyzed consists of 924 subjects. Each subject received a diffusion tensor imaging (DTI) scan, which is summarized as a 97×97 structural connectivity network, with nodes corresponding to 68 cortical surface ROIs and 19 subcortical ROIs following the Desikan-Killiany brain atlas,

and edges measuring the numbers of fibers connecting all pairs of ROIs (Liu et al., 2021). In addition, for each subject, four trait scores were recorded, including (i) the picture vocabulary test score, (ii) the oral reading recognition test score, (iii) the crystallized composite score, and (iv) the cognition total composite score.

We applied ACERL and sPCA to this data, and carried out two downstream tasks: predicting the subject’s trait scores, and identifying potentially important brain regions. We transformed the number of connecting fibers by $(1 + a)^{-1}$ and the trait score by $\log(a + 1)$. We randomly split the data, using 60% for training and the remaining 40% for testing. We repeated the split 50 times, and report the results based on 50 replications. We employed a support vector regression for subject trait prediction. We chose $r = 19$ as the dimension of the latent space, by the percentage of explained variance.

Table 4(b) reports the mean squared error (MSE) on the testing data, where we see that ACERL again outperforms sPCA, especially for the first two traits. We did not compare with the method of Liu et al. (2021) because they used additional information other than structural connectivity, and used different training-test sample split. Figure 3(b) reports the sparse edge adjacency matrix when setting the sparsity level at $s = 100$. There are four nodes with noticeably larger degrees, corresponding to four brain regions: left superior temporal cortex, left insula, right banks of superior temporal sulcus, and right superior temporal cortex. These regions are closely related to reading, speech, comprehension, and cognition. For instance, superior temporal cortex is heavily involved in auditory processing and speech perception, and superior temporal sulcus is important for voice encoding (Rupp et al., 2022). Meanwhile, the insula plays a key role in emotion regulation and cognitive control (Craig, 2009).

References

Bielak, P., Kajdanowicz, T., and Chawla, N. V. (2022). Attre2vec: Unsupervised attributed edge representation learning. *Information Sciences*, 592:1–15.

Cai, H., Zheng, V. W., and Chang, K. C.-C. (2018). A Comprehensive Survey of Graph Embedding: Problems, Techniques, and Applications . *IEEE Transactions on Knowledge & Data Engineering*, 30(09):1616–1637.

Cai, T. T., Han, R., and Zhang, A. R. (2022). On the non-asymptotic concentration of heteroskedastic wishart-type matrix.

Cai, T. T., Ma, Z., and Wu, Y. (2013). Sparse pca: Optimal rates and adaptive estimation. *Annals of Statistics*, 41(6):3074–3110.

Candès, E. J. and Recht, B. (2009). Exact matrix completion via convex optimization. *Foundations of Computational Mathematics*, 9(6):717–772.

Chen, T., Kornblith, S., Norouzi, M., and Hinton, G. (2020). A simple framework for contrastive learning of visual representations. In *International conference on machine learning*, pages 1597–1607. PMLR.

Craig, A. D. (2009). How do you feel—now? the anterior insula and human awareness. *Nature reviews neuroscience*, 10(1):59–70.

Cui, P., Wang, X., Pei, J., and Zhu, W. (2018). A survey on network embedding. *IEEE transactions on knowledge and data engineering*, 31(5):833–852.

Di Martino, A., Yan, C.-G., Li, Q., Denio, E., Castellanos, F. X., Alaerts, K., and et al (2014). The autism brain imaging data exchange: Towards a large-scale evaluation of the intrinsic brain architecture in autism. *Molecular Psychiatry*, 19:659–667.

Eckart, C. and Young, G. (1936). The approximation of one matrix by another of lower rank. *Psychometrika*, 1(3):211–218.

Edgar, J. C., Heiken, K., Chen, Y.-H., Herrington, J. D., Chow, V., Liu, S., Bloy, L., Huang, M., Pandey, J., Cannon, K. M., et al. (2015). Resting-state alpha in autism spectrum disorder and alpha associations with thalamic volume. *Journal of autism and developmental disorders*, 45:795–804.

Eilam-Stock, T., Wu, T., Spagna, A., Egan, L. J., and Fan, J. (2016). Neuroanatomical alterations in high-functioning adults with autism spectrum disorder. *Frontiers in neuroscience*, 10:237.

Essen, D. C. V., Smith, S. M., Barch, D. M., Behrens, T. E., Yacoub, E., and Ugurbil, K. (2013). The wu-minn human connectome project: An overview. *NeuroImage*, 80:62 – 79. Mapping the Connectome.

Fornito, A., Zalesky, A., and Breakspear, M. (2013). Graph analysis of the human connectome: Promise, progress, and pitfalls. *NeuroImage*, 80:426–444.

Gao, S. and Ma, Z. (2023). Sparse gca and thresholded gradient descent.

Goyal, P., HosseiniMardi, H., Ferrara, E., and Galstyan, A. (2018). Embedding networks with edge attributes. In *Proceedings of the 29th on Hypertext and Social Media*, HT ’18, page 38–42, New York, NY, USA. Association for Computing Machinery.

Grover, A. and Leskovec, J. (2016). node2vec: Scalable feature learning for networks. In *Proceedings of the 22nd ACM SIGKDD international conference on Knowledge discovery and data mining*, pages 855–864.

Gui, Y., Ma, C., and Ma, Z. (2025). Multi-modal contrastive learning adapts to intrinsic dimensions of shared latent variables. *arXiv preprint arXiv:2505.12473*.

Gui, Y., Ma, C., and Zhong, Y. (2023). Unraveling projection heads in contrastive learning: Insights from expansion and shrinkage. *arXiv preprint arXiv:2306.03335*.

Hadsell, R., Chopra, S., and LeCun, Y. (2006). Dimensionality reduction by learning an invariant mapping. In *2006 IEEE Computer Society Conference on Computer Vision and Pattern Recognition (CVPR’06)*, volume 2, pages 1735–1742.

Hamilton, W., Ying, Z., and Leskovec, J. (2017). Inductive representation learning on large graphs. *Advances in neural information processing systems*, 30.

He, X., Zhou, Y., Zhou, Z., Bai, S., and Bai, X. (2018). Triplet-center loss for multi-view 3d object retrieval. In *Proceedings of the IEEE Conference on Computer Vision and Pattern Recognition (CVPR)*.

Holland, P. W., Laskey, K. B., and Leinhardt, S. (1983). Stochastic blockmodels: First steps. *Social networks*, 5(2):109–137.

Ji, W., Deng, Z., Nakada, R., Zou, J., and Zhang, L. (2023). The power of contrast for feature learning: A theoretical analysis. *Journal of Machine Learning Research*, 24(330):1–78.

Jin, C., Netrapalli, P., Ge, R., Kakade, S. M., and Jordan, M. I. (2019). A short note on concentration inequalities for random vectors with subgaussian norm.

Jo, J., Baek, J., Lee, S., Kim, D., Kang, M., and Hwang, S. J. (2021a). Edge representation learning with hypergraphs. In Beygelzimer, A., Dauphin, Y., Liang, P., and Vaughan, J. W., editors, *Advances in Neural Information Processing Systems*.

Jo, J., Baek, J., Lee, S., Kim, D., Kang, M., and Hwang, S. J. (2021b). Edge representation learning with hypergraphs.

Johnstone, I. M. and Lu, A. Y. (2009). On consistency and sparsity for principal components analysis in high dimensions. *Journal of the American Statistical Association*, 104(486):682–693.

Kipf, T. N. and Welling, M. (2016). Semi-supervised classification with graph convolutional networks. *arXiv preprint arXiv:1609.02907*.

Kumar, A., Sabharwal, Y., and Sen, S. (2004). A simple linear time $(1 + \sqrt{\epsilon})$ -approximation algorithm for k-means clustering in any dimensions. In *45th Annual IEEE Symposium on Foundations of Computer Science*, pages 454–462.

Lei, J. and Rinaldo, A. (2015). Consistency of spectral clustering in stochastic block models. *The Annals of Statistics*, 43(1).

Lin, L. and Mei, S. (2025). A statistical theory of contrastive learning via approximate sufficient statistics. *arXiv preprint arXiv:2503.17538*.

Liu, M., Zhang, Z., and Dunson, D. B. (2021). Graph auto-encoding brain networks with applications to analyzing large-scale brain imaging datasets. *Neuroimage*, 245:118750.

Narayanan, A., Chandramohan, M., Venkatesan, R., Chen, L., Liu, Y., and Jaiswal, S. (2017). graph2vec: Learning distributed representations of graphs. *arXiv preprint arXiv:1707.05005*.

Ou, M., Cui, P., Pei, J., Zhang, Z., and Zhu, W. (2016). Asymmetric transitivity preserving graph embedding. In *Proceedings of the 22nd ACM SIGKDD International Conference on Knowledge Discovery and Data Mining*, KDD ’16, page 1105–1114, New York, NY, USA. Association for Computing Machinery.

Perozzi, B., Al-Rfou, R., and Skiena, S. (2014). Deepwalk: Online learning of social representations. In *Proceedings of the 20th ACM SIGKDD international conference on Knowledge discovery and data mining*, pages 701–710.

Roweis, S. T. and Saul, L. K. (2000). Nonlinear dimensionality reduction by locally linear embedding. *science*, 290(5500):2323–2326.

Rupp, K., Hect, J. L., Remick, M., Ghuman, A., Chandrasekaran, B., Holt, L. L., and Abel, T. J. (2022). Neural responses in human superior temporal cortex support coding of voice representations. *PLoS biology*, 20(7):e3001675.

Seghouane, A.-K., Shokouhi, N., and Koch, I. (2019). Sparse principal component analysis with preserved sparsity pattern. *IEEE Transactions on Image Processing*, 28(7):3274–3285.

Ten Berge, J. M. (1977). Orthogonal procrustes rotation for two or more matrices. *Psychometrika*, 42:267–276.

Tu, S., Boczar, R., Simchowitz, M., Soltanolkotabi, M., and Recht, B. (2016). Low-rank solutions of linear matrix equations via procrustes flow.

Vershynin, R. (2011). Introduction to the non-asymptotic analysis of random matrices.

Vu, V. Q., Cho, J., Lei, J., and Rohe, K. (2013). Fantope projection and selection: A near-optimal convex relaxation of sparse pca. *Advances in neural information processing systems*, 26.

Vu, V. Q. and Lei, J. (2013). Minimax sparse principal subspace estimation in high dimensions. *The Annals of Statistics*, 41(6):2905–2947.

Wainwright, M. J. (2019). *High-dimensional statistics: A non-asymptotic viewpoint*, volume 48. Cambridge university press.

Wang, C., Wang, C., Wang, Z., Ye, X., and Yu, P. S. (2020). Edge2vec: Edge-based social network embedding. *ACM Transactions on Knowledge Discovery from Data (TKDD)*, 14(4):1–24.

Wang, H., Yang, R., and Xiao, X. (2024). Effective edge-wise representation learning in edge-attributed bipartite graphs.

Wang, S. (2023). Self-supervised metric learning in multi-view data: A downstream task perspective. *Journal of the American Statistical Association*, 118(544):2454–2467.

Wang, S. (2025). On linear separation capacity of self-supervised representation learning. *Journal of Machine Learning Research*, to appear.

Wang, Y. X. R., Li, L., and Li, J. J. (2021). Network modeling in biology: Statistical methods for gene and brain networks. *Statistical Science*, 36(1):68–80.

Weyl, H. (1912). Das asymptotische Verteilungsgesetz der Eigenwerte linearer partieller Differentialgleichungen (mit einer Anwendung auf die Theorie der Hohlraumstrahlung). *Mathematische Annalen*, 71:441–479.

Xia, J., Wu, L., Chen, J., Hu, B., and Li, S. Z. (2022). Simgrace: A simple framework for graph contrastive learning without data augmentation. In *Proceedings of the ACM web conference 2022*, pages 1070–1079.

Xu, J. and Hsu, D. (2019). On the number of variables to use in principal component regression.

Xu, Q. and Qu, A. (2025). Representation retrieval learning for heterogeneous data integration. *arXiv preprint arXiv:2503.09494*.

You, Y., Chen, T., Sui, Y., Chen, T., Wang, Z., and Shen, Y. (2020). Graph contrastive learning with augmentations. *Advances in neural information processing systems*, 33:5812–5823.

Yu, Y., Wang, T., and Samworth, R. J. (2014). A useful variant of the Davis–Kahan theorem for statisticians.

Zhang, A. R., Cai, T. T., and Wu, Y. (2022). Heteroskedastic pca: Algorithm, optimality, and applications. *The Annals of Statistics*, 50(1):53–80.

Zhang, D., Yin, J., Zhu, X., and Zhang, C. (2020). Network Representation Learning: A Survey . *IEEE Transactions on Big Data*, 6(01):3–28.

Zhu, Y., Liu, M., Huang, W., and Ji, S. (2021). Graph contrastive learning with adaptive augmentation. In *Proceedings of the Web Conference 2021 (WWW)*, pages 2069–2080. ACM.

Zhu, Y., Xu, Y., Yu, Q., Liu, Z., Wu, C., Wang, J., and Lin, J. (2020). Graph contrastive learning with augmentations. In *Advances in Neural Information Processing Systems (NeurIPS)*.

Zoltowski, A. R., Lyu, I., Failla, M., Mash, L. E., Dunham, K., Feldman, J. I., Woynaroski, T. G., Wallace, M. T., Barquero, L. A., Nguyen, T. Q., et al. (2021). Cortical morphology in autism: findings from a cortical shape-adaptive approach to local gyration indexing. *Cerebral Cortex*, 31(11):5188–5205.

Supplementary Appendix

Abstract

In this Appendix, Section A collects a number of auxiliary lemmas from the literature that facilitate our proofs. Sections B, C, and D provide the proofs for the main theoretical results in Sections 3, 4, and 5, respectively.

A Auxiliary Lemmas

The auxiliary lemmas include the ones related to matrix algebra, concentration inequalities, community detection, and miscellaneous technical lemmas.

A.1 Lemmas related to matrix algebra

Lemma A.1 (The Eckart-Young-Mirsky Theorem in Eckart and Young (1936)). *For the singular value decomposition $A = U\Sigma V^T$, the best rank- k approximation of A with respect to the Frobenius norm is given by $\text{rank}_k(A) = \sum_{i=1}^k \sigma_i u_i v_i^T$. That is, for any matrix B of rank at most k , $\|A - \text{rank}_k(A)\|_F \leq \|A - B\|_F$.*

Lemma A.2 (Theorem 2 in Yu et al. (2014)). *Let $\Sigma, \widehat{\Sigma} \in \mathbb{R}^{p \times p}$ be symmetric matrices, with eigenvalues $\lambda_1 \geq \dots \geq \lambda_p$ and $\widehat{\lambda}_1 \geq \dots \geq \widehat{\lambda}_p$ respectively. Suppose $1 \leq r \leq s \leq p$, and $\min(\lambda_{r-1} - \lambda_r, \lambda_s - \lambda_{s+1}) > 0$, where $\lambda_0 = \infty$ and $\lambda_{p+1} = -\infty$. Let $d = s - r + 1$. Let $V = (v_r, v_{r+1}, \dots, v_s) \in \mathbb{R}^{p \times d}$, and $\widehat{V} = (\widehat{v}_r, \widehat{v}_{r+1}, \dots, \widehat{v}_s) \in \mathbb{R}^{p \times d}$ have orthonormal columns satisfying $\Sigma v_j = \lambda_j v_j$ and $\widehat{\Sigma} \widehat{v}_j = \widehat{\lambda}_j \widehat{v}_j$, $j = r, r+1, \dots, s$. Then*

$$\|\sin \Theta(\widehat{V}, V)\|_F \leq \frac{2 \min\left(d^{\frac{1}{2}} \|\widehat{\Sigma} - \Sigma\|_{sp}, \|\widehat{\Sigma} - \Sigma\|_F\right)}{\min(\lambda_{r-1} - \lambda_r^*, \lambda_s - \lambda_{s+1})}.$$

Moreover, there exists an orthogonal matrix $\widehat{O} \in \mathbb{R}^{d \times d}$, such that

$$\|\widehat{V} \widehat{O} - V\|_F \leq \frac{2^{\frac{3}{2}} \min\left(d^{\frac{1}{2}} \|\widehat{\Sigma} - \Sigma\|_{sp}, \|\widehat{\Sigma} - \Sigma\|_F\right)}{\min(\lambda_{r-1} - \lambda_r^*, \lambda_s - \lambda_{s+1})}.$$

Lemma A.3 (Lemma 1 in Zhang et al. (2022)). *Suppose $U \in \mathbb{O}_{m,r}$. Recall that $I(U^*) = \max_i \|e_i^T U\|_2^2$, and $P_U = UU^\top$ is the projection matrix. Then for any matrix $A \in \mathbb{R}^{m \times m}$, we have $\|D(P_U(D(A)))\|_{sp} \leq I(U^*)\|D(A)\|_{sp}$, and $\|D(P_U A)\|_{sp} \leq \sqrt{I(U^*)}\|A\|_{sp}$.*

Lemma A.4 (Lemma 4 in Zhang et al. (2022)). *If $M \in \mathbb{R}^{p \times p}$ is any square matrix and $\Delta(M)$ is the matrix M with diagonal entries set to 0, then $\|\Delta(M)\|_{sp} \leq 2\|M\|_{sp}$.*

Lemma A.5 (Lemma 6 in Zhang et al. (2022)). *Suppose $M, E \in \mathbb{R}^{p_1 \times p_2}$, $\text{rank}(M) = r$, and $\widehat{U} = \text{SVD}_r(M+E)$, i.e., the leading r left singular vectors of $M+E$. If \widehat{U}_\perp is the orthogonal complement of \widehat{U} , then $\|P_{\widehat{U}_\perp} M\|_{sp} \leq 2\|E\|_{sp}$, and $\|P_{\widehat{U}_\perp} M\|_F \leq 2 \min \{\sqrt{r}\|E\|, \|E\|_F\}$.*

Lemma A.6 (Weyl's inequality in Weyl (1912)). *Let A, B be two $p \times p$ Hermitian matrices and $\lambda_i(A)$ be the i th eigenvalue of A . Then, for $1 \leq l, j \leq p$,*

$$\begin{aligned} \lambda_l(A+B) &\leq \lambda_j(A) + \lambda_k(B), \quad \text{for } l \geq j+k-1, \\ \lambda_j(A) + \lambda_l(B) &\leq \lambda_{j+l-p}(A+B), \quad \text{for } j+l \geq p. \end{aligned}$$

Lemma A.7 (Lemma 5.4 in Tu et al. (2016)). *For any $U, X \in \mathbb{R}^{p \times r}$, we have*

$$\text{dist}^2(U, X) \leq \frac{1}{2(\sqrt{2}-1)\sigma_r^2(X)} \|UU^\top - XX^\top\|_F^2.$$

Lemma A.8 (Theorem 2 in Ten Berge (1977)). *The function $g(H) = \text{tr}(H^\top X^\top L)$, where H varies without restriction over the set of orthonormal matrices of order $r \times r$, is maximized if and only if $H^\top X^\top L$ is symmetric and positive semi-definite (SPSD). Let $X^\top L = PDQ^{*\top}$ be an Eckart-Young decomposition of $X^\top L$. Letting $H = PQ^{*\top}$, then $H^\top X^\top L = Q^*DQ^{*\top}$. Besides, $Q^*DQ^{*\top}$ is SPSD, which is both necessary and sufficient for attaining the best least-squares fit.*

Lemma A.9 (Theorem 3.3 in Vu et al. (2013)). *If $\lambda \geq \|\widehat{\Sigma} - \Sigma\|_{\infty, \infty}$ and $s \geq \|\widehat{U}\widehat{U}^\top - U_\Sigma U_\Sigma^\top\|_{2,0}$, then*

$$\|\widehat{U}\widehat{U}^\top - U_\Sigma U_\Sigma^\top\|_{sp} \leq \frac{4s\lambda}{\sigma_{(r)}^2 - \sigma_{(r+1)}^2}.$$

A.2 Lemmas related to concentration inequalities

Lemma A.10 (Lemma 2 in Zhang et al. (2022)). *Suppose $E \in \mathbb{R}^{p_1 \times p_2}$ has independent sub-Gaussian entries, $\text{Var}(E_{ij}) = \sigma_{ij}^2$, $\sigma_{ij}^2 = \max_i \sum_j \sigma_{ij}^2 = \max_j \sum_i \sigma_{ij}^2 = \max_{ij} \sigma_{ij}^2$. Suppose*

$$\left\| \frac{E_{ij}}{\sigma_{ij}} \right\|_{\psi_2} := \max_{q \geq 1} q^{-\frac{1}{2}} \left(\mathbb{E} \left| \frac{E_{ij}}{\sigma_{ij}} \right|^q \right)^{1/q} \leq \kappa.$$

Let $V \in \mathbb{O}_{p_2, r}$ be a fixed orthogonal matrix. Then

$$\begin{aligned} \mathbb{P}(\|EV\|_{sp} \geq 2(\sigma_C + x)) &\leq 2 \exp \left(5r - \min \left\{ \frac{x^4}{\kappa^4 \sigma_{(1)}^2 \sigma_C^2}, \frac{x^2}{\kappa^2 \sigma_{(1)}^2} \right\} \right), \\ \mathbb{E}[\|EV\|_{sp}] &\lesssim \sigma_C + \kappa r^{-\frac{1}{4}} (\sigma_{(1)} \sigma_C)^{\frac{1}{4}} + \kappa r^{\frac{1}{2}} \sigma_{(1)}. \end{aligned}$$

Lemma A.11 (Theorem 5.39 in Vershynin (2011)). *Let A be an $N \times n$ matrix whose rows A_i are independent sub-Gaussian isotropic random vectors in \mathbb{R}^n . Then for every $x \geq 0$, with probability at least $1 - 2 \exp(-cx^2)$,*

$$\sqrt{N} - C\sqrt{n} - x \leq \sigma_{\min}(A) \leq \sigma_{\max}(A) \leq \sqrt{N} + C\sqrt{n} + x,$$

where $C = C_K$, $c = c_K > 0$ depend only on the sub-Gaussian norm $K = \max_i \|A_i\|_{\psi_2}$ of the rows.

Lemma A.12 (Theorem 6.5 in Wainwright (2019)). *There are universal constants $\{c_j\}_{j=0}^3$, such that, for any row-wise σ -sub-Gaussian random matrix $X \in \mathbb{R}^{n \times d}$, the sample covariance $\widehat{\Sigma} = \frac{1}{n} \sum_{i=1}^n x_i x_i^\top$ satisfies the bounds*

$$\mathbb{E} \left[e^{\lambda \|\widehat{\Sigma} - \Sigma\|_{sp}} \right] \leq e^{c_0 \lambda^2 \sigma^4 / n + 4d}, \quad \text{for all } |\lambda| < \frac{n}{64e^2 \sigma^2}.$$

Consequently,

$$\mathbb{P} \left(\frac{\|\widehat{\Sigma} - \Sigma\|_{sp}}{\sigma^2} \geq c_1 \left(\sqrt{\frac{d}{n}} + \frac{d}{n} \right) + x \right) \leq c_2 e^{-c_3 n \min\{x, x^2\}}, \quad \text{for all } x \geq 0.$$

Lemma A.13 (Theorem 6 in Cai et al. (2022)). *Suppose Z is a $p_1 \times p_2$ random matrix with independent mean-zero sub-Gaussian entries. If there exist $\sigma_1, \dots, \sigma_p$ such that $\|Z_{ij}/\sigma_i\|_{\psi_2} \leq C_k$ for constant $C_k > 0$, then*

$$\mathbb{E} [\|ZZ^T - \mathbb{E}ZZ^T\|_{sp}] \lesssim \sum_i \sigma_i^2 + \sqrt{p_2 \sum_i \sigma_i^2} \cdot \max_i \sigma_i.$$

Lemma A.14 (Lemma 1 in Jin et al. (2019)). *Suppose a random vector $X \in \mathbb{R}^d$ is (σ/\sqrt{d}) -sub-Gaussian, then we have*

$$\mathbb{P}(\|X - \mathbb{E}[X]\|_2 \geq x) \leq 2e^{-\frac{x^2}{16\sigma^2}}$$

A.3 Lemmas related to community detection

Lemma A.15 (Lemma 5.3 in Lei and Rinaldo (2015)). *For $\epsilon > 0$ and any two matrices $\widehat{\Gamma}, \Gamma \in \mathbb{R}^{p \times G}$, such that $\Gamma = \Theta Y$, where $Y \in \mathbb{R}^{G \times G}$ and $\Theta \in \mathbb{M}_{v,G}$, the set of membership matrices. Let $(\widehat{\Theta}, \widehat{Y})$ be a $(1 + \epsilon)$ -approximate solution to the k -means problem, which means it satisfies $\|\widehat{\Theta}\widehat{Y} - \widehat{\Gamma}\|_F^2 \leq (1 + \epsilon) \min_{\Theta \in \mathbb{M}_{v,G}, Y \in \mathbb{R}^{G \times G}} \|\Theta Y - \widehat{\Gamma}\|_F^2$. Define $\tilde{\Gamma} = \widehat{\Theta}\widehat{Y}$.*

For any $\delta_g \leq \min_{l \neq g} \|Y_{l*} - Y_{g*}\|$, define $S_g = \{i \in H_g(\Theta) : \|\tilde{\Gamma}_{i*} - \Gamma_{i*}\| \geq \delta_g/2\}$, where for any matrix A , $A_{\mathcal{I}*}$ denotes the submatrix consisting of rows indexed by \mathcal{I} . Then,

$$\sum_{g=1}^G |S_g| \delta_g^2 \leq (16 + 8\epsilon) \|\widehat{\Gamma} - \Gamma\|_F^2. \quad (\text{A.1})$$

Moreover, if

$$(16 + 8\epsilon) \|\widehat{\Gamma} - \Gamma\|_F^2 / \delta_g^2 < p_g, \quad \text{for all } g, \quad (\text{A.2})$$

then there exists a $G \times G$ permutation matrix J , such that $\widehat{\Theta}_{H*} = \Theta_{H*} J$, where $H = \bigcup_{g=1}^G (H_g \setminus S_g)$.

Lemma A.16 (Lemma 2.1 in Lei and Rinaldo (2015)). Suppose $B \in \mathbb{R}^{G \times G}$ is symmetric and of full rank, and $\Theta \in \mathbb{R}^{p \times G}$ is a membership matrix. Let $\Gamma D \Gamma^\top$ be the eigen-decomposition of $L = \Theta B \Theta^\top$. Then $\Gamma = \Theta Y$ where $Y \in \mathbb{R}^{G \times G}$ and

$$\|Y_{g*} - Y_{l*}\| = \sqrt{p_g^{-1} + p_l^{-1}}, \quad \text{for all } 1 \leq g < l \leq G.$$

Lemma A.17 (Lemma 5.1 in Lei and Rinaldo (2015)). Suppose $L \in \mathbb{R}^{p \times p}$ is a rank G symmetric matrix with smallest nonzero singular value λ_G . Let A be any symmetric matrix, and $\widehat{\Gamma}, \Gamma \in \mathbb{R}^{p \times G}$ be the G leading eigenvectors of A and L , respectively. Then there exists a $G \times G$ orthogonal matrix O , such that

$$\|\widehat{\Gamma} - \Gamma O\|_F \leq \frac{2\sqrt{2G}}{\lambda_G} \|A - L\|_{sp}.$$

A.4 Miscellaneous lemmas

Lemma A.18 (Modified from Lemma B.19 in Ji et al. (2023)). Suppose $O \in \mathbb{O}_{d,r}$, for any $\widehat{O} \in \mathbb{O}_{d,r}$, with $\|\sin \Theta(\widehat{O}, O)\|_{sp} \leq \frac{\sigma_{(1)}^2}{\kappa_\Sigma} \wedge \frac{1}{2}$. Then,

$$\begin{aligned} \inf_{w \in \mathbb{R}^r} \mathbb{E}_0 \left[l_c \left(\mathbb{1} \left\{ F(w^\top \widehat{O}^\top x_0) \geq \frac{1}{2} \right\} \right) \right] - \inf_{w \in \mathbb{R}^r} \mathbb{E}_0 \left[l_c \left(\mathbb{1} \left\{ F(w^\top O^\top x_0) \geq \frac{1}{2} \right\} \right) \right] \lesssim \\ \left[\left\{ \kappa_\Sigma \left(1 + \frac{1}{\sigma_{(1)}^2} \right) \right\}^3 + \frac{\kappa_\Sigma}{\sigma_{(1)}^2} \left(1 + \sigma_{(1)}^2 \right)^2 \right] \|\sin \Theta(\widehat{O}, O^*)\|_{sp}. \end{aligned}$$

Lemma A.19 (Lemma B.20 in Ji et al. (2023)). Suppose $Q^* \in \mathbb{O}_{d,r}$, for any $\widehat{O} \in \mathbb{O}_{d,r}$,

with $\sigma_{(1)}^2(1 + \sigma_{(1)}^2) - \kappa_\Sigma \left(r - \left\| \sin \Theta(\widehat{O}, O) \right\|_F^2 \right) \geq 0$. Then,

$$\begin{aligned} \inf_{w \in \mathbb{R}^r} \mathbb{E}_0 \left[l_c \left(\mathbb{1} \left\{ F(w^\top \widehat{O}^\top x_0) \geq \frac{1}{2} \right\} \right) \right] - \inf_{w \in \mathbb{R}^r} \mathbb{E}_0 \left[l_c \left(\mathbb{1} \left\{ F(w^\top O^\top x_0) \geq \frac{1}{2} \right\} \right) \right] &\gtrsim \\ \frac{\left(\sigma_{(1)}^2 + 1 \right)^{\frac{3}{2}}}{\left(\sigma_{(1)}^2 + \kappa_\Sigma \right)^{\frac{3}{2}} \sigma_{(1)}^2} \left\{ \frac{\sigma_{(1)}^2}{1 + \sigma_{(1)}^2} - \kappa_\Sigma \left(r - \left\| \sin \Theta(\widehat{O}, O) \right\|_F^2 \right) \right\}. \end{aligned}$$

Lemma A.20 (Lemma B.7 in Gao and Ma (2023)). Define L^* as a global minimizer of the function $f(L)$, and $H_X = \arg \min_{H \in \mathbb{O}_{r,r}} \|XH - L^*\|_F$. Define a function $f(L)$ to be β -smooth at L , if for all Z , we have

$$\text{vec}(Z)^\top \nabla^2 f(L) \text{vec}(Z) \leq \beta \|Z\|_F^2.$$

Suppose that f is β -smooth within a ball $\mathcal{B}(L^*) = \{L : \|L - L^*\|_F \leq R\}$ and that $\nabla f(L)P = \nabla f(LP)$ for any orthonormal matrix P . Assume that for any $L \in \mathcal{B}(L^*)$ and any Z , we have $\text{vec}(ZH_Z - L^*)^\top \nabla^2 f(L) \text{vec}(ZH_Z - L^*) \geq \alpha \|ZH_Z - L^*\|_F^2$. In addition, if $\eta \leq \frac{1}{\beta}$, then using gradient descent with $\text{dist}(L_t, L^*) \leq R$, we have $\text{dist}^2(L_{t+1}, L^*) \leq (1 - \alpha\eta) \text{dist}^2(L_t, L^*)$. Moreover, with $\text{dist}(L_0, L^*) \leq R$, we have $\text{dist}^2(L_t, L^*) \leq (1 - \alpha\eta)^t \text{dist}^2(L_0, L^*)$.

B Proofs for Section 3

We first present the proofs for the main theoretical results in Section 3. We introduce a number of supporting lemmas along the way, and defer the proofs of those lemmas to the end of this section.

B.1 Proof of Theorem 3.1

Proof. As mentioned in the Section 2.4, the coefficient $1/8$ in (2.5) was chosen for presentation simplicity. We now present a general version of the loss in Equation (2.5) by introducing a general parameter λ to control the penalty strength.

$$\begin{aligned} \mathcal{L}(V; \mathcal{D}, A) &= -\frac{1}{n} \sum_i \langle V^\top Ax_i, V^\top (I - A)x_i \rangle + \\ &\quad \frac{1}{n^2} \sum_{i,j} \langle V^\top Ax_i, V^\top (I - A)x_j \rangle + \frac{\lambda}{8} \|VV^\top\|_F^2. \quad (\text{B.1}) \end{aligned}$$

We will analyze this loss throughout the proof, and obtain the formulation in (2.5), by setting $\lambda = 1$. Correspondingly, at the inner iteration t of the outer iteration k , denote the

parameter matrices as $\widehat{V}_{(t)}^{(k)}, \tilde{V}_{(t)}^{(k)} \in \mathbb{R}^{d \times r}$. Define

$$V^* = \frac{Q^*}{\sqrt{\lambda}}. \quad (\text{B.2})$$

Since in this theorem we focus solely on the k th iteration, we simplify the notation by omitting the superscripts $(k), (k-1)$. Also, recall the expected loss,

$$\mathcal{L}(V) = \mathbb{E}_A[\mathcal{L}(V; \mathcal{D}, A)]. \quad (\text{B.3})$$

Since we always consider the same dataset \mathcal{D} , we abbreviate $\mathcal{L}(V; \mathcal{D})$ as $\mathcal{L}(V)$ for notational simplicity.

First, we have the following lemma that helps simplifies the loss function.

Lemma B.1. *If A is generated by (2.2) with the masking parameter $p = (p_1, \dots, p_d)^\top \in [0, 1]^d$, while omitting the constant, the loss function (B.3) can be written as,*

$$\mathcal{L}(V) = \frac{\lambda}{2} \left\| VV^\top - \frac{1}{\lambda} (\Delta(M) + P^2 D(M)) \right\|_F^2. \quad (\text{B.4})$$

where $M = \frac{1}{n} XX^\top - \frac{1}{n^2} X1_n 1_n^\top X^\top$, $X \in \mathbb{R}^{d \times n} = (x_1, \dots, x_n)$, and $P = \text{diag}(p_1, \dots, p_d)$.

Without loss of generality, we write $Q^* = U^* \Lambda^{*\frac{1}{2}}$. Define the row support of U^* as S , and suppose $\mathcal{I} \supseteq S$. Define $\widehat{U}(\mathcal{I}) \in \mathbb{R}^{d \times r}$ as the solution of the optimization,

$$\max \langle N, FF^\top \rangle, \quad \text{such that } F^\top F = I_r, \quad \text{supp}(F) \subseteq \mathcal{I},$$

where we rewrite $N = \Delta(M) + P^2 D(M)$.

We further define $\widehat{\Lambda}_r(\mathcal{I})$ as the diagonal matrix formed by the first r eigenvalues of $(N)_{\mathcal{I}\mathcal{I}}$. Since $\text{supp}(\widehat{U}(\mathcal{I})) \subseteq \mathcal{I}$, we have that $\widehat{U}_{\mathcal{I}*}(\mathcal{I})$ is the solution of

$$\max \langle (N)_{\mathcal{I}\mathcal{I}}, LL^\top \rangle \quad \text{such that } L^\top L = I_r,$$

where, for any matrix A , $A_{\mathcal{I}*}$ denotes the submatrix consisting of rows indexed by \mathcal{I} . Moreover, $\text{supp}(U^*) = S \subseteq \mathcal{I}$, then $U_{\mathcal{I}*}$ is the solution of

$$\max \langle (Q^* Q^{*\top})_{\mathcal{I}\mathcal{I}}, LL^\top \rangle \quad \text{such that } L^\top L = I_r.$$

Moreover, define $\widehat{V}(\mathcal{I}) = \widehat{U}(\mathcal{I}) \left(\frac{\widehat{\Lambda}_r(\mathcal{I})}{\lambda} \right)^{\frac{1}{2}}$, and recall V^* as defined in (B.2). By Lemma

A.7, we have,

$$\begin{aligned}
\text{dist}(\widehat{V}(\mathcal{I}), V^*) &\leq \frac{1}{\sqrt{2\sqrt{2} - 2\lambda_r^* \sqrt{\lambda}}} \left\| \widehat{U}(\mathcal{I}) \widehat{\Lambda}_r(\mathcal{I}) \widehat{U}(\mathcal{I})^\top - U^* \Lambda^* U^{*\top} \right\|_F \\
&\leq \frac{\sqrt{2r}}{\sqrt{2\sqrt{2} - 2\lambda_r^* \sqrt{\lambda}}} \left\| \widehat{U}(\mathcal{I}) \widehat{\Lambda}_r(\mathcal{I}) \widehat{U}(\mathcal{I})^\top - U^* \Lambda^* U^{*\top} \right\|_{\text{sp}} \\
&\leq \frac{2\sqrt{2r}}{\sqrt{2\sqrt{2} - 2\lambda_r^* \sqrt{\lambda}}} \left\| (N - Q^* Q^{*\top})_{\mathcal{I}\mathcal{I}} \right\|_{\text{sp}} \\
&< \frac{9\sqrt{r}}{2\lambda_r^* \sqrt{\lambda}} W^{(k-1)}
\end{aligned} \tag{B.5}$$

Next, we characterize the progress of the gradient descent step using the following lemma. Recall $W^{(k-1)}$ is defined as the masking-adjusted covariance matrix estimation error from (3.2). We define the effective restricted set as $S_{(t)} = \text{supp}(\tilde{V}_{(t)}) \cup \text{supp}(\tilde{V}_{(t+1)}) \cup S$.

Lemma B.2. *Suppose $W^{(k-1)} < \lambda_r^{*2}/4$, and the step size η is chosen such that $\eta \leq \frac{1}{8W^{(k-1)} + \frac{85}{12}\lambda_1^{*2}}$. If*

$$\text{dist}(\widehat{V}_{(t)}, \widehat{V}(S_{(t)})) \leq \frac{\lambda_r^{*2}}{12\sqrt{\lambda(\lambda_1^{*2} + W^{(k-1)})}}, \tag{B.6}$$

then after the gradient step, we have

$$\text{dist}^2(\widehat{V}_{(t+1)}^o, \widehat{V}(S_{(t)})) \leq \left\{ 1 - \eta \left(\frac{17}{12} \lambda_r^{*2} - 4R^{(k-1)} \right) \right\} \text{dist}^2(\widehat{V}_{(t)}, \widehat{V}(S_{(t)})),$$

where $\widehat{V}_{(t+1)}^o \in \mathbb{R}^{d \times r}$ denotes a matrix that has the same entries as those in $\widehat{V}_{(t+1)}$ on $S_{(t)} \times [r]$ and zeros elsewhere.

Next, we present a lemma showing the property of truncation.

Lemma B.3 (Proposition B.6 in Gao and Ma (2023)). *Let V^* be as defined in (B.2). Suppose we perform hard thresholding by selecting the top s elements of $\widehat{V}_{(t+1)}$. Then we have*

$$\text{dist}^2(V^*, \tilde{V}_{(t+1)}) \leq \left\{ 1 + 2\sqrt{\frac{s^*}{s}} \left(1 + \sqrt{\frac{s^*}{s}} \right) \right\} \text{dist}^2(V^*, \widehat{V}_{(t+1)}).$$

Now, we turn to the proof of this theorem.

We first define the effective support in each step. Considering the situation in Lemma B.2 and the effective restricted set $S_{(t)}$, with the loss (B.4), the gradient descent step restricted to $S_{(t)}$ can be viewed as

$$\widehat{V}_{(t+1), S_{(t)}*} = \tilde{V}_{(t), S_{(t)}*} - 2\eta \left(-N_{S_{(t)} S_{(t)}} \tilde{V}_{(t), S_{(t)}*} + \lambda \tilde{V}_{(t), S_{(t)}*} \tilde{V}_{(t), S_{(t)}*}^\top \right).$$

Note that applying hard thresholding on $\widehat{V}_{(t+1)}^o$ is equivalent to applying hard thresholding on original $V_{(t+1)}$. This allows us to replace the intermediate update by $\widehat{V}_{(t+1)}^o$ and still obtain the same output sequence $\widehat{V}_{(t+1)}$. Thus, we will prove instead for the update using $N_{S_{(t)}S_{(t)}}$, then we can use Lemma B.2.

We achieve this by induction on t . Specifically, for $t = 1, 2, \dots$, we will prove that $\tilde{V}_{(t)}$ satisfies the radius condition (B.6), and that

$$\text{dist}(\tilde{V}_{(t)}, V^*) \leq \xi^{t-1} \text{dist}(\tilde{V}_{(1)}, V^*) + \frac{9\sqrt{r}}{(1-\xi)\lambda_r^* \sqrt{\lambda}} W^{(k-1)}. \quad (\text{B.7})$$

We start with the base case of $t = 1$. Since $\text{dist}(\tilde{V}_{(1)}, V^*) \leq \text{dist}(\tilde{V}_{(1)}, V^*)$, (B.7) holds trivially. To check the radius condition B.6, we have, by (B.5) and $W^{(k-1)} \leq \frac{c_3 \lambda_r^{*3}}{\lambda_1^* \sqrt{r}}$,

$$\text{dist}(\widehat{V}(S_{(1)}), V^*) \leq \frac{9\sqrt{r}}{2\lambda_r^* \sqrt{\lambda}} W^{(k-1)} < \frac{\lambda_r^{*2}}{24\sqrt{\lambda(\lambda_1^{*2} + W^{(k-1)})}}.$$

Moreover, by $\|\widehat{Q}^{(0)}\widehat{Q}^{(0)\top} - Q^*Q^{*\top}\|_F \leq \lambda_r^{*3}/(20\lambda_1^*)$, and Lemma A.7, we have

$$\text{dist}(\tilde{V}_{(1)}, \widehat{V}(S_{(1)})) \leq \text{dist}(\tilde{V}_{(1)}, V^*) + \text{dist}(\widehat{V}(S_{(1)}), V^*) \leq \frac{\lambda_r^{*2}}{12\sqrt{\lambda(\lambda_1^{*2} + W^{(k-1)})}}.$$

We then continue with the induction step. Suppose that $\tilde{V}_{(t)}$ satisfies the radius condition (B.6) and that the induction equation (B.7) is satisfied at step t . We aim to show that (B.6) and (B.7) hold for $\tilde{V}_{(t+1)}$.

In the gradient step, Lemma B.2 shows that under (B.6) on $\text{dist}(\tilde{V}_{(t)}, \widehat{V}(S_{(t)}))$, if we choose the step-size to be $\eta \leq \frac{1}{\beta}$, we have,

$$\text{dist}(\widehat{V}_{(t+1)}^o, \widehat{V}(S_{(t)})) \leq \sqrt{1 - \eta\alpha} \text{dist}(\tilde{V}_{(t)}, \widehat{V}(S_{(t)})),$$

where $\alpha = \frac{4}{3}\lambda_r^{*2} \leq \frac{17}{12}\lambda_r^{*2} - 4W^{(k-1)}$, $\beta = \frac{43}{6}\lambda_1^{*2} \geq 8W^{(k-1)} + \frac{85}{12}\lambda_1^{*2}$ given $W^{(k-1)} \leq \frac{c_3 \lambda_r^{*3}}{\lambda_1^* \sqrt{r}}$.

By Lemma B.3,

$$\text{dist}(\tilde{V}_{(t+1)}, V^*) \leq \sqrt{1 + 2\sqrt{\frac{s^*}{s}} \left(1 + \sqrt{\frac{s^*}{s}}\right)} \text{dist}(\widehat{V}_{(t+1)}^o, V^*).$$

Therefore,

$$\begin{aligned} \text{dist}(\widehat{V}_{(t+1)}^o, V^*) &\leq \text{dist}(\widehat{V}_{(t+1)}^o, \widehat{V}(S_{(t)})) + \text{dist}(\widehat{V}(S_{(t)}), V^*) \\ &\leq \sqrt{1 - \eta\alpha} \text{dist}(\tilde{V}_{(t)}, \widehat{V}(S_{(t)})) + \text{dist}(\widehat{V}(S_{(t)}), V^*) \\ &\leq \sqrt{1 - \eta\alpha} \text{dist}(\tilde{V}_{(t)}, V^*) + \left(\sqrt{1 - \eta\alpha} + 1\right) \text{dist}(\widehat{V}(S_{(t)}), V^*). \end{aligned}$$

Combining with (B.5), we have that,

$$\begin{aligned} \text{dist}(\tilde{V}_{(t+1)}, V^*) &\leq \sqrt{\left(1 + 2\sqrt{\frac{s^*}{s}}\left(1 + \sqrt{\frac{s^*}{s}}\right)\right)(1 - \eta\alpha) \text{dist}(\tilde{V}_{(t)}, V^*)} \\ &\quad + \sqrt{1 + 2\sqrt{\frac{s^*}{s}}\left(1 + \sqrt{\frac{s^*}{s}}\right)}(\sqrt{1 - \eta\alpha} + 1) \frac{9\sqrt{r}}{2\lambda_r^* \sqrt{\lambda}} W^{(k-1)}. \end{aligned}$$

By taking $s \geq \frac{64}{\alpha^2 \eta^2} s^*$, we ensure that

$$\xi \leq \sqrt{\left(1 + \frac{\alpha\eta}{4} + \frac{\alpha^2\eta^2}{32}\right)(1 - \alpha\eta)} \leq \sqrt{\left(1 - \frac{3\alpha\eta}{4} - \frac{7\alpha^2\eta^2}{32}\right)} \leq \sqrt{1 - \frac{3\alpha\eta}{4}} < 1 - \frac{3\alpha\eta}{8}, \quad (\text{B.8})$$

where $\xi = \sqrt{\left(1 + 2\sqrt{\frac{s^*}{s}}\left(1 + \sqrt{\frac{s^*}{s}}\right)\right)(1 - \eta\alpha)}$. Therefore,

$$\begin{aligned} \text{dist}(\tilde{V}_{(t+1)}, V^*) &\leq \xi \text{dist}(\tilde{V}_{(t)}, V^*) + \left(1 - \frac{3\alpha\eta}{8} + \sqrt{1 + \frac{\alpha\eta}{4} + \frac{\alpha^2\eta^2}{2}}\right) \frac{9\sqrt{r}}{2\lambda_r^* \sqrt{\lambda}} W^{(k-1)} \\ &\leq \xi \text{dist}(\tilde{V}_{(t)}, V^*) + \frac{9\sqrt{r}}{\lambda_r^* \sqrt{\lambda}} W^{(k-1)}. \end{aligned}$$

From (B.7) at the t step,

$$\begin{aligned} \text{dist}(\tilde{V}_{(t+1)}, V^*) &\leq \xi \left(\xi^{t-1} \text{dist}(\tilde{V}_{(1)}, V^*) + \frac{9\sqrt{r}}{(1 - \xi)\lambda_r^* \sqrt{\lambda}} W^{(k-1)} \right) + \frac{9\sqrt{r}}{\lambda_r^* \sqrt{\lambda}} W^{(k-1)} \\ &= \xi^t \text{dist}(\tilde{V}_{(1)}, V^*) + \frac{9\sqrt{r}}{(1 - \xi)\lambda_r^* \sqrt{\lambda}} W^{(k-1)}. \end{aligned}$$

This proves that (B.7) holds for $t + 1$ step.

Furthermore, by (B.8), we have,

$$\begin{aligned} \text{dist}(\tilde{V}_{(t+1)}, \widehat{V}(S_{(t+1)})) &\leq \text{dist}(\tilde{V}_{(t+1)}, V^*) + \text{dist}(\widehat{V}(S_{(t+1)}), V^*) \\ &\leq \xi^t \text{dist}(\tilde{V}_{(1)}, V^*) + \left(\frac{9}{1 - \xi} + \frac{9}{2}\right) \frac{\sqrt{r}}{\lambda_r^* \sqrt{\lambda}} W^{(k-1)} \\ &\leq \frac{\lambda_r^{*2}}{24\sqrt{\lambda(\lambda_1^{*2} + W^{(k-1)})}} + \left(\frac{24}{\alpha\eta} + 2\right) \frac{\sqrt{r}}{\lambda_r^* \sqrt{\lambda}} W^{(k-1)}. \end{aligned}$$

By $W^{(k-1)} \leq \frac{c_3 \lambda_r^{*3}}{\lambda_1^* \sqrt{r}}$, we have

$$\text{dist}(\tilde{V}_{(t+1)}, \widehat{V}(S_{(t+1)})) \leq \frac{\lambda_r^{*2}}{12\sqrt{\lambda(\lambda_1^{*2} + W^{(k-1)})}}.$$

By induction, we have that,

$$\begin{aligned} \text{dist}(\tilde{V}_{(t+1)}, V^*) &\leq \xi^t \text{dist}(\tilde{V}_{(1)}, V^*) + \frac{24\sqrt{r}}{\alpha\eta\lambda_r^* \sqrt{\lambda}} W^{(k-1)} \\ &\leq \xi^t \text{dist}(\tilde{V}_{(1)}, V^*) + \frac{3}{\lambda_r^*} \sqrt{\frac{sr}{s^* \lambda}} W^{(k-1)}. \end{aligned}$$

This completes the proof of Theorem 3.1. \square

B.2 Proof of Theorem 3.2

Proof. Suppose $s \geq s^*$. we define the event Ω_1 as

$$\Omega_1 = \left\{ \left\| \left(M - Q^* Q^{*\top} - \Sigma \right)_{\mathcal{I}\mathcal{I}} \right\|_{\text{sp}} \leq c'_1 (\lambda_1^{*2} + \sigma_{(1)}^{*2}) \left(\sqrt{\frac{s \log d}{n}} + \frac{s^2 \log d}{n} \right), \right. \\ \left. \text{for all } \mathcal{I} \subset [d] \text{ with } |\mathcal{I}| = 2s + s^* \right\}.$$

The following lemma ensure Ω_1 occurs with a high probability.

Lemma B.4. *Suppose $2s + s^* < n$. There exist a constant $c'_1 > 0$, such that $\mathbb{P}(\Omega_1) \geq 1 - ce^{-cs \log d}$.*

Under Ω_1 happens, we consider the loss $\mathcal{L}(V)$ in (B.4), and perform Algorithm 1.

Taking the masking parameter as (2.6) at the k th iteration, we have

$$\left(P^{(k)2} D(M) \right)_{e,e} = \begin{cases} M_{e,e} & \text{when } N_{e,e}^{(k-1)} \geq M_{e,e}, \\ N_{e,e}^{(k-1)} & \text{when } N_{e,e}^{(k-1)} < M_{e,e}, \end{cases}$$

where $P^{(k)} = \text{diag}(p_1^{(k)}, \dots, p_d^{(k)})$, and $\tilde{N}^{(k-1)} = \hat{Q}^{(k-1)} \hat{Q}^{(k-1)\top}$. Denote $\tilde{N}^{(k-1)} = \Delta(M) + P^{(k)2} D(M)$, and $\tilde{N}^{(0)} = N^{(0)} = \Delta(M)$.

After establishing Theorem 3.1 for the k th iteration, we set $\lambda = 1$ and analyze $W^{(k)} = \left\| \left(\tilde{N}^{(k)} - Q^* Q^{*\top} \right)_{\mathcal{I}\mathcal{I}} \right\|_{\text{sp}}$ as k increases, leveraging Theorem 3.1. The goal is to derive a recursive relationship between $W^{(k-1)}$ and $W^{(k)}$, and subsequently express $W^{(k)}$ in terms of T_0 . We claim that

$$W^{(k)} \leq 6T_0 + \frac{c'_2 s^* \lambda_1^{*2}}{2^k s r}, \quad (\text{B.9})$$

where $T_0 = 2c'_1 (\lambda_1^{*2} + \sigma_{(1)}^{*2}) \left(\sqrt{\frac{s \log d}{n}} + \frac{s^2 \log d}{n} \right)$ and c'_2 is a sufficiently small constant.

We start with the base case of $k = 1$. From Lemma A.4, we have

$$W^{(0)} = \|(\tilde{N}^{(0)} - Q^* Q^{*\top})_{\mathcal{I}\mathcal{I}}\|_{\text{sp}} \leq \left\| \left(\Delta(M) - Q^* Q^{*\top} - \Sigma \right)_{\mathcal{I}\mathcal{I}} \right\|_{\text{sp}} + D(Q^* Q^{*\top})_{\text{sp}} \\ \leq T_0 + \lambda_1^{*2} I(U^*) \leq T_0 + \frac{c_2 \lambda_1^{*2}}{r} \leq 6T_0 + \frac{c'_2 s^* \lambda_1^{*2}}{s r},$$

by $c_2 \leq \frac{c'_2 s^*}{s}$. Thus, $W^{(0)}$ satisfies (B.9).

Next we verify that $W^{(0)}$ meets the condition in Theorem 3.1. Since $W^{(0)} \leq 6T_0 + \frac{c_2 \lambda_1^{*2}}{r}$, and by that $s \log d \ll n$ and c_2 is sufficiently small, it follows that $W^{(0)} \leq \frac{c_3 \lambda_r^{*3}}{\lambda_1^* \sqrt{r}}$.

For our initializer $\widehat{Q}^{(0)}$, the assumption $\|\widehat{Q}^{(0)}\widehat{Q}^{(0)\top} - Q^*Q^{*\top}\|_F \leq \lambda_r^{*3}/(20\lambda_1^*)$ required by Theorem 3.1 is automatically satisfied. Given that $W^{(0)} \leq \frac{c_3\lambda_r^{*3}}{\lambda_1^*\sqrt{r}}$, the base case is verified. Therefore, both $W^{(0)}$ and $\widehat{Q}^{(0)}$ satisfy the initialization conditions in Theorem 3.1.

We then continue with the induction step. Suppose that

$$W^{(k-1)} \leq 6T_0 + \frac{c'_2 s^* \lambda_1^{*2}}{2^{k-1} sr} \leq \frac{c_3 \lambda_r^{*3}}{\lambda_1^* \sqrt{r}}, \quad \|\widehat{Q}^{(k-1)}\widehat{Q}^{(k-1)\top} - Q^*Q^{*\top}\|_F \leq \lambda_r^{*3}/(20\lambda_1^*).$$

At the k th iteration, we run

$$T^{(k)} = \Omega\left(\frac{\log\left(\frac{1}{\lambda_r^*} \sqrt{\frac{sr}{s^*}} W^{(k-1)}\right)}{\log\left(1 - \frac{\lambda_r^{*2}\eta}{2}\right)}\right)$$

By Assumptions 3.1 and 3.2, we have

$$T^{(k)} = \Omega\left(\log n \wedge \log\left(2^k r\right)\right).$$

Taking the output $\tilde{V}_{(T^{(k)})}^{(k)}$ as $\widehat{Q}^{(k)}$. By applying Theorem 3.1, we obtain that

$$\text{dist}\left(\widehat{Q}^{(k)}, Q^*\right) \leq \frac{49}{16\lambda_r^*} \sqrt{\frac{sr}{s^*}} W^{(k-1)}.$$

This implies that there exists an orthogonal matrix $O \in \mathbb{O}_{r,r}$, such that

$$\text{dist}\left(\widehat{Q}^{(k)}, Q^*\right) = \left\| \widehat{Q}^{(k)}O - Q^* \right\|_F \leq \frac{49}{16\lambda_r^*} \sqrt{\frac{sr}{s^*}} W^{(k-1)} \quad (\text{B.10})$$

Since c'_2 is sufficiently small,

$$\begin{aligned} \left\| \widehat{Q}^{(k)}\widehat{Q}^{(k)\top} - Q^*Q^{*\top} \right\|_F &= \left\| \widehat{Q}^{(k)}OO^\top\widehat{Q}^{(k)\top} - U^*U^{*\top} \right\|_F \\ &= \left\| \left(\widehat{Q}^{(k)}O - Q^* \right) O^\top\widehat{Q}^{(k)\top} + Q^* \left(O^\top\widehat{Q}^{(k)\top} - Q^{*\top} \right) \right\|_F \\ &\leq \left(\|\widehat{Q}^{(k)}\|_{\text{sp}} + \|Q\|_{\text{sp}} \right) \|\widehat{Q}^{(k)}O - Q\|_F \\ &\leq \frac{25\lambda_1^*}{4\lambda_r^*} \sqrt{\frac{sr}{s^*}} W^{(k-1)} \end{aligned} \quad (\text{B.11})$$

Then by Lemma A.2, we have,

$$\left\| \widehat{Q}^{(k)} \left(\widehat{Q}^{(k)\top}\widehat{Q}^{(k)} \right)^{-1} \widehat{Q}^{(k)\top} - U^*U^{*\top} \right\|_F \leq \frac{\sqrt{2}}{\lambda_r^{*2}} \|\widehat{Q}^{(k)}\widehat{Q}^{(k)\top} - Q^*Q^{*\top}\|_F \leq \frac{25\sqrt{2}\lambda_1^*}{4\lambda_r^{*3}} \sqrt{\frac{sr}{s^*}} W^{(k-1)} \quad (\text{B.12})$$

Since

$$\begin{aligned} W^{(k)} &= \left\| \left(\tilde{N}^{(k)} - Q^*Q^{*\top} \right)_{\mathcal{II}} \right\|_{\text{sp}} \leq \left\| \left(\Delta(M - Q^*Q^{*\top} - \Sigma) \right)_{\mathcal{II}} \right\|_{\text{sp}} \\ &\quad + \left\| \left(D(\tilde{N}^{(k)} - Q^*Q^{*\top}) \right)_{\mathcal{II}} \right\|_{\text{sp}} = T_0 + \left\| \left(D(\tilde{N}^{(k)} - Q^*Q^{*\top}) \right)_{\mathcal{II}} \right\|_{\text{sp}}, \end{aligned} \quad (\text{B.13})$$

we only need to analyze the diagonal term.

First, we bound the difference between

$$\left\| \left(D(\tilde{N}^{(k)} - Q^* Q^{*\top}) \right)_{\mathcal{II}} \right\|_{\text{sp}} \quad \text{and} \quad \left\| \left(D(N^{(k)} - Q^* Q^{*\top}) \right)_{\mathcal{II}} \right\|_{\text{sp}}.$$

Since $D(\tilde{N}^{(k)})$, $D(Q^* Q^{*\top})$ and $D(N^{(k)})$ are all diagonal and positive semi-definite, we analyze the difference by computing each entry.

If $N_{e,e}^{(k)} \geq (Q^* Q^{*\top})_{e,e}$, we have

$$\left| \min\{M_{e,e}, N_{e,e}^{(k)}\} - (Q^* Q^{*\top})_{e,e} \right| \leq \left| N_{e,e}^{(k)} - (Q^* Q^{*\top})_{e,e} \right|, \text{ i.e.}$$

$$\left| \tilde{N}_{e,e}^{(k)} - (Q^* Q^{*\top})_{e,e} \right| \leq \left| N_{e,e}^{(k)} - (Q^* Q^{*\top})_{e,e} \right|.$$

If $D(N^{(k)})_{e,e} < D(Q^* Q^{*\top})_{e,e}$, only when $D(M)_{e,e} < D(N^{(k)})_{e,e} < D(Q^* Q^{*\top})_{e,e}$, we have

$$D(Q^* Q^{*\top})_{e,e} - D(M)_{e,e} > D(Q^* Q^{*\top})_{e,e} - D(N^{(k)})_{e,e}.$$

In this situation,

$$\begin{aligned} D(Q^* Q^{*\top})_{e,e} - D(M)_{e,e} &\leq D(Q^* Q^{*\top} + \Sigma)_{e,e} - D(M)_{e,e} \leq \left\| \left(D(Q^* Q^{*\top} + \Sigma - M) \right)_{\mathcal{II}} \right\|_{\text{sp}} \\ &\leq \left\| \left(Q^* Q^{*\top} + \Sigma - M \right)_{\mathcal{II}} \right\|_{\text{sp}} \leq \frac{T_0}{2}. \end{aligned}$$

Combining the two situations, we have

$$\left\| \left(D(\tilde{N}^{(k)} - Q^* Q^{*\top}) \right)_{\mathcal{II}} \right\|_{\text{sp}} \leq \left\| \left(D(N^{(k)} - Q^* Q^{*\top}) \right)_{\mathcal{II}} \right\|_{\text{sp}} + \frac{T_0}{2}. \quad (\text{B.14})$$

Second, we bound $\left\| \left(D(N^{(k)} - Q^* Q^{*\top}) \right)_{\mathcal{II}} \right\|_{\text{sp}}$. Note that

$$\begin{aligned} \left\| \left(D(N^{(k)} - Q^* Q^{*\top}) \right)_{\mathcal{II}} \right\|_{\text{sp}} &= \left\| \left(D(\widehat{Q}^{(k)} \widehat{Q}^{(k)\top} - Q^* Q^{*\top}) \right)_{\mathcal{II}} \right\|_{\text{sp}} \\ &\leq \left\| D(\widehat{Q}^{(k)} \widehat{Q}^{(k)\top} - Q^* Q^{*\top}) \right\|_{\text{sp}}. \end{aligned} \quad (\text{B.15})$$

We focus on $\left\| D(\widehat{Q}^{(k)} \widehat{Q}^{(k)\top} - Q^* Q^{*\top}) \right\|_{\text{sp}}$. Define the projection matrix $P_Q = U^* U^{*\top}$ and $P_{Q^{(k)}} = \widehat{Q}^{(k)} (\widehat{Q}^{(k)\top} \widehat{Q}^{(k)})^{-1} \widehat{Q}^{(k)\top}$, we have $P_{Q^{(k)}} \widehat{Q}^{(k)} \widehat{Q}^{(k)\top} = \widehat{Q}^{(k)} \widehat{Q}^{(k)\top}$. Note the following decomposition,

$$\begin{aligned} D(\widehat{Q}^{(k)} \widehat{Q}^{(k)\top} - Q^* Q^{*\top}) &= D(P_Q (\widehat{Q}^{(k)} \widehat{Q}^{(k)\top} - Q^* Q^{*\top})) - D(P_{\widehat{Q}_{\perp}^{(k)}} Q^* Q^{*\top}) \\ &\quad + D((P_{\widehat{Q}^{(k)}} - P_Q) (\widehat{Q}^{(k)} \widehat{Q}^{(k)\top} - Q^* Q^{*\top})). \end{aligned}$$

By Lemma A.3 and (B.11), we have

$$\begin{aligned} \|D\left(P_Q\left(\widehat{Q}^{(k)}\widehat{Q}^{(k)\top} - Q^*Q^{*\top}\right)\right)\|_{\text{sp}} &\leq \sqrt{I(U^*)}\left\|\widehat{Q}^{(k)}\widehat{Q}^{(k)\top} - Q^*Q^{*\top}\right\|_{\text{sp}} \\ &\leq \frac{25\sqrt{2}\lambda_1^*}{4\lambda_r^*}\sqrt{\frac{sr}{s^*}I(U^*)}W^{(k-1)}. \end{aligned} \quad (\text{B.16})$$

By Lemmas A.3, A.5 and (B.11), we have

$$\left\|D\left(P_{\widehat{Q}_\perp^{(k)}}Q^*Q^{*\top}\right)\right\|_{\text{sp}} \leq 2\sqrt{I(U^*)}\left\|\widehat{Q}^{(k)}\widehat{Q}^{(k)\top} - Q^*Q^{*\top}\right\|_{\text{sp}} \leq \frac{25\sqrt{2}\lambda_1^*}{2\lambda_r^*}\sqrt{\frac{sr}{s^*}I(U^*)}W^{(k-1)}. \quad (\text{B.17})$$

By (B.11) and (B.12), we have

$$\begin{aligned} &\left\|D\left(P_{\widehat{Q}^{(k)}} - P_Q\right)\left(\widehat{Q}^{(k)}\widehat{Q}^{(k)\top} - Q^*Q^{*\top}\right)\right\|_{\text{sp}} \\ &\leq \left\|P_{\widehat{Q}^{(k)}} - P_Q\right\|_{\text{sp}}\left\|\widehat{Q}^{(k)}\widehat{Q}^{(k)\top} - Q^*Q^{*\top}\right\|_{\text{sp}} \\ &\leq \frac{25\sqrt{2}\lambda_1^*}{4\lambda_r^*}\sqrt{\frac{sr}{s^*}W^{(k-1)}}\left\|\widehat{Q}^{(k)}\left(\widehat{Q}^{(k)\top}\widehat{Q}^{(k)}\right)^{-1}\widehat{Q}^{(k)\top} - U^*U^{*\top}\right\|_{\text{sp}} \\ &\leq \frac{625\lambda_1^{*2}sr}{8\lambda_r^{*4}s^*}W^{(k-1)^2}. \end{aligned} \quad (\text{B.18})$$

Combining (B.15), (B.16), (B.17) and (B.18), we have

$$\left\|\left(D(N^{(k)} - Q^*Q^{*\top})\right)_{\mathcal{II}}\right\|_{\text{sp}} \leq \frac{75\lambda_1^*}{4\lambda_r^*}\sqrt{\frac{sr}{s^*}I(U^*)}W^{(k-1)} + \frac{625\lambda_1^{*2}sr}{16\lambda_r^{*4}s^*}W^{(k-1)^2}. \quad (\text{B.19})$$

Moreover, by combining (B.13), (B.14) and (B.19), we obtain that

$$W^{(k)} \leq \frac{3}{2}T_0 + \frac{75\sqrt{2}\lambda_1^*}{4\lambda_r^*}\sqrt{\frac{sr}{s^*}I(U^*)}W^{(k-1)} + \frac{625\lambda_1^{*2}sr}{8\lambda_r^{*4}s^*}W^{(k-1)^2}. \quad (\text{B.20})$$

Finally, since (B.9) holds for $k-1$, we have

$$\begin{aligned} W^{(k)} &\leq \frac{3}{2}T_0 + \frac{75\sqrt{2}\lambda_1^*}{4\lambda_r^*}\sqrt{\frac{sr}{s^*}I(U^*)}\left(6T_0 + \frac{c'_2s^*\lambda_1^{*2}}{2^{k-1}sr}\right) + \frac{625\lambda_1^{*2}sr}{8\lambda_r^{*4}s^*}\left(6T_0 + \frac{c'_2s^*\lambda_1^{*2}}{2^{k-1}sr}\right)^2 \\ &\leq \left(\frac{3}{2} + \frac{225\sqrt{2}\lambda_1^*}{2\lambda_r^*}\sqrt{\frac{sr}{s^*}I(U^*)} + \frac{1875\lambda_1^{*4}c'_2}{2^{k+1}\lambda_r^{*4}} + \frac{5625\lambda_1^{*2}sr}{2\lambda_r^{*4}s^*}T_0\right)T_0 \\ &\quad + \left(\frac{75\sqrt{2}\lambda_1^*}{2\lambda_r^*}\sqrt{\frac{sr}{s^*}I(U^*)} + \frac{625\lambda_1^{*4}c'_2}{2^{k+1}\lambda_r^{*4}}\right)\frac{c'_2s^*\lambda_1^{*2}}{2^k sr}. \end{aligned}$$

Using the bounds $I(U^*) \leq \frac{c_1}{r} \leq \frac{c'_2s}{s'r}$ and c'_2 is sufficiently small, along with the assumption $s \log d \ll n$, we obtain that, for $k \geq 1$,

$$\begin{cases} \frac{3}{2} + \frac{225\sqrt{2}\lambda_1^*}{2\lambda_r^*}\sqrt{\frac{sr}{s^*}I(U^*)} + \frac{1875\lambda_1^{*4}c'_2}{2^{k+1}\lambda_r^{*4}} + \frac{5625\lambda_1^{*2}sr}{2\lambda_r^{*4}s^*}T_0 \leq 6 \\ \frac{75\sqrt{2}\lambda_1^*}{2\lambda_r^*}\sqrt{\frac{sr}{s^*}I(U^*)} + \frac{625\lambda_1^{*4}c'_2}{2^{k+1}\lambda_r^{*4}} \leq 1. \end{cases}$$

Therefore,

$$W^{(k)} \leq 6T_0 + \frac{c'_2 s^* \lambda_1^{*2}}{2^k s r}.$$

Furthermore, we verify that $W^{(k)}$ and $\widehat{Q}^{(k)}$ satisfy the conditions required in Theorem 3.1. First, since $W^{(k)} \leq 6T_0 + \frac{c'_2 s^* \lambda_1^{*2}}{2^k s r}$, and by $s \log d \ll n$ and c'_2 is sufficiently small, it follows that $W^{(k)} \leq \frac{c_3 \lambda_r^{*3}}{\lambda_1^* \sqrt{r}}$. Second, from (B.11), we have,

$$\left\| \widehat{Q}^{(k)} \widehat{Q}^{(k)\top} - Q^* Q^{*\top} \right\|_F \leq \frac{25\lambda_1^*}{4\lambda_r^*} \sqrt{\frac{sr}{s^*}} W^{(k-1)} \leq \frac{\lambda_r^{*3}}{20\lambda_1^*}.$$

Thus, both conditions are satisfied, and the induction is complete.

Substituting $T_0 = 2c'_1(\lambda_1^{*2} + \sigma_{(1)}^{*2}) \left(\sqrt{\frac{s \log d}{n}} + \frac{s^2 \log d}{n} \right)$, we perform $K = \Omega(\log n)$ iterations. By Assumptions 3.1 and 3.2, and (B.11), we have,

$$\left\| \widehat{Q}^{(K)} \widehat{Q}^{(K)\top} - Q^* Q^{*\top} \right\|_F \lesssim \frac{\lambda_1^*}{\lambda_r^*} \sqrt{\frac{sr}{s^*}} (\lambda_1^{*2} + \sigma_{(1)}^{*2}) \left(\sqrt{\frac{s \log d}{n}} + \frac{s^2 \log d}{n} \right) \lesssim \frac{s}{s^*} \sqrt{\frac{s^* r \log d}{n}}.$$

This completes the proof of Theorem 3.2. \square

B.3 Proof of Corollary 3.1

Proof. Our proof focuses on the estimator from the outer iteration. This is sufficient, because the inner loop's gradient descent converges to the global minimizer with a high probability. As established in Lemma B.6, this convergence is guaranteed because the loss function (3.1) is convex with a high probability. We still consider the loss $\mathcal{L}(V)$ in (B.4), and perform Algorithm 1 without the hard thresholding step.

Similar as before, we define the event Ω_2 as

$$\Omega_2 = \left\{ \left\| M - Q^* Q^{*\top} - \Sigma \right\|_{\text{sp}} \leq c'_3 (\lambda_1^{*2} + \sigma_{(1)}^{*2}) \sqrt{\frac{d + c'_4}{n}} \right\},$$

where $c'_4 = o(n)$ is a positive constant. The following lemma ensures that Ω_2 occurs with a high probability.

Lemma B.5. *Suppose $d < n$. There exist constants $c'_3, c'_4 > 0$ and $c'_4 = o(n)$, such that $\mathbb{P}(\Omega_2) \geq 1 - ce^{-c'_4 \sqrt{d+c'_4} (\frac{\sqrt{n}}{d} \wedge \sqrt{d+c'_4})}$.*

Under Ω_2 , the next lemma characterizes the solution for the inner iteration.

Lemma B.6. *Suppose Assumptions 3.2 and 3.5 hold, and that $r \ll n$ and $d \ll n$. Let \widehat{V} be the minimizer of the loss (B.4). Then, with probability at least $1 - ce^{-c'_4 \sqrt{d+c'_4} (\frac{\sqrt{n}}{d} \wedge \sqrt{d+c'_4})}$,*

we have

$$\widehat{V}\widehat{V}^\top = \frac{1}{\lambda} \text{rank}_r (\Delta(M) + P^2 D(M)). \quad (\text{B.21})$$

Accordingly, when we set $\lambda = 1$ and choose the masking parameter as (2.6) during the k th outer iteration, denoting $\widehat{Q}^{(k)}$ as the output of the k th outer iteration, we have

$$\left(P^{(k)^2} D(M) \right)_{e,e} = \begin{cases} M_{e,e} & \text{when } N_{e,e}^{(k-1)} \geq M_{e,e} \\ N_{e,e}^{(k-1)} & \text{when } N_{e,e}^{(k-1)} < M_{e,e} \end{cases}$$

where $P^{(k)} = \text{diag}(p_1^{(k)}, \dots, p_d^{(k)})$, and $N^{(k-1)} = \widehat{Q}^{(k-1)} \widehat{Q}^{(k-1)\top}$.

Moreover, denote $\tilde{N}^{(k-1)} = \Delta(M) + P^{(k)^2} D(M)$, and $\tilde{N}^{(0)} = N^{(0)} = \Delta(M)$. So we take $\lambda = 1$, the solution of loss B.4 at the k th outer iteration is $N^{(k)} = \text{rank}_r(\tilde{N}^{(k-1)})$.

Next, we analyze the initial error $W^{(0)} = \left\| \tilde{N}^{(0)} - Q^* Q^{*\top} \right\|_{\text{sp}}$, and the evolution of iterations' error $W^{(k)} = \left\| \tilde{N}^{(k)} - Q^* Q^{*\top} \right\|_{\text{sp}}$.

For the initial error $W^{(0)}$, we have

$$W^{(0)} = \left\| \Delta(M) - \Delta(Q^* Q^{*\top}) \right\|_{\text{sp}} + \left\| D(Q^* Q^{*\top}) \right\|_{\text{sp}} \leq T_0 + \lambda_1^{*2} I(U^*),$$

where $T_0 = 2c_1(\lambda_1^{*2} + \sigma_{(1)}^{*2})\sqrt{\frac{d+c'_4}{n}}$ by (B.35).

Next, we establish an upper bound for $W^{(k)}$ based on $W^{(k-1)}$. Since

$$\begin{aligned} W^{(k)} &= \left\| \left(\tilde{N}^{(k)} - Q^* Q^{*\top} \right)_{\mathcal{II}} \right\|_{\text{sp}} \leq \left\| \left(\Delta(M) - Q^* Q^{*\top} - \Sigma \right)_{\mathcal{II}} \right\|_{\text{sp}} + \\ &\quad \left\| \left(D(\tilde{N}^{(k)} - Q^* Q^{*\top}) \right)_{\mathcal{II}} \right\|_{\text{sp}} = T_0 + \left\| \left(D(\tilde{N}^{(k)} - Q^* Q^{*\top}) \right)_{\mathcal{II}} \right\|_{\text{sp}}, \end{aligned} \quad (\text{B.22})$$

we only need to analyze the diagonal term.

First, we bound the difference between

$$\left\| D(\tilde{N}^{(k)}) - D(Q^* Q^{*\top}) \right\|_{\text{sp}} \quad \text{and} \quad \left\| D(N^{(k)}) - D(Q^* Q^{*\top}) \right\|_{\text{sp}}.$$

Since $D(\tilde{N}^{(k)})$, $D(Q^* Q^{*\top})$ and $D(N^{(k)})$ are all diagonal and positive semi-definite, we can analyze the difference by computing each entry.

If $N_{e,e}^{(k)} \geq (Q^* Q^{*\top})_{e,e}$, we have

$$\left| \min\{M_{e,e}, N_{e,e}^{(k)}\} - (Q^* Q^{*\top})_{e,e} \right| \leq \left| N_{e,e}^{(k)} - (Q^* Q^{*\top})_{e,e} \right|, \text{i.e.}$$

$$\left| \tilde{N}_{e,e}^{(k)} - (Q^* Q^{*\top})_{e,e} \right| \leq \left| N_{e,e}^{(k)} - (Q^* Q^{*\top})_{e,e} \right|.$$

If $D(N^{(k)})_{e,e} < D(Q^*Q^{*\top})_{e,e}$, only when $D(M)_{e,e} < D(N^{(k)})_{e,e} < D(Q^*Q^{*\top})_{e,e}$, we have

$$D(Q^*Q^{*\top})_{e,e} - D(M)_{e,e} > D(Q^*Q^{*\top})_{e,e} - D(N^{(k)})_{e,e}.$$

In this situation,

$$\begin{aligned} D(Q^*Q^{*\top})_{e,e} - D(M)_{e,e} &\leq D(Q^*Q^{*\top} + \Sigma)_{e,e} - D(M)_{e,e} \leq \left\| D(Q^*Q^{*\top} + \Sigma) - D(M) \right\|_{\text{sp}} \\ &\leq \left\| Q^*Q^{*\top} + \Sigma - M \right\|_{\text{sp}} \leq \frac{T_0}{2}. \end{aligned}$$

Combining the two situations, we have

$$\left\| D(\tilde{N}^{(k)}) - D(Q^*Q^{*\top}) \right\|_{\text{sp}} \leq \left\| D(N^{(k)}) - D(Q^*Q^{*\top}) \right\|_{\text{sp}} + \frac{T_0}{2}. \quad (\text{B.23})$$

Second, we bound $\left\| D(N^{(k)}) - D(Q^*Q^{*\top}) \right\|_{\text{sp}}$. Denote $\tilde{U}^{(k)}$ as the first r th eigenvector of $\tilde{N}^{(k)}$. Then by definition,

$$D(N^{(k)} - Q^*Q^{*\top}) = D\left(P_{\tilde{U}^{(k-1)}}\tilde{N}^{(k-1)} - Q^*Q^{*\top}\right).$$

We decompose

$$Q^*Q^{*\top} = P_{\tilde{U}^{(k-1)}}Q^*Q^{*\top} + P_{\tilde{U}_{\perp}^{(k-1)}}Q^*Q^{*\top}.$$

Then

$$D(N^{(k)} - Q^*Q^{*\top}) = D\left(P_{\tilde{U}^{(k-1)}}\left(\tilde{N}^{(k-1)} - Q^*Q^{*\top}\right)\right) - D\left(P_{\tilde{U}_{\perp}^{(k-1)}}Q^*Q^{*\top}\right).$$

Next, we analyze $D\left(P_{\tilde{U}^{(k-1)}}\left(\tilde{N}^{(k-1)} - Q^*Q^{*\top}\right)\right)$. Let $P_{\tilde{U}^{(k-1)}} = P_{U^*} + (P_{\tilde{U}^{(k-1)}} - P_{U^*})$.

Then

$$\begin{aligned} D(N^{(k)} - Q^*Q^{*\top}) &= D\left(P_{U^*}\left(\tilde{N}^{(k-1)} - Q^*Q^{*\top}\right)\right) - D\left(P_{\tilde{U}_{\perp}^{(k-1)}}Q^*Q^{*\top}\right) \\ &\quad + D\left((P_{\tilde{U}^{(k-1)}} - P_{U^*})\left(\tilde{N}^{(k-1)} - Q^*Q^{*\top}\right)\right). \end{aligned}$$

By Lemma A.3,

$$\left\| D(P_{U^*}\left(\tilde{N}^{(k-1)} - Q^*Q^{*\top}\right)) \right\|_{\text{sp}} \leq \sqrt{I(U^*)} \left\| \tilde{N}^{(k-1)} - Q^*Q^{*\top} \right\|_{\text{sp}} = \sqrt{I(U^*)} W^{(k-1)}. \quad (\text{B.24})$$

By Lemmas A.3 and A.5,

$$\begin{aligned} \left\| D(P_{\tilde{U}_{\perp}^{(k-1)}}Q^*Q^{*\top}) \right\|_{\text{sp}} &= \left\| D(P_{\tilde{U}_{\perp}^{(k-1)}}Q^*Q^{*\top}P_Q) \right\|_{\text{sp}} \leq \sqrt{I(U^*)} \left\| P_{\tilde{U}_{\perp}^{(k-1)}}Q^*Q^{*\top} \right\|_{\text{sp}} \\ &\leq 2\sqrt{I(U^*)} \left\| \tilde{N}^{(k-1)} - Q^*Q^{*\top} \right\|_{\text{sp}} = 2\sqrt{I(U^*)} W^{(k-1)}. \end{aligned} \quad (\text{B.25})$$

Note that

$$\begin{aligned}
\left\| \tilde{U}^{(k-1)} \tilde{U}^{(k-1)\top} - U^{*\top} \right\|_{\text{sp}} &\leq 2 \left\| \sin \Theta(\tilde{U}^{(k-1)}, U^*) \right\|_{\text{sp}} = 2 \left\| \tilde{U}_{\perp}^{(k-1)\top} U^* \right\|_{\text{sp}} \\
&\leq 2 \left\| \tilde{U}_{\perp}^{(k-1)\top} U^* U^{*\top} Q^* Q^{*\top} \right\| \cdot \sigma_r^{-1}(U^{*\top} Q^* Q^{*\top}) \\
&\leq 2 \left\| \tilde{U}_{\perp}^{(k-1)\top} Q^* Q^{*\top} \right\| \cdot \sigma_r^{-1}(Q^* Q^{*\top}) \\
&\leq \frac{4}{\lambda_r^{*2}} \left\| \tilde{N}^{(k-1)} - Q^* Q^{*\top} \right\|_{\text{sp}}
\end{aligned}$$

Then

$$\|D(P_{\tilde{U}^{(k-1)}} - P_{U^*})(\tilde{N}^{(k-1)} - Q^* Q^{*\top})\|_{\text{sp}} \leq \|P_{\tilde{U}^{(k-1)}} - P_{U^*}\|_{\text{sp}} W^{(k-1)} \leq \frac{4}{\lambda_r^{*2}} W^{(k-1)^2}. \quad (\text{B.26})$$

Combining (B.24), (B.25) and (B.26), we have

$$\left\| D(N^{(k)}) - D(Q^* Q^{*\top}) \right\|_{\text{sp}} \leq 3\sqrt{I(U^*)} W^{(k-1)} + \frac{4}{\lambda_r^{*2}} W^{(k-1)^2} \quad (\text{B.27})$$

Moreover, combining (B.22), (B.23) and (B.27), we obtain that

$$W^{(k)} \leq \frac{3}{2} T_0 + 3\sqrt{I(U^*)} W^{(k-1)} + \frac{4}{\lambda_r^{*2}} W^{(k-1)^2}. \quad (\text{B.28})$$

Finally, we use induction to show $W^{(k)} \leq 3T_0 + 2^{-k-7}\lambda_r^{*2}$.

We start with the base case of $k = 0$. By Assumption 3.5, $W^{(0)} \leq T_0 + \lambda_1^{*2} I(U^*) \leq 3T_0 + 2^{-7}\lambda_r^{*2}$.

We then continue with the induction step. Suppose $W^{(k-1)} \leq 3T_0 + 2^{-k-6}\lambda_r^{*2}$. We have

$$\begin{aligned}
W^{(k)} &\leq \frac{3}{2} T_0 + 3\sqrt{I(U^*)} \left(3T_0 + 2^{-k-6}\lambda_r^{*2} \right) + \frac{4}{\lambda_r^{*2}} \left(3T_0 + 2^{-k-6}\lambda_r^{*2} \right)^2 \\
&= \frac{3}{2} T_0 + 9\sqrt{I(U^*)} T_0 + 6\sqrt{I(U^*)} 2^{-k-7}\lambda_r^{*2} + 3 \cdot 2^{-k-4} T_0 + \frac{36}{\lambda_r^{*2}} T_0^2 + 2^{-k-3} 2^{-k-7}\lambda_r^{*2} \\
&= \left(\frac{3}{2} + 9\sqrt{I(U^*)} + 3 \cdot 2^{-k-4} + \frac{36}{\lambda_r^{*2}} T_0 \right) T_0 + \left(6\sqrt{I(U^*)} + 2^{-k-3} \right) 2^{-k-7}\lambda_r^{*2}
\end{aligned}$$

By Assumption 3.5, $r \ll n$ and $d \ll n$, we have $\sqrt{I(U^*)} \leq \frac{1}{12}$ and $T_0 \leq \frac{\lambda_r^{*2}}{72}$. Therefore, for any $k \geq 1$,

$$\begin{cases} \frac{3}{2} + 9\sqrt{I(U^*)} + 3 \cdot 2^{-k-4} + \frac{36}{\lambda_r^{*2}} T_0 \leq 3 \\ 6\sqrt{I(U^*)} + 2^{-k-3} \leq 1. \end{cases}$$

We have $W^{(k)} \leq 3T_0 + 2^{-k-7}\lambda_r^{*2}$. Furthermore, by applying (B.27) again, we obtain that

$$\left\| N^{(k+1)} - Q^* Q^{*\top} \right\|_{\text{sp}} \leq T_0 + 3\sqrt{I(U^*)} W^{(k)} + \frac{4}{\lambda_r^{*2}} R^{(k)^2} \leq 3T_0 + 2^{-k-8}\lambda_r^{*2},$$

which implies that

$$\left\| \widehat{Q}^{(k+1)} \widehat{Q}^{(k+1)\top} - Q^* Q^{*\top} \right\|_{\text{sp}} \leq 3T_0 + 2^{-k-8} \lambda_r^{*2}.$$

Since $T_0 = 2c'_3(\lambda_1^{*2} + \sigma_{(1)}^{*2})\sqrt{\frac{d+c'_4}{n}}$, we perform $K = O(\log n)$ iterations. Then

$$\left\| \widehat{Q}^{(K)} \widehat{Q}^{(K)\top} - Q^* Q^{*\top} \right\|_{\text{sp}} \lesssim (\lambda_1^{*2} + \sigma_{(1)}^{*2})\sqrt{\frac{d+c'_4}{n}}.$$

By taking $c'_4 = d$, with probability at least $1 - ce^{-c\sqrt{\frac{n}{d}}\wedge d}$, we obtain that,

$$\left\| \widehat{Q}^{(K)} \widehat{Q}^{(K)\top} - Q^* Q^{*\top} \right\|_{\text{sp}} \lesssim \sqrt{\frac{d}{n}}.$$

This completes the proof of Corollary 3.1. \square

B.4 Proofs of supporting lemmas

B.4.1 Proof of Lemma B.1

Proof. Note that we can rewrite the expected loss $\mathcal{L}(V)$ in (3.1) as

$$\begin{aligned} \mathcal{L}(V) &= -\frac{1}{n} \mathbb{E}_A \left[\langle V^\top A X, V^\top (I - A) X \rangle \right] + \frac{1}{n^2} \mathbb{E}_A \left[\langle V^\top A X 1_n, V^\top (I - A) X 1_n \rangle \right] + \Pi(V) \\ &= \mathbb{E}_A \left[-\frac{1}{n} \text{tr} \left(X^\top A^\top V V^\top (I - A) X \right) + \frac{1}{n^2} \text{tr} \left(1_n^\top X^\top A^\top V V^\top (I - A) X 1_n \right) \right] + \Pi(V) \\ &= \frac{\lambda}{8} \|V V^\top\|_F^2 - \mathbb{E}_A \left[\frac{1}{n} \text{tr} \left(G^\top G (I - A) X X^\top A^\top \right) - \frac{1}{n^2} \text{tr} \left(V V^\top (I - A) X 1_n 1_n^\top X^\top A^\top \right) \right] \\ &= \frac{\lambda}{8} \mathbb{E}_A \left[\left\| V V^\top - \frac{4}{\lambda} (I - A) \left(\frac{1}{n} X X^\top - \frac{1}{n^2} X 1_n 1_n^\top X^\top \right) A \right\|_F^2 + C(X, A) \right]. \end{aligned}$$

Consider the matrix $(I - A)MA$. For the off-diagonal entry (e, e') , $e \neq e'$, we have

$$\mathbb{E}[(1 - a_e)(a_{e'})M_{e,e'}] = \mathbb{E}[(1 - a_e)]\mathbb{E}[a_{e'}]M_{e,e'} = \frac{1}{4}M_{e,e'}.$$

For the diagonal entry (e, e) , we have

$$\mathbb{E}[(1 - a_e)a_e M_{e,e}] = \mathbb{E}[(1 - a_e)a_e]M_{e,e} = \frac{p_e^2}{4}M_{e,e}.$$

Then, we can further rewrite the loss as

$$\mathcal{L}(V) = \frac{\lambda}{8} \left\| V V^\top - \frac{1}{\lambda} (\Delta(M) + P^2 D(M)) \right\|_F^2 + C(X).$$

This completes the proof of Lemma B.1. \square

B.4.2 Proof of Lemma B.2

Proof. Due to the sparsity of $\widehat{V}_{(t)}, \tilde{V}_{(t)}$, at step t , we can consider the restricted loss function,

$$f_t(L) = \frac{\lambda}{2} \left\| LL^\top - \frac{1}{\lambda} N_{(t)} \right\|_F^2,$$

where we denote $N_{S_{(t)}S_{(t)}}$ by $N_{(t)}$ for simplicity in the proof.

We begin with the gradient expression,

$$\frac{1}{2} \nabla f_t(L) = -N_{(t)}L + \lambda LL^\top L. \quad (\text{B.29})$$

Let $L_{(t)} = \tilde{V}_{t,S_{(t)}*}$. During the gradient descent, the update rule becomes $L_{(t+1)} = L_{(t)} - \eta \nabla f_t(L_{(t)})$. We have that $L_{(t+1)} = V_{(t+1),S_{(t)}*}$, which holds because $\text{supp}(\tilde{V}_{(t)}) \subseteq S_{(t)}$. So we work on the distance involving $L_{(t)}$ and $L_{(t+1)}$.

We leverage Lemma A.20. First, we define the minimizer of $f_t(L)$ as $L_{(t)}^*$. Under the condition $\|N_{(t)} - (Q^*Q^{*\top})_{S_{(t)}S_{(t)}}\|_{\text{sp}} \leq W^{(k-1)} < \frac{\lambda_r^{*2}}{4} < \frac{\lambda_r^{*2}}{2}$, applying the Weyl's inequality in Lemma A.6, we have the following eigenvalue bounds for $\tilde{N}_{(t)}$

$$\lambda_i(N_{(t)}) > \frac{\lambda_r^{*2}}{2}, \quad i \leq r, \quad \lambda_i(N_{(t)}) > -\frac{\lambda_r^{*2}}{2}, \quad i > r,$$

where $\lambda_j(A)$ is the j th largest eigenvalue value of A . This implies that the largest r eigenvalues of $N_{(t)}$ are also the largest r singular values. By Lemma A.1,

$$L_{(t)}^* L_{(t)}^{*\top} = \widehat{Q}_{S_{(t)}*}(S_{(t)}) \frac{\widehat{\Lambda}_r(S_{(t)})}{\lambda} \widehat{Q}_{S_{(t)}*}(S_{(t)})^\top.$$

Then we can take $L_{(t)}^* = \widehat{V}_{S_{(t)}*}(S_{(t)})$, up to an orthogonal transformation.

Next, we check the conditions in Lemma A.20 one by one. It is straightforward to verify the condition $\nabla f_t(L)P = \nabla f_t(LP)$ by (B.29). Next we derive the expression for $\text{vec}(Z)^\top \nabla^2 f_t(L) \text{vec}(Z)$. The gradient expression in the vectorized form is

$$\frac{1}{2} \text{vec} \nabla f_t(L) = -\left(I_r \otimes N_{(t)}\right) \text{vec}(L) + \lambda \left(I_r \otimes LL^\top\right) \text{vec}(L).$$

For the first term,

$$\frac{\partial -\left(I_r \otimes N_{(t)}\right) \text{vec}(L)}{\partial \text{vec}(L)} = -I_r \otimes N_{(t)}.$$

Henceforth,

$$(z_1^\top \quad \cdots \quad z_r^\top) \begin{pmatrix} -N_{(t)} & 0 & \cdots & 0 \\ 0 & -N_{(t)} & \cdots & 0 \\ \vdots & \vdots & \ddots & \vdots \\ 0 & 0 & \cdots & -N_{(t)} \end{pmatrix} \begin{pmatrix} z_1 \\ \vdots \\ z_r \end{pmatrix} = \langle ZZ^\top, -N_{(t)} \rangle.$$

For the second term, recalling that $L \in \mathbb{R}^{d \times r}$, its vectorized form can be written as,

$$\text{vec}(L) = (l_1^\top, l_2^\top, \dots, l_r^\top)^\top,$$

where $l_i \in \mathbb{R}^d$ represents the i th column of L . Note that $LL^\top = \sum_{i=1}^r l_i l_i^\top$, and

$$(I_r \otimes LL^\top) \text{vec}(L) = \begin{pmatrix} \sum_{i=1}^r l_i l_i^\top l_1 \\ \sum_{i=1}^r l_i l_i^\top l_2 \\ \vdots \\ \sum_{i=1}^r l_i l_i^\top l_r \end{pmatrix}.$$

We then compute the gradient of $\sum_{i=1}^r l_i l_i^\top l_j$ with respect to l_j . When $j \neq k$,

$$\frac{\partial \sum_{i=1}^r l_i l_i^\top l_j}{\partial l_k} = \frac{\partial l_k l_k^\top l_j}{\partial l_k} = l_j^\top l_k I_d + l_j l_k^\top.$$

When $j = k$,

$$\frac{\partial \sum_{i=1}^r l_i l_i^\top l_j}{\partial l_k} = \frac{\partial \sum_{i=1}^r l_i l_i^\top l_j}{\partial l_j} = \frac{\partial l_j l_j^\top l_j}{\partial l_j} + \sum_{i \neq j} \frac{\partial l_i l_i^\top l_j}{\partial l_j} = LL^\top + l_j^\top l_j I_d + l_j l_j^\top.$$

Henceforth,

$$\begin{aligned} (z_1^\top \ \dots \ z_r^\top) \begin{pmatrix} LL^\top & 0 & \dots & 0 \\ 0 & LL^\top & \dots & 0 \\ \vdots & \vdots & \ddots & \vdots \\ 0 & 0 & \dots & LL^\top \end{pmatrix} \begin{pmatrix} z_1 \\ \vdots \\ z_r \end{pmatrix} &= \langle ZZ^\top, LL^\top \rangle, \\ (z_1^\top \ \dots \ z_r^\top) \begin{pmatrix} l_1^\top l_1 I_d & l_1^\top l_2 I_d & \dots & l_1^\top l_r I_d \\ l_2^\top l_1 I_d & l_2^\top l_2 I_d & \dots & l_2^\top l_r I_d \\ \vdots & \vdots & \ddots & \vdots \\ l_r^\top l_1 I_d & l_r^\top l_2 I_d & \dots & l_r^\top l_r I_d \end{pmatrix} \begin{pmatrix} z_1 \\ \vdots \\ z_r \end{pmatrix} &= \langle L^\top L, Z^\top Z \rangle, \\ (z_1^\top \ \dots \ z_r^\top) \begin{pmatrix} l_1 l_1^\top & l_1 l_2^\top & \dots & l_1 l_r^\top \\ l_2 l_1^\top & l_2 l_2^\top & \dots & l_2 l_r^\top \\ \vdots & \vdots & \ddots & \vdots \\ l_r l_1^\top & l_r l_2^\top & \dots & l_r l_r^\top \end{pmatrix} \begin{pmatrix} z_1 \\ \vdots \\ z_r \end{pmatrix} &= \langle Z^\top L, L^\top Z \rangle. \end{aligned}$$

Combining the above results together, we define

$$\begin{aligned} g_t(L, Z) &= \frac{1}{2} \text{vec}(Z)^\top \nabla^2 f_t(L) \text{vec}(Z) = \\ &\quad - \langle N_{(t)}, ZZ^\top \rangle + \lambda \langle ZZ^\top, LL^\top \rangle + \lambda \langle Z^\top Z, L^\top L \rangle + \lambda \langle Z^\top L, L^\top Z \rangle. \quad (\text{B.30}) \end{aligned}$$

Next, we verify the smoothness condition and the strong convexity condition under a proper radius condition.

For the smoothness condition, suppose $\|L - L_{(t)}^*\|_F \leq \delta$. By the condition $\|N_{(t)} - (Q^*Q^{*\top})_{S_{(t)}S_{(t)}}\|_{\text{sp}} \leq W^{(k-1)}$, we have

$$\begin{aligned} \|L_{(t)}^*\|_{\text{sp}} &= \|\widehat{V}_{S_{(t)}^*}(S_{(t)})\|_{\text{sp}} = \|\widehat{Q}_{S_{(t)}^*}(S_{(t)})\left(\frac{\widehat{\Lambda}_r(S_{(t)})}{\lambda}\right)^{\frac{1}{2}}\|_{\text{sp}} \leq \sqrt{\frac{\lambda_1^{*2} + W^{(k-1)}}{\lambda}}, \\ \lambda_{\max}(-N_{(t)}) &\leq W^{(k-1)}, \end{aligned}$$

where $\lambda_{\max}(A)$ is the maximum eigenvalue of A . We analyze each term.

$$\begin{aligned} \langle -N_{(t)}, ZZ^\top \rangle &\leq W^{(k-1)}\|Z\|_F^2, \\ \langle LL^\top, ZZ^\top \rangle &\leq \|LL^\top\|_{\text{sp}}\|Z\|_F^2 \leq \left(\delta + \sqrt{\frac{\lambda_1^{*2} + W^{(k-1)}}{\lambda}}\right)^2\|Z\|_F^2, \\ \langle L^\top L, ZZ^\top \rangle &\leq \|L^\top L\|_{\text{sp}}\|Z\|_F^2 \leq \left(\delta + \sqrt{\frac{\lambda_1^{*2} + W^{(k-1)}}{\lambda}}\right)^2\|Z\|_F^2, \\ \langle Z^\top L, L^\top Z \rangle &\leq \|Z^\top L\|_F\|L^\top Z\|_F \leq \|L\|_{\text{sp}}\|L^\top\|_{\text{sp}}\|Z\|_F^2 \leq \left(\delta + \sqrt{\frac{\lambda_1^{*2} + W^{(k-1)}}{\lambda}}\right)^2\|Z\|_F^2. \end{aligned}$$

Combining the above results, we have,

$$g_t(L, Z) \leq \left(W^{(k-1)} + 3\lambda\left(\delta + \sqrt{\frac{\lambda_1^{*2} + W^{(k-1)}}{\lambda}}\right)^2\right)\|Z\|_F^2.$$

We then choose

$$\beta = 2W^{(k-1)} + 6\lambda\left(\delta + \sqrt{\frac{\lambda_1^{*2} + W^{(k-1)}}{\lambda}}\right)^2.$$

For the strong convexity condition, denoting $\tilde{Z} = ZH_Z - L_{(t)}^*$, we have

$$\begin{aligned} g_t(L_{(t)}^*, \tilde{Z}) &= -\langle N_{(t)}, \tilde{Z}\tilde{Z}^\top \rangle + \lambda\langle L_{(t)}^*L_{(t)}^{*\top}, \tilde{Z}\tilde{Z}^\top \rangle + \lambda\langle L_{(t)}^{*\top}L_{(t)}^*, \tilde{Z}^\top \tilde{Z} \rangle + \lambda\langle \tilde{Z}^\top L_{(t)}^*, L_{(t)}^{*\top}\tilde{Z} \rangle \\ &= \underbrace{\langle \tilde{Z}\widehat{\Lambda}_r(S_{(t)})\tilde{Z}^\top, I \rangle}_{D_1} + \underbrace{\langle \lambda L_{(t)}^*L_{(t)}^{*\top} - N_{(t)}, \tilde{Z}\tilde{Z}^\top \rangle}_{D_1} + \underbrace{\lambda\langle \tilde{Z}^\top L_{(t)}^*, L_{(t)}^{*\top}\tilde{Z} \rangle}_{D_2} \end{aligned}$$

For D_1 , $L_{(t)}^*L_{(t)}^{*\top} = \widehat{Q}_{S_{(t)}^*}(S_{(t)})\frac{\widehat{\Lambda}_r(S_{(t)})}{\lambda}\widehat{Q}_{S_{(t)}^*}(S_{(t)})^\top$. Denote

$$N_{(t)} = \widehat{Q}_{S_{(t)}^*}(S_{(t)})\widehat{\Lambda}_r(S_{(t)})\widehat{Q}_{S_{(t)}^*}(S_{(t)})^\top + \widehat{Q}_{S_{(t)}^*}(S_{(t)})_\perp\widehat{\Lambda}_r(S_{(t)})\widehat{Q}_{S_{(t)}^*}(S_{(t)})_\perp^\top,$$

where we define the remaining eigenvectors by $\widehat{Q}_{S_{(t)}^*}(S_{(t)})_\perp$ and the rest of eigenvalues by the diagonal entries of $\widehat{\Lambda}_r(S_{(t)})$. Then,

$$\begin{aligned} D_1 &\geq (\lambda_r^{*2} - W^{(k-1)})\langle \tilde{Z}\tilde{Z}^\top, I \rangle + \langle -\widehat{Q}_{S_{(t)}^*}(S_{(t)})_\perp\widehat{\Lambda}_r(S_{(t)})\widehat{Q}_{S_{(t)}^*}(S_{(t)})_\perp^\top, \tilde{Z}\tilde{Z}^\top \rangle \\ &= \langle \tilde{Z}\tilde{Z}^\top, \widehat{Q}_{S_{(t)}^*}(S_{(t)})\left((\lambda_r^* - W^{(k-1)})I - \widehat{\Lambda}_r(S_{(t)})\right)\widehat{Q}_{S_{(t)}^*}(S_{(t)})^\top \rangle \\ &\geq (\lambda_r^{*2} - 2R^{(k-1)})\|\tilde{Z}\|_F^2 \end{aligned}$$

$$\begin{aligned}
D_2 &= \langle (ZH_Z - L_{(t)}^*)^\top L_{(t)}^*, L_{(t)}^{*\top} (ZH_Z - L_{(t)}^*) \rangle \\
&= \langle (ZH_Z)^\top L_{(t)}^*, L_{(t)}^{*\top} (ZH_Z) \rangle - 2 \langle L_{(t)}^{*\top} L_{(t)}^*, L_{(t)}^{*\top} ZH_Z \rangle + \langle L_{(t)}^{*\top} L_{(t)}^*, L_{(t)}^{*\top} L_{(t)}^* \rangle
\end{aligned}$$

By Lemma A.8, there exists Z_1 , such that $Z_1 Z_1 = L_{(t)}^{*\top} ZH_Z$. Then,

$$D_2 = \langle Z_1^\top Z_1, Z_1^\top Z_1 \rangle + \langle L_{(t)}^{*\top} L_{(t)}^*, L_{(t)}^{*\top} L_{(t)}^* \rangle - 2 \langle L_{(t)}^{*\top} L_{(t)}^*, Z_1 Z_1 \rangle = \|Z_1^\top Z_1 - L_{(t)}^{*\top} L_{(t)}^*\|_F^2 \geq 0$$

Now for a general L , we have,

$$\begin{aligned}
|g_t(L, \tilde{Z}) - g_t(L_{(t)}^*, \tilde{Z})| &\leq \lambda \left| \langle \tilde{Z} \tilde{Z}^\top, (LL^\top - L_{(t)}^* L_{(t)}^{*\top}) \rangle \right| + \lambda \left| \langle \tilde{Z}^\top \tilde{Z}, (L^\top L - L_{(t)}^{*\top} L_{(t)}^*) \rangle \right| \\
&\quad + \lambda \left| \langle \tilde{Z}^\top L, L^\top \tilde{Z} \rangle - \langle \tilde{Z}^\top L_{(t)}^*, L_{(t)}^{*\top} \tilde{Z} \rangle \right|.
\end{aligned}$$

For each of the three terms on the right-hand-side of the above equation, we have

$$\begin{aligned}
\left| \langle \tilde{Z} \tilde{Z}^\top, LL^\top - L_{(t)}^* L_{(t)}^{*\top} \rangle \right| &\leq \|\tilde{Z}\|_F^2 \|LL^\top - L_{(t)}^* L_{(t)}^{*\top}\|_{\text{sp}} \leq \|\tilde{Z}\|_F^2 (\|L\|_{\text{sp}} + \|L_{(t)}^{*\top}\|_{\text{sp}}) \|L - L_{(t)}^*\|_{\text{sp}}, \\
\left| \langle \tilde{Z}^\top \tilde{Z}, L^\top L - L_{(t)}^{*\top} L_{(t)}^* \rangle \right| &\leq \|\tilde{Z}\|_F^2 \|L^\top L - L_{(t)}^{*\top} L_{(t)}^*\|_{\text{sp}} \leq \|\tilde{Z}\|_F^2 (\|L^\top\|_{\text{sp}} + \|L_{(t)}^*\|_{\text{sp}}) \|L - L_{(t)}^*\|_{\text{sp}}, \\
\left| \langle \tilde{Z}^\top L, L^\top \tilde{Z} \rangle - \langle \tilde{Z}^\top L_{(t)}^*, L_{(t)}^{*\top} \tilde{Z} \rangle \right| &= \text{tr}(\tilde{Z}^\top \tilde{Z} L - \tilde{Z}^\top \tilde{Z} L_{(t)}^*) \\
&\leq \|\tilde{Z}\|_F^2 \|L + L_{(t)}^*\|_{\text{sp}} \|L - L_{(t)}^*\|_{\text{sp}} \leq \|\tilde{Z}\|_F^2 (\|L\|_{\text{sp}} + \|L_{(t)}^*\|_{\text{sp}}) \|L - L_{(t)}^*\|_{\text{sp}}.
\end{aligned}$$

Therefore,

$$|g_t(L, \tilde{Z}) - g_t(L_{(t)}^*, \tilde{Z})| \leq 3\lambda \left(\delta + 2\sqrt{\frac{\lambda_1^{*2} + W^{(k-1)}}{\lambda}} \right) \|L - L_{(t)}^*\|_F \|\tilde{Z}\|_F^2.$$

Then, under the radius condition $\|L - L_{(t)}^*\|_F \leq \delta$, we obtain that

$$g_t(L, \tilde{Z}) \geq \left(\lambda_r^{*2} - 2W^{(k-1)} - 3\lambda \left(\delta + 2\sqrt{\frac{\lambda_1^{*2} + W^{(k-1)}}{\lambda}} \right) \delta \right) \|\tilde{Z}\|_F^2.$$

Letting $\delta < \frac{\lambda_r^{*2}}{12\sqrt{\lambda(\lambda_1^{*2} + W^{(k-1)})}}$, we have that,

$$\lambda\delta^2 < \frac{\lambda_r^{*4}}{144(\lambda_1^{*2} + W^{(k-1)})} < \frac{\lambda_r^{*2}}{144}, \quad \lambda\delta\sqrt{\frac{\lambda_1^{*2} + W^{(k-1)}}{\lambda}} < \frac{\lambda_r^{*2}}{12}.$$

It implies that,

$$\begin{aligned}
\alpha &= 2\lambda_r^{*2} - 4W^{(k-1)} - 6\lambda\delta^2 - 6\lambda\delta\sqrt{\frac{\lambda_1^{*2} + W^{(k-1)}}{\lambda}} \geq \frac{17}{12}\lambda_r^{*2} - 4W^{(k-1)}, \\
\beta &= 2W^{(k-1)} + 6\lambda\delta^2 + 6(\lambda_1^{*2} + W^{(k-1)}) + 12\lambda\delta\sqrt{\frac{\lambda_1^{*2} + W^{(k-1)}}{\lambda}} \\
&\leq 8W^{(k-1)} + \left(\frac{1}{12} + 6 + 1 \right) \lambda_1^{*2} = 8W^{(k-1)} + \frac{85}{12}\lambda_1^{*2}.
\end{aligned}$$

When $\eta \leq \frac{1}{8W^{(k-1)} + \frac{85}{12}\lambda_1^{*2}}$, expanding the matrix of size $|S_{(t)}| \times r$ to $d \times r$ by filling in zeros, we obtain that

$$\text{dist}^2(\widehat{V}_{(t+1)}^o, \widehat{V}(S_{(t)})) \leq \left(1 - \eta \left(\frac{17}{12}\lambda_r^{*2} - 4W^{(k-1)}\right)\right) \text{dist}^2(\widehat{V}_{(t)}, \widehat{V}(S_{(t)})).$$

This completes the proof of B.2. \square

B.4.3 Proof of Lemma B.4

Proof. We control the error on the subset \mathcal{I} of $M - Q^*Q^{*\top} - \Sigma$. For a fixed \mathcal{I} , applying the concentration inequality of Wishart-type matrices in Lemma A.12, and taking $x = \sqrt{\frac{2s+s^*+c}{n}}$, we have

$$\mathbb{P}\left(\left\|\left(\frac{1}{n}XX^\top - \mathbb{E}\left[\frac{1}{n}XX^\top\right]\right)_{\mathcal{I}\mathcal{I}}\right\|_{\text{sp}} \gtrsim (\lambda_1^{*2} + \sigma_{(1)}^{*2})\sqrt{\frac{2s+s^*+c}{n}}\right) \lesssim e^{-(2s+s^*+c)}.$$

Taking $c = 2(2s+s^*)\log\frac{de}{2s+s^*}$, we obtain that

$$\begin{aligned} \mathbb{P}\left(\left\|\left(\frac{1}{n}XX^\top - \mathbb{E}\left[\frac{1}{n}XX^\top\right]\right)_{\mathcal{I}\mathcal{I}}\right\|_{\text{sp}} \gtrsim (\lambda_1^{*2} + \sigma_{(1)}^{*2})\sqrt{\frac{(2s+s^*)\log d}{n}}\right) \\ \lesssim \left(\frac{2s+s^*}{de}\right)^{2s+s^*} e^{-(2s+s^*)\log d}. \end{aligned} \quad (\text{B.31})$$

Moreover,

$$\mathbb{P}\left(\|\tilde{x}_{\mathcal{I}}\|_2^2 \geq (\lambda_1^{*2} + \sigma_{(1)}^{*2})x^2\right) \leq e^{-\frac{x^2 n}{2(2s+s^*)}}.$$

Taking $x^2 = 4\frac{(2s+s^*)^2 \log d}{n}$, we have

$$\mathbb{P}\left(\|\tilde{x}_{\mathcal{I}}\|_2^2 \gtrsim (\lambda_1^{*2} + \sigma_{(1)}^{*2})\frac{(2s+s^*)^2 \log d}{n}\right) \lesssim \left(\frac{2s+s^*}{de}\right)^{2s+s^*} e^{-(2s+s^*)\log d}. \quad (\text{B.32})$$

Combining (B.31) and (B.32) and $s' \geq s$, we obtain that

$$\begin{aligned} \mathbb{P}\left(\left\|(M - Q^*Q^{*\top} - \Sigma)_{\mathcal{I}\mathcal{I}}\right\|_{\text{sp}} \gtrsim (\lambda_1^{*2} + \sigma_{(1)}^{*2})\left(\sqrt{\frac{s \log d}{n}} + \frac{s^2 \log d}{n}\right)\right) \\ \lesssim \left(\frac{2s+s^*}{de}\right)^{2s+s^*} e^{-(2s+s^*)\log d}. \end{aligned}$$

Since there are $\binom{d}{2s+s^*}$ possible subsets, we use the union bound to get

$$\begin{aligned} \mathbb{P}\left(\left\|(M - Q^*Q^{*\top} - \Sigma)_{\mathcal{I}\mathcal{I}}\right\|_{\text{sp}} \gtrsim (\lambda_1^{*2} + \sigma_{(1)}^{*2})\left(\sqrt{\frac{s \log d}{n}} + \frac{s^2 \log d}{n}\right), \right. \\ \left. \exists \mathcal{I} \subset [d] \text{ with } |\mathcal{I}| = 2s+s^*\right) \lesssim \binom{d}{2s+s^*} \left(\frac{2s+s^*}{de}\right)^{2s+s^*} e^{-(2s+s^*)\log d}. \end{aligned}$$

Using the binomial coefficient bound

$$\binom{d}{2s+s^*} \leq \left(\frac{de}{2s+s^*}\right)^{2s+s^*},$$

there exist $c'_1 > 0$, such that $\mathbb{P}(\Omega_1) \geq 1 - ce^{-cs \log d}$.

This completes the proof of Lemma B.4. \square

B.4.4 Proof of Lemma B.5

Proof. Since $x_i = Qz_i + \xi_i$, we have $\text{Cov}(x_i) = Q^*Q^{*\top} + \Sigma$. Moreover, z_i and ξ_i are the sub-Gaussian random vectors with parameters λ_1^{*2} and $\sigma_{(1)}^{*2}$. Therefore, x_i is also the sub-Gaussian random vector with the parameter $\lambda_1^{*2} + \sigma_{(1)}^{*2}$. Write

$$M - Q^*Q^{*\top} - \Sigma = \frac{1}{n}XX^\top - Q^*Q^{*\top} - \Sigma - \frac{1}{n}\bar{X}\bar{X}^\top,$$

where $\bar{X} = \frac{1}{n}X1_n1_n^\top$.

First, we note that $\mathbb{E}[\frac{1}{n}XX^\top] = Q^*Q^{*\top} + \Sigma$. Applying the concentration inequality of Wishart-type matrices in Lemma A.12, and taking $x = \sqrt{\frac{d+c'_4}{n}}$, we obtain that

$$\mathbb{P}\left(\left\|\frac{1}{n}XX^\top - \mathbb{E}\left[\frac{1}{n}XX^\top\right]\right\|_{\text{sp}} \gtrsim (\lambda_1^{*2} + \sigma_{(1)}^{*2})\left(\sqrt{\frac{d+c'_4}{n}} + \frac{d}{n}\right)\right) \lesssim e^{-(d+c'_4)}. \quad (\text{B.33})$$

Second, we note that each column of \tilde{X} is the same. So we can rewrite it as

$$\frac{1}{n}\bar{X}\bar{X}^\top = \bar{x}\bar{x}^\top,$$

where $\bar{x} = \frac{1}{n}\sum_{i=1}^n x_i$. Since x_i 's are independent zero mean sub-Gaussian random vectors, by Lemma A.14, we have

$$\mathbb{P}\left(\|\tilde{x}\|_2^2 \gtrsim (\lambda_1^{*2} + \sigma_{(1)}^{*2})\sqrt{\frac{d+c'_4}{n}}\right) \lesssim e^{-\frac{\sqrt{(d+c'_4)n}}{d}}.$$

Then

$$\mathbb{P}\left(\left\|\frac{1}{n}\tilde{X}\tilde{X}^\top\right\|_{\text{sp}} \gtrsim (\lambda_1^{*2} + \sigma_{(1)}^{*2})\sqrt{\frac{d+c'_4}{n}}\right) \lesssim e^{-\frac{\sqrt{(d+c'_4)n}}{d}}. \quad (\text{B.34})$$

Under the assumption that $r < d, d < n$, combining (B.33) and (B.34), we have

$$\mathbb{P}\left(\left\|M - Q^*Q^{*\top} - \Sigma\right\|_{\text{sp}} \gtrsim (\lambda_1^{*2} + \sigma_{(1)}^{*2})\sqrt{\frac{d+c'_4}{n}}\right) \lesssim e^{-\sqrt{d+c'_4}(\frac{\sqrt{n}}{d} \wedge \sqrt{d+c'_4})}.$$

Then there exist $c'_3, c'_4 > 0$, such that $\mathbb{P}(\Omega_2) \geq 1 - ce^{-c'_4\sqrt{d+c'_4}(\frac{\sqrt{n}}{d} \wedge \sqrt{d+c'_4})}$.

This completes the proof of Lemma B.5. \square

B.4.5 Proof of Lemma B.6

Proof. We control the singular value of $\Delta(M) + P^2D(M)$. Under the event Ω_1 , noting that Σ is diagonal, we have

$$\Delta(M) = Q^*Q^{*\top} - D(Q^*Q^{*\top}) + \Delta(M - Q^*Q^{*\top} - \Sigma).$$

Applying Lemma A.4, we obtain that

$$\|\Delta(M - Q^*Q^{*\top} - \Sigma)\|_{\text{sp}} \leq 2c'_3(\lambda_1^{*2} + \sigma_{(1)}^{*2})\sqrt{\frac{d+c'_4}{n}}. \quad (\text{B.35})$$

Since $d \ll n$ and $c'_4 = o(n)$, we have $2c'_3(\lambda_1^{*2} + \sigma_{(1)}^{*2})\sqrt{\frac{d+c'_4}{n}} < \frac{\lambda_r^{*2}}{4}$. Moreover, by Assumptions 3.2 and 3.5, we have $\|D(Q^*Q^{*\top})\|_{\text{sp}} = \lambda_1^{*2}I(U^*) \leq c_3\lambda_1^{*2} < \frac{\lambda_r^{*2}}{4}$. By Weyl's inequality in Lemma A.6, we have that

$$\begin{aligned} \lambda_i(\Delta(M)) &\geq \lambda_r^{*2} - \|D(Q^*Q^{*\top}) - \Delta(M - Q^*Q^{*\top} - \Sigma)\|_{\text{sp}} > \frac{\lambda_r^{*2}}{2}, \quad i \leq r, \\ \lambda_i(\Delta(M)) &\geq -\|D(Q^*Q^{*\top}) - \Delta(M - Q^*Q^{*\top} - \Sigma)\|_{\text{sp}} > -\frac{\lambda_r^{*2}}{2}, \quad i > r. \end{aligned} \quad (\text{B.36})$$

Moreover, noting that $M = \frac{1}{n}(X - \tilde{X})(X - \tilde{X})^\top$, we have

$$\lambda_i(\Delta(M) + P^2D(M)) \geq \lambda_i(\Delta(M)). \quad (\text{B.37})$$

We have already proved that the largest r eigenvalues of $\Delta(M) + P^2D(M)$ are also the largest r singular values according to (B.36) and (B.37). By Lemma A.1, the minimizer \hat{V} of loss B.4 $\mathcal{L}(V)$ satisfies $\hat{V}\hat{V}^\top = \frac{1}{\lambda} \text{rank}_r(\Delta(M) + P^2D(M))$.

This completes the proof of Lemma B.6. \square

C Proofs for Section 4

C.1 Proof of Theorem 4.1

Proof. Note that

$$\begin{aligned} \inf_{w \in \mathbb{R}^r} \mathbb{E}_0[l_c(\delta_{\hat{Q}, w})] &= \inf_{w \in \mathbb{R}^r} \mathbb{E}_0\left[l_c\left(\mathbb{1}\left\{F(w^\top(\hat{Q}^\top\hat{Q})^{-1}\hat{Q}^\top x_0) \geq \frac{1}{2}\right\}\right)\right] \\ &= \inf_{w \in \mathbb{R}^r} \mathbb{E}_0\left[l_c\left(\mathbb{1}\left\{F(w^\top(\hat{Q}^\top\hat{Q})^{-\frac{1}{2}}\hat{Q}^\top x_0) \geq \frac{1}{2}\right\}\right)\right]. \end{aligned}$$

Similarly, for Q , we have,

$$\inf_{w \in \mathbb{R}^r} \mathbb{E}_0[l_c(\delta_{Q, w})] = \inf_{w \in \mathbb{R}^r} \mathbb{E}_0\left[l_c\left(\mathbb{1}\left\{F(w^\top(Q^{*\top}Q^*)^{-\frac{1}{2}}Q^{*\top} x_0) \geq \frac{1}{2}\right\}\right)\right].$$

Also note that $\widehat{Q}(\widehat{Q}^\top \widehat{Q})^{-\frac{1}{2}}, Q^*(Q^{*\top} Q^*)^{-\frac{1}{2}} \in \mathbb{O}_{d,r}$, by Lemma A.1,

$$\left\| \sin \Theta(\widehat{Q}(\widehat{Q}^\top \widehat{Q})^{-\frac{1}{2}}, Q^*(Q^{*\top} Q^*)^{-\frac{1}{2}}) \right\|_F \leq E(\widehat{Q}).$$

Since we have $E(\widehat{Q}) \leq \frac{\sigma_{(1)}^{*2}}{\kappa_\Sigma} \wedge \frac{1}{2}$, applying Lemma A.18, we have

$$\begin{aligned} \inf_{w \in \mathbb{R}^r} \mathbb{E}_0 \left[l_c(\delta_{\widehat{Q},w}) \right] - \inf_{w \in \mathbb{R}^r} \mathbb{E}_0 [l_c(\delta_{Q^*,w})] &\lesssim \\ &\left(\left(\kappa_\Sigma \left(1 + \frac{1}{\sigma_{(1)}^{*2}} \right) \right)^3 + \frac{\kappa_\Sigma}{\sigma_{(1)}^{*2}} \left(1 + \sigma_{(1)}^{*2} \right)^2 \right) \left\| \sin \Theta(\widehat{Q}(\widehat{Q}^\top \widehat{Q})^{-\frac{1}{2}}, Q^*) \right\|_{\text{sp}}. \end{aligned}$$

By the assumption $\sigma_{(1)}^{*2}, \kappa_\Sigma \asymp 1$, we obtain that,

$$\inf_{w \in \mathbb{R}^r} \mathbb{E}_0 \left[l_c(\delta_{\widehat{Q},w}) \right] - \inf_{w \in \mathbb{R}^r} \mathbb{E}_0 [l_c(\delta_{Q^*,w})] \lesssim E(\widehat{Q}).$$

This completes the proof of Theorem 4.1. \square

C.2 Proof of Theorem 4.2

Proof. We show that, for any $e \in \mathcal{C}$ and $e' \notin \mathcal{C}$, the following inequality holds,

$$\|\widehat{q}_e\|_2 \geq \|\widehat{q}_{e'}\|_2.$$

By the triangle inequality, we have

$$\begin{aligned} \|\widehat{q}_e\|_2 &\geq \|q_e\|_2 - \|\widehat{q}_e - q_e\|_2, \\ \|\widehat{q}_{e'}\|_2 &\leq \|q_{e'}\|_2 + \|\widehat{q}_{e'} - q_{e'}\|_2. \end{aligned}$$

Since $e' \notin \mathcal{C}$, we have $\|q_{e'}\|_2 = 0$, which simplifies the second inequality to:

$$\|\widehat{q}_{e'}\|_2 \leq \|\widehat{q}_{e'} - q_{e'}\|_2.$$

By Theorem 3.2 and the assumption

$$\|q_e\|_2 \gtrsim \frac{s}{s^*} \sqrt{\frac{s^* r \log d}{n}},$$

we have that

$$\|\widehat{q}_e\|_2 - \|\widehat{q}_{e'}\|_2 \geq 0.$$

This completes the proof of Theorem 4.2. \square

C.3 Proof of Theorem 4.3

Proof. We first provide a more detailed description of the community detection procedure based on edge embedding. We then analyze its behavior.

Algorithm S.2 Node community detection based on edge embedding.

- 1: **Input:** Edge embeddings matrix $\widehat{Q} \in \mathbb{R}^{d \times r}$; Number of clusters G .
- 2: **Output:** Partition of nodes into G communities.
- 3: Initialize the node similarity matrix $\widehat{S} \in \mathbb{R}^{v \times v}$ with all entries set to 0.
- 4: **for** each edge $e \in [d]$ **do**
- 5: Compute the l_2 -norm of the edge embeddings and update the similarity matrix:

$$\widehat{S}_{u_e u'_e} = \widehat{S}_{u'_e u_e} \leftarrow \|\widehat{q}_e\|_2.$$

- 6: **end for**
- 7: Compute the normalized Laplacian matrix:

$$\widehat{L} \leftarrow \widehat{D}^{-\frac{1}{2}} \widehat{S} \widehat{D}^{-\frac{1}{2}},$$

where \widehat{D} is the diagonal degree matrix with $\widehat{D}_{vv} = \sum_{v'} \widehat{S}_{v,v'}$.

- 8: Compute $\widehat{\Gamma} \in \mathbb{R}^{p \times G}$, the matrix of the leading G eigenvectors of \widehat{L} (ordered by absolute eigenvalue).
- 9: Solve the k -means clustering problem with $\widehat{\Gamma}$ as input. Let $(\widehat{\Theta}, \widehat{Y})$ be a $(1 + \epsilon)$ -approximate solution to the k -means problem which means it satisfies $\|\widehat{\Theta} \widehat{Y} - \widehat{\Gamma}\|_F^2 \leq (1 + \epsilon) \min_{\Theta \in \mathbb{M}_{v,G}, Y \in \mathbb{R}^{G \times G}} \|\Theta Y - \widehat{\Gamma}\|_F^2$, where $\mathbb{M}_{v,G}$ is the set of membership matrices
- 10: **Return:** The membership matrix $\widehat{\Theta}$.

In our analysis, we first bound $\|\widehat{L} - L\|_{\text{sp}}$.

$$\begin{aligned} \|\widehat{L} - L\|_{\text{sp}} &= \left\| \widehat{D}^{-\frac{1}{2}} \widehat{S} \widehat{D}^{-\frac{1}{2}} - \widehat{D}^{-\frac{1}{2}} S \widehat{D}^{-\frac{1}{2}} + \widehat{D}^{-\frac{1}{2}} S \widehat{D}^{-\frac{1}{2}} - D^{-\frac{1}{2}} S D^{-\frac{1}{2}} \right\|_{\text{sp}} \\ &\leq \left(\left\| D^{-\frac{1}{2}} \right\|_{\text{sp}} + \left\| \widehat{D}^{-\frac{1}{2}} \right\|_{\text{sp}} \right)^2 \left\| \widehat{S} - S \right\|_{\text{sp}} + \left(2 \left\| D^{-\frac{1}{2}} \right\|_{\text{sp}} + \left\| \widehat{D}^{-\frac{1}{2}} \right\|_{\text{sp}} \right) \|S\|_{\text{sp}} \left\| \widehat{D}^{-\frac{1}{2}} - D^{-\frac{1}{2}} \right\|_{\text{sp}}. \end{aligned}$$

Note that

$$E(\widehat{Q}) = \left\| \widehat{Q} \widehat{Q}^\top - Q^* Q^{*\top} \right\|_F.$$

Therefore,

$$\left\| \widehat{S} - S \right\|_{\text{sp}} = \left\| \Delta(\widehat{S} - S) \right\|_{\text{sp}} + \rho_G \leq E(\widehat{Q}) + \rho_G,$$

Moreover,

$$\left\| D^{-\frac{1}{2}} \right\|_{\text{sp}} = \frac{1}{\sqrt{\min_{i \in [v]} D_{ii}}} = \frac{1}{\sqrt{v\tau_v}}.$$

By $|\widehat{D}_{ii} - D_{ii}| = |\sum_{j \neq i} (\widehat{S}_{ij} - S_{ij})| \leq \sqrt{v} E(\widehat{Q})$, we have that

$$\left| \frac{1}{\sqrt{\widehat{D}_{ii}}} - \frac{1}{\sqrt{D_{ii}}} \right| = \left| \frac{\sqrt{D_{ii}} - \sqrt{\widehat{D}_{ii}}}{\sqrt{\widehat{D}_{ii}}\sqrt{D_{ii}}} \right| = \left| \frac{D_{ii} - \widehat{D}_{ii}}{D_{ii}\sqrt{\widehat{D}_{ii}} + \widehat{D}_{ii}\sqrt{D_{ii}}} \right| \leq \frac{\sqrt{v} E(\widehat{Q})}{\tau_v^{\frac{3}{2}} v^{\frac{3}{2}} - \tau_v^{\frac{1}{2}} v^{\frac{3}{2}} E(\widehat{Q})}.$$

With the assumption $E(\widehat{Q}) = o(\tau_v \sqrt{v} \wedge \rho_G)$, we have

$$\left\| \widehat{D}^{-\frac{1}{2}} - D^{-\frac{1}{2}} \right\|_{\text{sp}} \leq \frac{2E(\widehat{Q})}{\tau_v^{\frac{3}{2}} v}.$$

Combining these results yields

$$\left\| \widehat{L} - L \right\|_{\text{sp}} \leq \left(\frac{1}{\sqrt{\tau_v v}} + \frac{2E(\widehat{Q})}{\tau_v^{\frac{3}{2}} v} \right)^2 (E(\widehat{Q}) + \rho_G) + \left(\frac{2}{\sqrt{\tau_v v}} + \frac{2E(\widehat{Q})}{\tau_v^{\frac{3}{2}} v} \right) \frac{2E(\widehat{Q})}{\tau_v^{\frac{3}{2}} v} \|S\|_{\text{sp}}.$$

By Lemma A.17, there exists an orthogonal matrix $O \in \mathbb{O}_{G,G}$, such that

$$\left\| \widehat{\Gamma} - \Gamma O \right\|_F \leq \frac{2\sqrt{2}G}{\lambda_G} \left\| \widehat{L} - L \right\|_{\text{sp}}.$$

where $\widehat{\Gamma}, \Gamma$ are the corresponding eigenvector matrices.

Note that $L = D^{-\frac{1}{2}} S D^{-\frac{1}{2}} = D^{-\frac{1}{2}} \Theta B \Theta^\top D^{-\frac{1}{2}} = \Theta B_L \Theta^\top$, where $B_L = D_B^{-\frac{1}{2}} B D_B^{-\frac{1}{2}}$ and $D_B = \text{diag}(B\Theta^\top \mathbf{1}_v)$. Since B is symmetric, full rank, and positive definite, it follows that B_L is also symmetric and full rank. By Lemma A.16, there exists Y , such that $W O = \Theta Y O = \Theta Y'$, where $\|Y_{g*} - Y_{l*}\| = \sqrt{v_g^{-1} + v_l^{-1}}$.

Next, we leverage Lemma A.15. We choose

$$\delta_g = \sqrt{\frac{1}{v_g} + \frac{1}{\max\{v_\ell : \ell \neq g\}}}.$$

Then $v_g \delta_g^2 \geq 1$. We next check the condition (A.2). When $E(\widehat{Q}) = o(\tau_v \sqrt{v} \wedge \rho_G)$, we have

$$(16 + 8\epsilon) \left\| \widehat{\Gamma} - \Gamma O \right\|_F^2 \leq \frac{8G^2}{\lambda_G^2} \left\| \widehat{L} - L \right\|_{\text{sp}}^2 \leq 128(2 + \epsilon) \frac{\rho_G^2 K^2}{\tau_v^2 v^2 \lambda_G^2}.$$

We then have $128(2 + \epsilon) \frac{\rho_G^2 G^2}{\tau_v^2 v^2 \lambda_G^2} \leq 1 \leq \min_{1 \leq g < G} v_g \delta_g^2$. By (A.1),

$$\sum_{g=1}^G |S_g| \left(\frac{1}{v_g} + \frac{1}{\max\{v_\ell : \ell \neq g\}} \right) \leq 128(2 + \epsilon) \frac{\rho_G^2 K^2}{\tau_v^2 v^2 \lambda_G^2},$$

which implies that

$$\widehat{L}(\widehat{\Theta}, \Theta) \leq \max_{1 \leq g \leq G} \frac{|S_g|}{v_g} \leq \sum_{g=1}^G \frac{|S_g|}{v_g} \leq 128(2 + \epsilon) \frac{\rho_G^2 K^2}{\tau_v^2 v^2 \lambda_G^2}.$$

Recalling that v'_{\max} is the second largest community size, we obtain that

$$L(\widehat{\Theta}, \Theta) \leq \frac{1}{v} \sum_{g=1}^G |S_g| \leq 128(2 + \epsilon) \frac{\rho_G^2 G^2 v'_{\max}}{\tau_v^2 v^3 \lambda_G^2}.$$

This completest the proof of Theorem 4.3. \square

D Proofs for Section 5

D.1 Proof of Theorem 5.1

Proof. Recall that $Q^*Q^{*\top} = U^*\Lambda^*U^{*\top}$, where $\Lambda^* = \text{diag}(\lambda_1^{*2}, \dots, \lambda_r^{*2})$ with $\lambda_1^{*2} \geq \dots \geq \lambda_r^{*2}$, and $U^* \in \mathbb{R}^{d \times r}$. For a matrix A , let $\text{supp}(A)$ denote the indices of non-zero rows, i.e., $\text{supp}(A) = \{i \in [n] : \|A_{i*}\|_2 > 0\}$ where A_{i*} denotes the i -th row of A .

Since to establish lower bounds, it suffices to consider the least favorable case among the given parameter space, i.e., $(Q^*, \Sigma^*) \in \mathcal{M}_s$, in the following, we establish the lower bound by focusing on this least favorable case. Specifically, we consider a scenario as follows: suppose $\sigma_i^{*2} = c_\sigma$ for all $i \in \text{supp}(Q^*)$ and $\sigma_{(r)}^{*2} > c_\sigma + \lambda_1^{*2}$. Consider $\text{supp}(Q^*) = [s]$ and $\sigma_{s+i}^{*2} = \sigma_{(i)}^{*2}$ for $i \in [r]$, which means the first r th eigenvalues are $(\sigma_{s+1}^{*2}, \dots, \sigma_{s+r}^{*2})$. Then

$$Q^* = \begin{pmatrix} Q_{[s]}^* \\ 0 \end{pmatrix},$$

where $Q_{[s]}^*$ represents the first r rows corresponding to the support $\text{supp}(Q^*) = [s]$. Note that

$$Q^*Q^{*\top} = U^*\Lambda^*U^{*\top} = \begin{pmatrix} U_{[s]}^* \\ 0 \end{pmatrix} \Lambda^* \begin{pmatrix} U_{[s]}^{*\top} & 0 \end{pmatrix}.$$

For Σ , we have $\sigma_i^{*2} = c_\sigma$ for $i \leq s$. Then

$$\Sigma = \begin{pmatrix} U_{[s]}^* & 0 \\ 0 & I_{d-s} \end{pmatrix} \begin{pmatrix} c_\sigma I_s & 0 \\ 0 & \text{diag}(\sigma_{s+1}^{*2}, \dots, \sigma_d^{*2}) \end{pmatrix} \begin{pmatrix} U_{[s]}^{*\top} & 0 \\ 0 & I_{d-s} \end{pmatrix}.$$

Combining the above results, we have,

$$\mathbb{E}[XX^\top] = \begin{pmatrix} U_{[s]}^* & 0 \\ 0 & I_{d-s} \end{pmatrix} \begin{pmatrix} c_\sigma I_s + \Lambda^* & 0 \\ 0 & \text{diag}(\sigma_{s+1}^{*2}, \dots, \sigma_d^{*2}) \end{pmatrix} \begin{pmatrix} U_{[s]}^{*\top} & 0 \\ 0 & I_{d-s} \end{pmatrix}.$$

By the assumption $\sigma_{(r)}^{*2} > c_\sigma + \lambda_1^{*2}$, we get that the first r leading eigenvectors of $\mathbb{E}[XX^\top]$ are $U_x = (e_{s+1}, \dots, e_{s+r})$, where $\{e_i\}_{i=1}^d$ represents the canonical basis. So the distance between U_x and U^* is

$$\begin{aligned} \|U_x U_x^\top - U^* U^{*\top}\|_F^2 &= \text{tr} \left((U_x U_x^\top - U^* U^{*\top})^\top (U_x U_x^\top - U^* U^{*\top}) \right) \\ &= \text{tr} (U_x U_x^\top + U^* U^{*\top}) = 2r. \end{aligned}$$

Moreover, by Assumption 5.1, with probability at least $1 - ce^{-cs \log d}$, we have

$$\|\widehat{U}_x \widehat{U}_x^\top - U^* U^{*\top}\|_F \geq \|U_x U_x^\top - U^* U^{*\top}\|_F - \|\widehat{U}_x \widehat{U}_x^\top - U_x U_x^\top\|_F \gtrsim \sqrt{r}.$$

Therefore,

$$\sup_{(Q^*, \Sigma) \in \mathcal{M}_s} \mathbb{P}\left(\left\|\widehat{U}_x \widehat{U}_x^\top - U^* U^{*\top}\right\|_F \gtrsim \sqrt{r}\right) \geq 1 - ce^{-cs \log d}.$$

This completes the proof of Theorem 5.1. \square

D.2 Proof of Theorem 5.2

Proof. First, we observe that

$$\begin{aligned} \inf_{w \in \mathbb{R}^r} \mathbb{E}_0\left[l_c\left(\delta'_{\widehat{U}_x, w}\right)\right] &= \inf_{w \in \mathbb{R}^r} \mathbb{E}_0\left[l_c\left(\mathbb{1}\left\{F\left(w^\top \widehat{\Lambda}_r^{-\frac{1}{2}} \widehat{U}_x^\top x_0\right) \geq \frac{1}{2}\right\}\right)\right] \\ &= \inf_{w \in \mathbb{R}^r} \mathbb{E}_0\left[l_c\left(\mathbb{1}\left\{F\left(w^\top \widehat{U}_x^\top x_0\right) \geq \frac{1}{2}\right\}\right)\right] \\ &= \inf_{w \in \mathbb{R}^r} \mathbb{E}_0\left[l_c\left(\mathbb{1}\left\{F\left(w^\top (\widehat{U}_x^\top \widehat{U}_x)^{-\frac{1}{2}} \widehat{U}_x^\top x_0\right) \geq \frac{1}{2}\right\}\right)\right]. \end{aligned}$$

Moreover,

$$\begin{aligned} \inf_{w \in \mathbb{R}^r} \mathbb{E}_0[l_c(\delta_{Q^*, w})] &= \inf_{w \in \mathbb{R}^r} \mathbb{E}_0\left[l_c\left(\mathbb{1}\left\{F(w^\top (Q^{*\top} Q^*)^{-\frac{1}{2}} Q^{*\top} x_0) \geq \frac{1}{2}\right\}\right)\right] \\ &= \inf_{w \in \mathbb{R}^r} \mathbb{E}_0\left[l_c\left(\mathbb{1}\left\{F\left(w^\top U^{*\top} x_0\right) \geq \frac{1}{2}\right\}\right)\right]. \end{aligned}$$

By Lemma A.19, and under the condition

$$E_U^2(\widehat{U}) \geq r - \frac{\sigma_{(1)}^{*2}}{\kappa_\Sigma(1 + \sigma_{(1)}^{*2})} + \frac{c_6}{\kappa_\Sigma},$$

we have

$$\inf_{w \in \mathbb{R}^r} \mathbb{E}_0\left[l_c\left(\delta'_{\widehat{U}_x, w}\right)\right] - \inf_{w \in \mathbb{R}^r} \mathbb{E}_0[l_c(\delta_{Q^*, w})] \gtrsim \frac{\left(\sigma_{(1)}^{*2} + 1\right)^{\frac{3}{2}}}{\left(\sigma_{(1)}^{*2} + \kappa_\Sigma\right)^{\frac{3}{2}} \sigma_{(1)}^{*2}} c_6.$$

Therefore, there exists a constant c_P , which depends only on c_6 , $\sigma_{(1)}^{*2}$, and κ_Σ , such that:

$$\inf_{w \in \mathbb{R}^r} \mathbb{E}_0\left[l_c\left(\delta'_{\widehat{U}_x, w}\right)\right] - \inf_{w \in \mathbb{R}^r} \mathbb{E}_0[l_c(\delta_{Q^*, w})] \geq c_P.$$

This completes the proof of Theorem 5.2. \square